ENCLOSURE 6

TENNESSEE VALLEY AUTHORITY
BROWNS FERRY NUCLEAR PLANT (BFN)
UNITS 1, 2, AND 3

TECHNICAL SPECIFICATIONS (TS) CHANGES TS-431 AND TS-418
EXTENDED POWER UPRATE (EPU)

CALCULATION PACKAGE 0006982.304

Attached is Calculation Package 0006982.304, "Extended Power Uprate Main Steam Line Strain Gauge Vibration Monitoring."

Structural Integrity Associates, Inc.	File No.: 0006982.304
CALCULATION PACKAGE	**Project No.:** 0006982.00

PROJECT NAME:

Extended Power Uprate Main Steam Line Strain Gauge Vibration Monitoring

CONTRACT NO.:

CWA P4463

CLIENT:	**PLANT:** Browns Ferry Units 1, 2 & 3
Tennessee Valley Authority (TVA)	

CALCULATION TITLE:

Comparison Study of Substructure and Submodel Analysis using ANSYS

Document Revision	Affected Pages	Revision Description	Project Manager Approval Signature & Date	Preparer(s) & Checker(s) Signatures & Date
0	1-97, A1-A4, Computer Files	Initial Issue	K. K. Fujikawa 10/30/08	S. B. Kok 10/30/08 R. Gnagne 10/30/08 M. Qin 10/30/08

Table of Contents

1.0 INTRODUCTION 8
1.1 Background Information 8
1.2 Validation Methodology 8
1.3 Nomenclature 9
2.0 STRUCTURE DESCRIPTION AND MATERIAL PROPERTIES 10
3.0 FINITE ELEMENT MODEL DEVELOPMENT 11
3.1 Model Descriptions and Boundary Conditions 12
3.1.1 Full Shell Model 12
3.1.2 Full Solid Model 13
3.1.3 Shell Submodel #1 14
3.1.4 Solid Submodel #1 15
3.1.5 Shell Submodel #2 16
3.1.6 Solid Submodel #2 18
3.2 Finite Element Mesh 20
3.3 Stress Paths 22
4.0 LOAD CASES 24
4.1 Static Analysis Load Cases 24
4.2 Dynamic Analysis Load Cases 25
5.0 STATIC ANALYSIS RESULTS 26
5.1 Static Load Case #1 26
5.1.1 Full Shell Finite Element Analysis 26
5.1.2 Full Solid Finite Element Analysis 27
5.1.3 Substructure Analysis Using Shell Submodel #1 29
5.1.4 Substructure Analysis Using Shell Submodel #2 30
5.1.5 Substructure Analysis Using Solid Submodel #1 31
5.1.6 Substructure Analysis Using Solid Submodel #2 33
5.1.7 Submodel Analysis Using Submodel #1 35
5.1.8 Submodel Analysis Using Submodel #2 40
5.2 Static Load Case #2 45
5.2.1 Full Shell Finite Element Analysis 45
5.2.2 Full Solid Finite Element Analysis 46
5.2.3 Substructure Analysis Using Shell Submodel #1 48

5.2.4 Substructure Analysis Using Shell Submodel #2 ..... *49*
5.2.5 Substructure Analysis Using Solid Submodel #1 ..... *50*
5.2.6 Substructure Analysis Using Solid Submodel #2 ..... *52*
5.2.7 Submodel Analysis Using Submodel #1 ..... *54*
5.2.8 Submodel Analysis Using Submodel #2 ..... *59*
6.0 DYNAMIC ANALYSIS RESULTS 64
6.1 Structural Modal Frequencies 64
6.2 Structural Damping Values 65
6.3 Time History Analysis Integration Time Step 65
6.4 Dynamic Load Case #1 66
6.4.1 Full Shell Finite Element Analysis *66*
6.4.2 Substructure Analysis Using Shell Submodel #2 ..... *70*
6.4.3 Substructure Analysis Using Solid Submodel #2 ..... *72*
6.4.4 Submodel Analysis Using Submodel #2 ..... *74*
6.5 Dynamic Load Case #2 79
6.5.1 Full Shell Finite Element Analysis *79*
6.5.2 Substructure Analysis Using Shell Submodel #2 ..... *83*
6.5.3 Substructure Analysis Using Solid Submodel #2 ..... *85*
6.5.4 Submodel Analysis Using Submodel #2 ..... *87*
7.0 SUMMARY STRESS REDUCTION FACTORS 92
7.1 Static Analysis SRF 92
7.2 Dynamic Analysis SRF 93
8.0 DISCUSSIONS 94
8.1 Static Analysis 94
8.2 Dynamic Analysis 95
9.0 CONCLUSIONS 96
10.0 REFERENCES 97

Appendix A - Computer Files A1

List of Tables

Table 2-1 Key Dimensions 10
Table 5-1 Full Solid Model Baseline Analysis SRF for Static Load Case #1 28
Table 5-2 Substructure Analysis (Submodel #1) SRF for Static Load Case #1 32
Table 5-3 Substructure Analysis (Submodel #2) SRF for Static Load Case #1 34
Table 5-4 Submodel Analysis (Submodel #1) SRF for Static Load Case #1 39
Table 5-5 Submodel Analysis (Submodel #2) SRF for Static Load Case #1 44
Table 5-6 Full Solid Model Baseline Analysis SRF for Static Load Case #2 47
Table 5-7 Substructure Analysis (Submodel #1) SRF for Static Load Case #2 51
Table 5-8 Substructure Analysis (Submodel #2) SRF for Static Load Case #2 53
Table 5-9 Submodel Analysis (Submodel #1) SRF for Static Load Case #2 58
Table 5-10 Submodel Analysis (Submodel #2) SRF for Static Load Case #2 63
Table 6-1 Structural Vertical (Y direction) Modal Frequencies 64
Table 6-2 Structural Horizontal (Z direction) Modal Frequencies 64
Table 6-3 Substructure Dynamic Analysis (Submodel #2) SRF for Dynamic Load Case #1 73
Table 6-4 Submodel Analysis (Submodel #2) SRF for Dynamic Load Case #1 78
Table 6-5 Substructure Dynamic Analysis (Submodel #2) SRF for Dynamic Load Case #2 86
Table 6-6 Submodel Analysis (Submodel #2) SRF for Dynamic Load Case #2 91
Table 7-1 Summary SRF for Static Load Case #1 92
Table 7-2 Summary SRF for Static Load Case #2 92
Table 7-3 Summary SRF for Dynamic Load Case #1 93
Table 7-4 Summary SRF for Dynamic Load Case #2 93

List of Figures

Figure 3-1 Full Shell Model 12
Figure 3-2 Full Solid Model 13
Figure 3-3 Shell Submodel #1 14
Figure 3-4 Solid Submodel #1 15
Figure 3-5 Shell Submodel #2 16
Figure 3-6 Solid Submodel #2 18
Figure 3-7 Shell Finite Element Model Mesh 20
Figure 3-8 Solid Finite Element Model Mesh 21
Figure 3-9 Solid Finite Element Model Stress Paths (Side View) 22
Figure 3-10 Solid Finite Element Model Stress Paths (Top View) 23
Figure 5-1 Full Shell Model Stress Plot for Case #1 (Full Shell Model Baseline Analysis) 26
Figure 5-2 Full Solid Model Analysis Stress Plot for Load Case #1 (Full Solid Model Baseline Analysis) 27
Figure 5-3 Substructure Analysis using Shell Submodel #1 Stress Plot for Load Case #1 29
Figure 5-4 Substructure Analysis using Shell Submodel #2 Stress Plot for Load Case #1 30
Figure 5-5 Substructure Analysis using Solid Submodel #1 Stress Plot for Load Case #1 31
Figure 5-6 Substructure Analysis using Solid Submodel #2 Stress Plot for Load Case #1 33
Figure 5-7 Submodel Analysis using Submodel #1 Applied Displacements for Load Case #1 35
Figure 5-8 Submodel Analysis using Submodel #1 Stress Profile Comparison for Load Case #1 36
Figure 5-9 Submodel Analysis using Submodel #1 Shell Model Stress Plot for Load Case #1 37
Figure 5-10 Submodel Analysis using Submodel #1 Solid Model Stress Plot for Load Case #1 38
Figure 5-11 Submodel Analysis using Submodel #2 Applied Displacements for Load Case #1 40
Figure 5-12 Submodel Analysis using Submodel #2 Stress Profile Comparison for Load Case #1 41
Figure 5-13 Submodel Analysis using Submodel #2 Shell Model Stress Plot for Load Case #1 42
Figure 5-14 Submodel Analysis using Submodel #2 Solid Model Stress Plot for Load Case #1 43
Figure 5-15 Full Shell Model Stress Plot for Case #2 (Full Shell Model Baseline Analysis) 45
Figure 5-16 Full Solid Model Analysis Stress Plot for Load Case #2 (Full Solid Model Baseline Analysis) 46
Figure 5-17 Substructure Analysis using Shell Submodel #1 Stress Plot for Load Case #2 48

Figure 5-18 Substructure Analysis using Shell Submodel #2 Stress Plot for Load Case #2 49

Figure 5-19 Substructure Analysis using Solid Submodel #1 Stress Plot for Load Case #2 50

Figure 5-20 Substructure Analysis using Solid Submodel #2 Stress Plot for Load Case #2 52

Figure 5-21 Submodel Analysis using Submodel #1 Applied Loads for Load Case #2 54

Figure 5-22 Submodel Analysis using Submodel #1 Stress Profile Comparison for Load Case #2 .. 55

Figure 5-23 Submodel Analysis using Submodel #1 Shell Model Stress Plot for Load Case #2 56

Figure 5-24 Submodel Analysis using Submodel #1 Solid Model Stress Plot for Load Case #2 57

Figure 5-25 Submodel Analysis using Submodel #2 Applied Loads for Load Case #2 59

Figure 5-26 Submodel Analysis using Submodel #2 Stress Profile Comparison for Load Case #2 ... 60

Figure 5-27 Submodel Analysis using Submodel #2 Shell Model Stress Plot for Load Case #2 61

Figure 5-28 Submodel Analysis using Submodel #2 Solid Model Stress Plot for Load Case #2 62

Figure 6-1 Full Shell Model Dynamic Analysis Vertical Transient Displacement for Load Case #1 66

Figure 6-2 Full Shell Model Dynamic Analysis Nodal Stress Intensity for Load Case #1 67

Figure 6-3 Full Shell Model Dynamic Analysis Vertical Displacement Plot for Load Case #1 (Full Shell Model Baseline Analysis) 68

Figure 6-4 Full Shell Model Dynamic Analysis Maximum Stress Plot for Load Case #1 (Full Shell Model Baseline Analysis) 69

Figure 6-5 Substructure Analysis using Shell Submodel #2 Vertical Displacement Plot for Load Case #1 70

Figure 6-6 Substructure Analysis using Shell Submodel #2 Stress Plot for Load Case #1 71

Figure 6-7 Substructure Analysis using Solid Submodel #2 Stress Plot for Load Case #1 72

Figure 6-8 Submodel Analysis using Submodel #2 Applied Displacements for Load Case #1 74

Figure 6-9 Submodel Analysis using Submodel #2 Stress Profile Comparison for Load Case #1 75

Figure 6-10 Submodel Analysis using Submodel #2 Shell Model Stress Plot for Load Case #1 76

Figure 6-11 Submodel Analysis using Submodel #2 Solid Model Stress Plot for Load Case #1 77

Figure 6-12 Full Shell Model Dynamic Analysis Horizontal Transient Displacement for Load Case #2 79

Figure 6-13 Full Shell Model Dynamic Analysis Nodal Stress Intensity for Load Case #2 80

Figure 6-14 Full Shell Model Dynamic Analysis Horizontal Displacement Plot for Load Case #2 (Full Shell Model Baseline Analysis) 81

Figure 6-15 Full Shell Model Dynamic Analysis Maximum Stress Plot for Load Case #2 (Full Shell Model Baseline Analysis) 82

Figure 6-16 Substructure Analysis using Shell Submodel #2 Horizontal Displacement Plot for Load Case #2 83

Figure 6-17 Substructure Analysis using Shell Submodel #2 Stress Plot for Load Case #2 84

Figure 6-18 Substructure Analysis using Solid Submodel #2 Stress Plot for Load Case #2 85

Figure 6-19 Submodel Analysis using Submodel #2 Applied Horizontal Loads for Load Case #2 ... 87

Figure 6-20 Submodel Analysis using Submodel #2 Stress Profile Comparison for Load Case #2 ... 88

Figure 6-21 Submodel Analysis using Submodel #2 Shell Model Stress Plot for Load Case #2 89

Figure 6-22 Submodel Analysis using Submodel #2 Solid Model Stress Plot for Load Case #2 90

1.0 INTRODUCTION

1.1 Background Information

This calculation addresses United States Nuclear Regulatory Commission (NRC) request for additional information (RAI) #199/156 (Reference 3) pertaining to Tennessee Valley Authority (TVA) Browns Ferry Units 1 and 2 extended power uprate (EPU) licensing application.

In the stress assessment of the Unit 1 steam dryer, TVA has employed submodel analysis approach to determine a stress reduction factor (SRF) and apply it to the shell analysis stress in the full shell model steam dryer analysis. NRC has noted that the submodel analysis approach is different from a typical substructure analysis approach, as employed in the general purpose finite element code such as ANSYS (References 4 & 5). This calculation validates the submodel analysis approach by specifically addressing the following issues:

1. An analysis of the problem using a typical substructure analysis approach.
2. An analysis of the problem applying the submodel analysis approach, by applying "loads" to match the stress intensity along a line common to the full shell model and the shell submodel.
3. An analysis of the problem applying the submodel analysis approach, by applying "displacements" to match the stress intensity along a line common to the full shell model and the shell submodel.
4. A comparison of the results obtained in (1) using the typical substructure analysis approach with those in (2) and (3) using the submodel analysis approach.

1.2 Validation Methodology

The submodel analysis approach will be validated using two analysis options: (1) static analysis and (2) dynamic time history analysis. In both the static and dynamic time history analyses, the submodel analysis approach will be compared with the typical substructure analysis approach.

In addition to the requested comparison of the two approaches, the following additional analyses are performed to provide more benchmark comparison:

- Perform a static analysis using a full solid model, which models in the detailed weld configuration. This full solid model analysis provides the most accurate information, since this does not include any inherent assumption or approximation associated with substructure or submodel analysis techniques.
- In the static analysis, two submodels are developed: one submodel is 1/2 the size of the full model, and the other is 3/4 the size of the full model. The two different sized models will provide some additional data for comparison, and establish if the size of the submodel influences the analysis results.

1.3 Nomenclature

The key terminology used in the calculation is defined as follows.

Submodel

This refers to a subpart of the full model that has been developed for use in either the substructure analysis or the submodel analyses.

Substructure Analysis

Substructure analysis refers to a typical analysis approach, as employed in the general purpose finite element codes such as ANSYS. In this approach, the displacements from the full model analysis are interpolated and mapped onto the nodes on the appropriate submodel boundaries. These nodal displacements along the boundaries and any loads applied to the local region determine the solution of the submodel.

Submodel Analysis

In a submodel analysis, two submodels are created: one is based on shell elements and the other solid elements. The shell submodel is used to match the stress profile in the submodel with the corresponding stress profile of the full shell model. This matching of stress profile is an iterative process. This is performed by applying loads or displacements, typically along a line. When a close match of the stress profile is achieved, the established loads or displacements can then be applied to the corresponding solid submodel stress analysis. Appropriate boundary conditions are required to be applied to the submodel boundaries. A stress reduction factor (SRF) is calculated by comparing the solid submodel result to the corresponding full shell model result. The SRF is then applied to the appropriate stresses in the full model shell analysis.

Stress Reduction Factor (SRF)

This refers to the ratio of the maximum solid submodel linearized stress intensity and the maximum full shell model stress intensity, at the location of interest. Mathematically, SRF is defined as "Solid Submodel Maximum Linearized $P_m + P_b$ Stress Intensity (along solid submodel stress paths) / Full Shell Model Maximum $P_m + P_b$ Stress Intensity".

2.0 STRUCTURE DESCRIPTION AND MATERIAL PROPERTIES

Structure Description

With reference to Figure 3-1, the structure used for this study consists of:

- A 10" x 40" x 1/2" thick vertical plate.
- A 6" x 12" x 1/4" thick horizontal plate.
- The 1/4" horizontal plate is welded to the 1/2" vertical plate using double-sided 1/4" fillet weld. The fillet weld is wrapped around at both ends of the horizontal plate.
- The vertical plate is restrained at the top and at the bottom. The vertical edges of the vertical plate are not restrained.
- A-240, Type 304 stainless steel material properties at 550°F (Reference 1) are assumed for all components.

Table 2-1
Key Dimensions

Component	Thickness / Size (in)	Modeled Dimensions (in x in)
Vertical Plate	1/2"	10" (width) x 40" (height)
Horizontal Plate	1/4"	6" (width) x 12" (long)
Weld (1)	1/4"	Along the entire connection.

Note: (1) The fillet weld is modeled in the solid finite element models, on both sides.

Material Properties

Modulus of Elasticity	=	25.55E6	psi (Reference 2)
Poisson's Ratio	=	0.30	

3.0 FINITE ELEMENT MODEL DEVELOPMENT

There are a total of 6 finite element models used in this study:

1. The full shell model (see Figure 3-1). This model is used to establish the Shell Baseline Analysis.
2. The full solid model (see Figure 3-2). This model is used to establish the Solid Baseline Analysis.
3. The shell submodel #1 (see Figure 3-3). This shell submodel is 1/2 the size of the full shell model. This model is used in the submodel analysis to match the stress intensity along the weld line.
4. The solid submodel #1 (see Figure 3-4). This solid submodel corresponds to the shell submodel as shown in Figure 3-3. This model is used to establish the stress reduction factor (SRF).
5. The shell submodel #2 (see Figure 3-5). This shell submodel is 3/4 the size of the full shell model. This model is used in the submodel analysis to match the stress intensity along the weld line.
6. The solid submodel #2 (see Figure 3-6). This solid submodel corresponds to the shell submodel as shown in Figure 3-5. This model is used to establish the stress reduction factor (SRF).

A typical finite element mesh of the shell model is shown in Figure 3-7, and a typical finite element mesh of the solid model is shown in Figure 3-8.

Detailed weld configurations are modeled in the solid finite element models. The top two edges of the vertical plates are fixed, and the two vertical edges are free, i.e. not restrained(see Figure 3-1).

The boundary conditions are identified for each of the finite element model in the figures.

3.1 Model Descriptions and Boundary Conditions

3.1.1 Full Shell Model

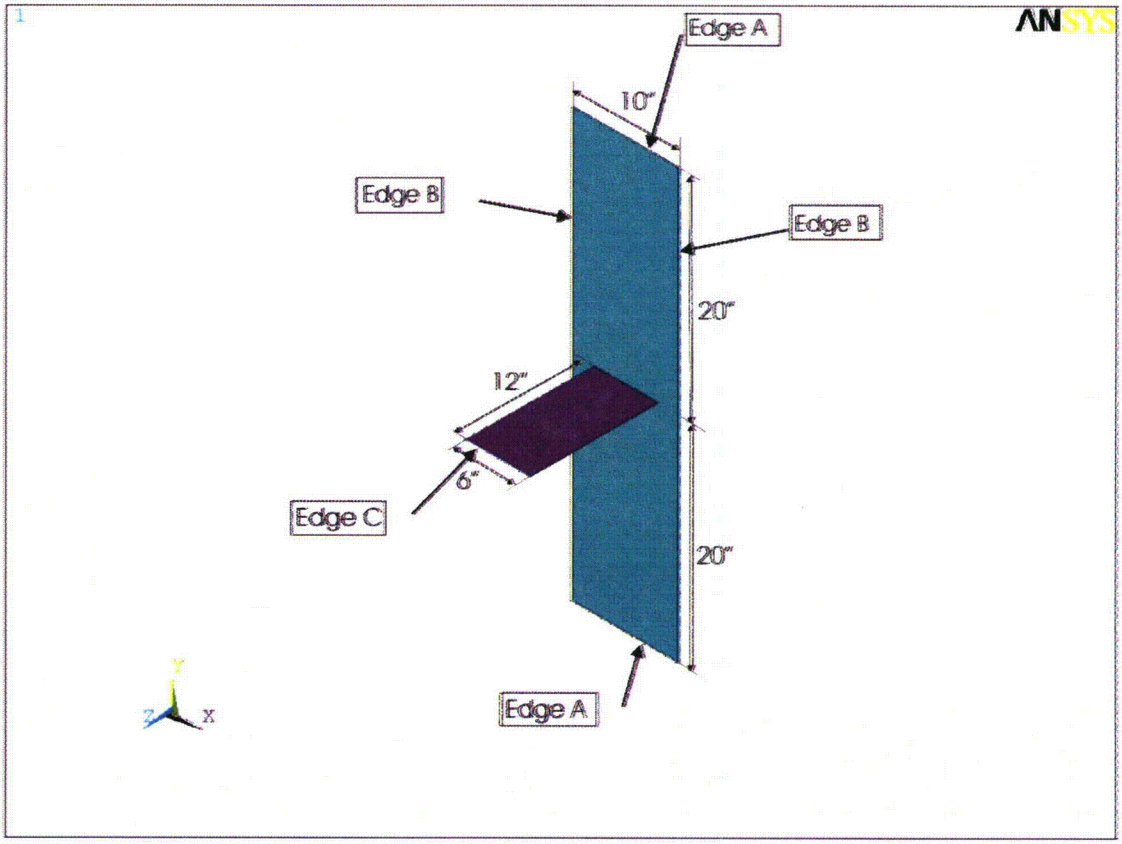

Figure 3-1
Full Shell Model

Boundary Conditions

Edge A: Fixed

Edge B: Free (i.e., not restrained)

Edge C: Applied Load

3.1.2 *Full Solid Model*

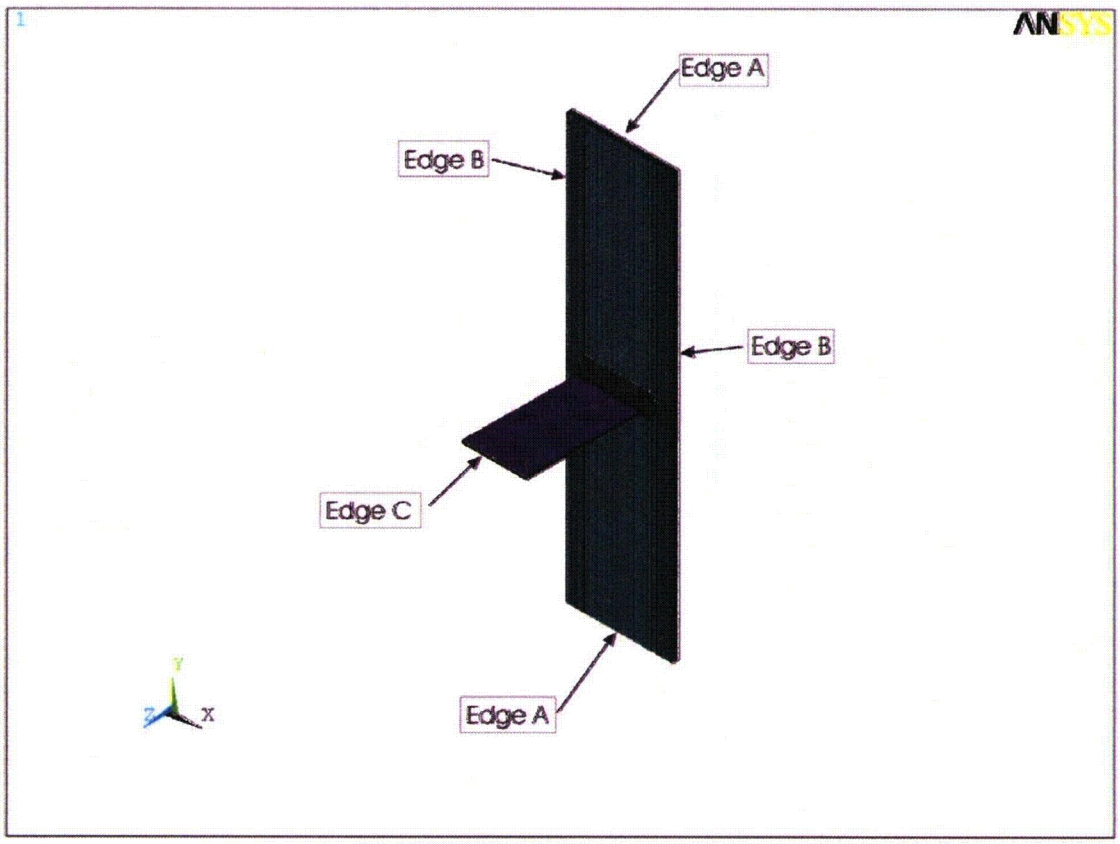

Figure 3-2
Full Solid Model

Boundary Conditions

Edge A: Fixed

Edge B: Free (i.e., not restrained)

Edge C: Applied Load

3.1.3 Shell Submodel #1

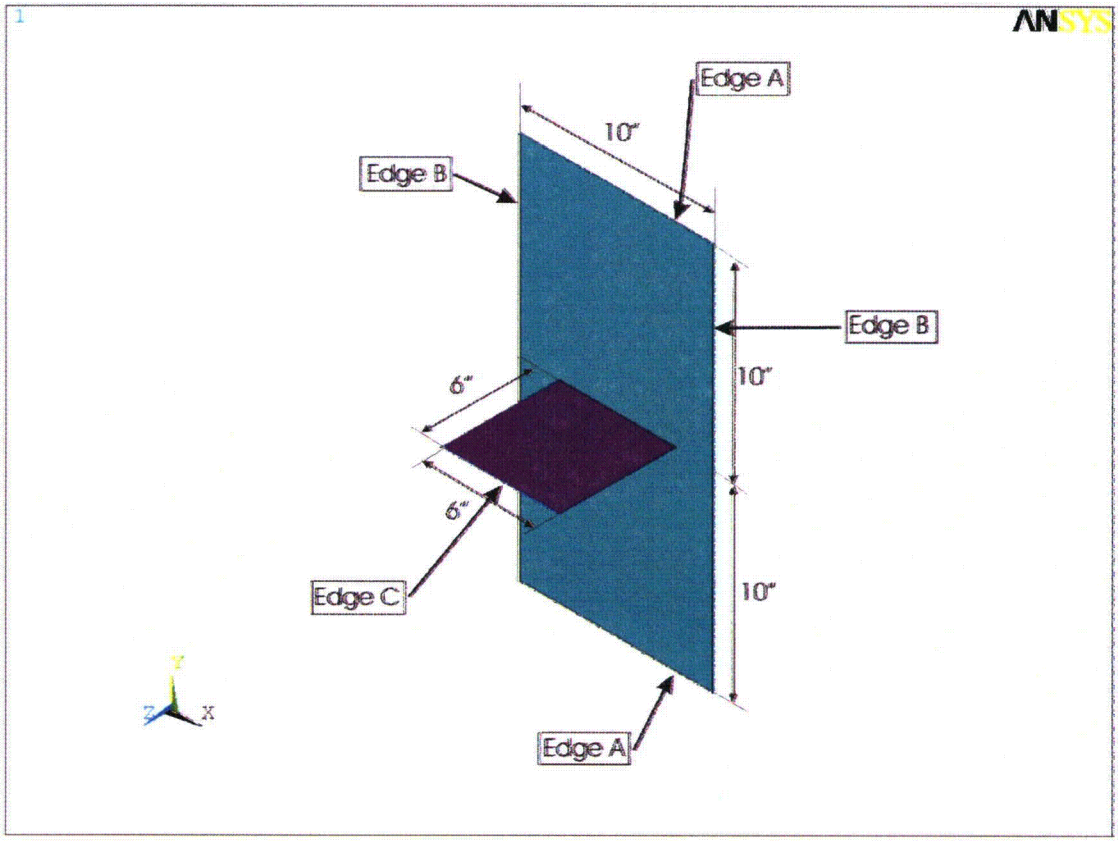

Figure 3-3
Shell Submodel #1

Substructure Analysis Boundary Conditions

Edge A: Applied Displacements

Edge B: Free (i.e., not restrained)

Edge C: Applied Displacements

Submodel Analysis Boundary Conditions

Static Load Cases #1

Edge A: Fixed

Edge B: Free (i.e., not restrained)

Edge C: Applied Displacements

Static Load Case #2

Edge A: Restrained in X & Z translations

Edge B: Free (i.e., not restrained)

Edge C: Applied Load.

3.1.4 Solid Submodel #1

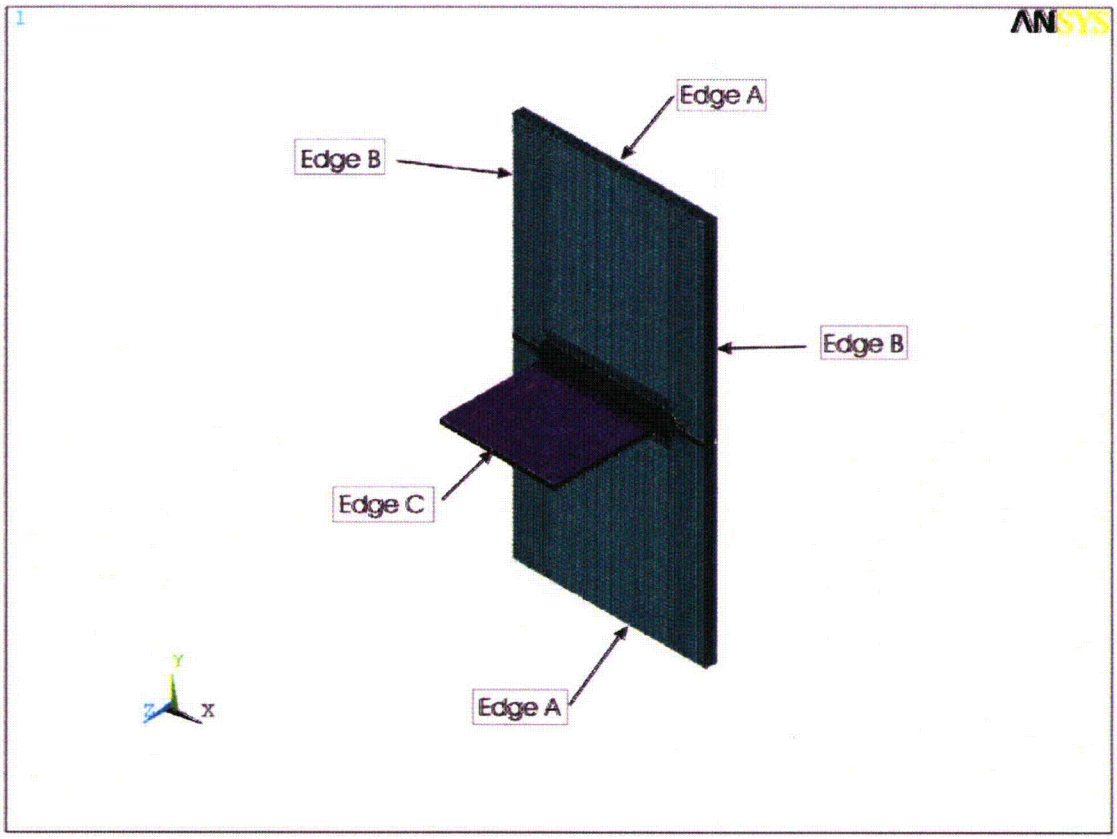

Figure 3-4
Solid Submodel #1

Substructure Analysis Boundary Conditions

Edge A: Applied Displacements

Edge B: Free (i.e., not restrained)

Edge C: Applied Displacements

Submodel Analysis Boundary Conditions

Static Load Cases #1

Edge A: Fixed

Edge B: Free (i.e., not restrained)

Edge C: Applied Displacements

Static Load Case #2

Edge A: Restrained in X & Z translations

Edge B: Free (i.e., not restrained)

Edge C: Applied Load.

3.1.5 Shell Submodel #2

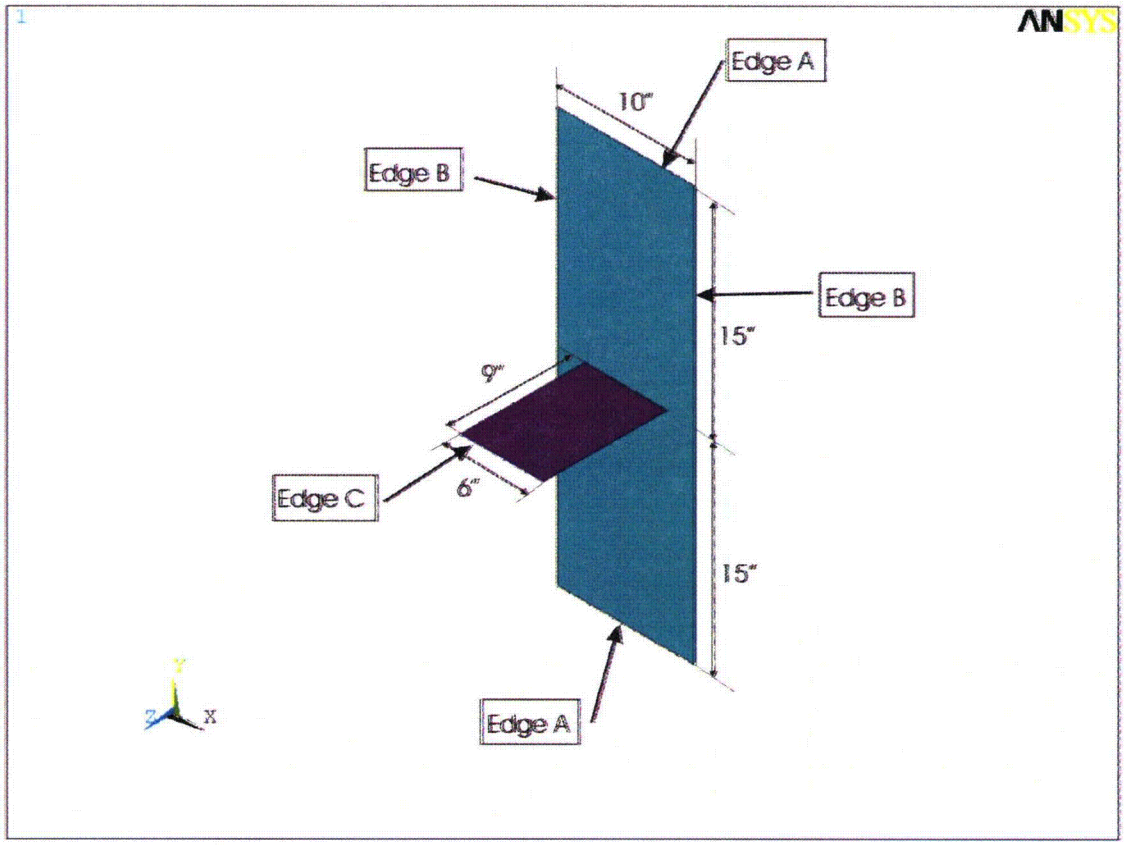

Figure 3-5
Shell Submodel #2

Substructure Analysis Boundary Conditions

Edge A: Applied Displacements

Edge B: Free (i.e., not restrained)

Edge C: Applied Displacements

Submodel Analysis Boundary Conditions

Static Load Cases #1

Edge A: Fixed

Edge B: Free (i.e., not restrained)

Edge C: Applied Displacements

Static Load case #2

Edge A: Fixed

Edge B: Free (i.e., not restrained)

Edge C: Applied Load

Dynamic Load Cases #1

Edge A: Fixed

Edge B: Free (i.e., not restrained)

Edge C: Applied Displacements

Dynamic Load Case #2

Edge A: Restrained in X & Z translations

Edge B: Applied Load

Edge C: Fixed

3.1.6 Solid Submodel #2

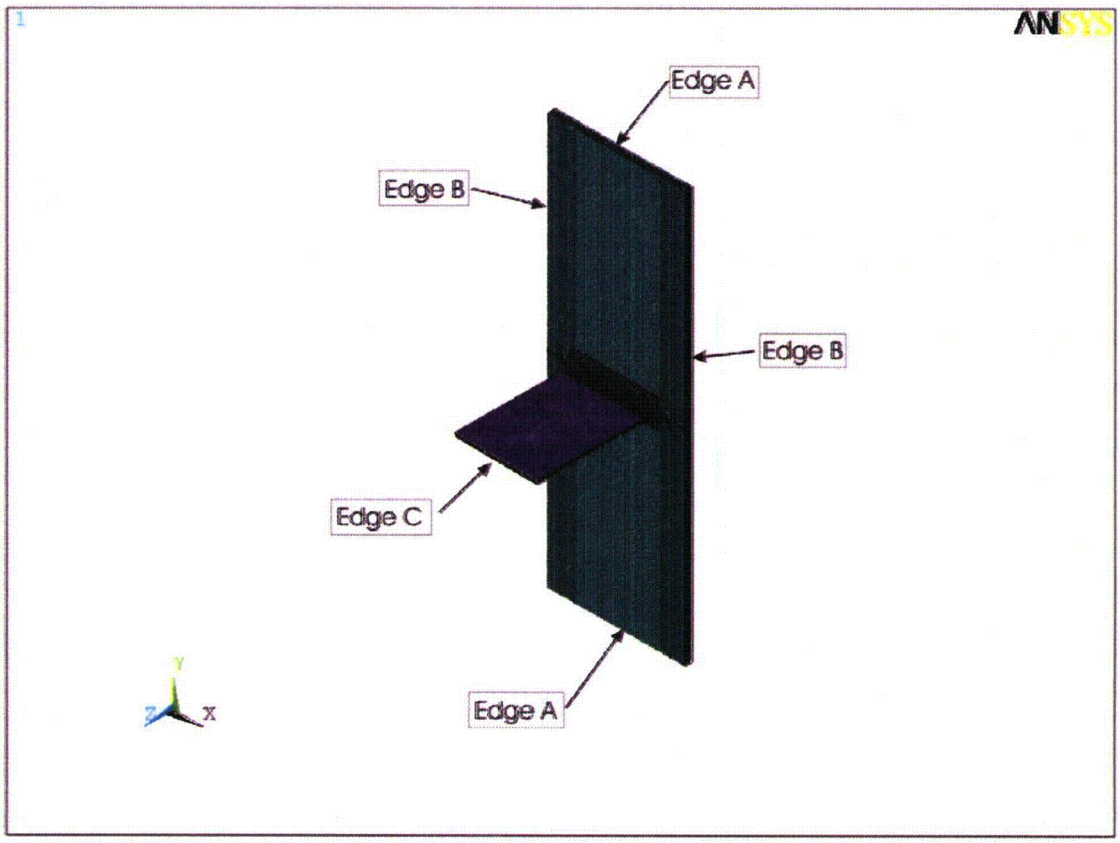

Figure 3-6
Solid Submodel #2

Substructure Analysis Boundary Conditions

Edge A: Applied Displacements

Edge B: Free (i.e., not restrained)

Edge C: Applied Displacements

Submodel Analysis Boundary Conditions

Static Load Cases #1

Edge A: Fixed

Edge B: Free (i.e., not restrained)

Edge C: Applied Displacements

Static Load case #2

Edge A: Fixed

Edge B: Free (i.e., not restrained)

Edge C: Applied Load

Dynamic Load Cases #1

Edge A: Fixed

Edge B: Free (i.e., not restrained)

Edge C: Applied Displacements

Dynamic Load Case #2

Edge A: Restrained in X & Z translations

Edge B: Applied Load

Edge C: Fixed

3.2 Finite Element Mesh

Shell Finite Element Model

The shell finite element model is modeled using SHELL63 elements. A regular mesh size of 0.25" is used for the shell finite element models. The full shell model consists of approximately 7,800 nodes and 7,600 shell elements. The following Figure 3-7 shows the finite element mesh for the shell finite element models.

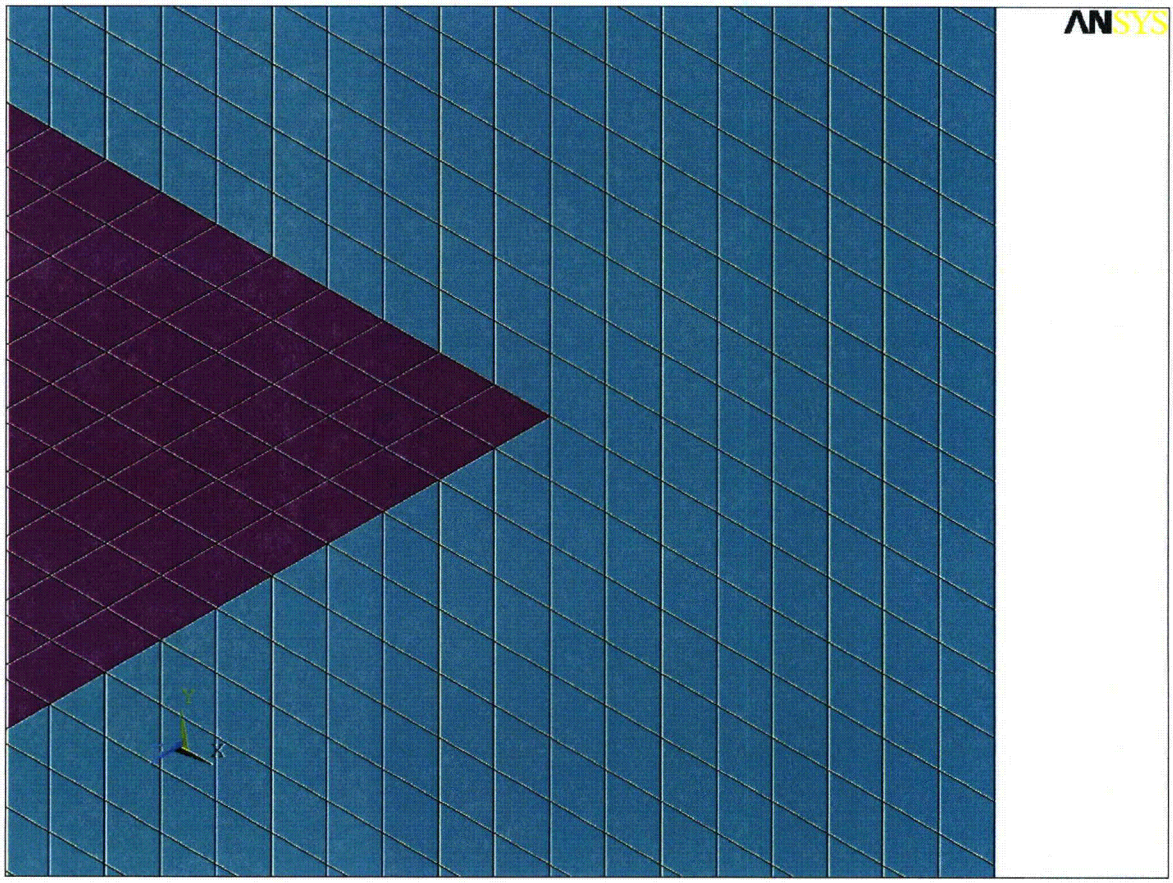

Figure 3-7
Shell Finite Element Model Mesh

Solid Finite Element Model

The solid finite element model is modeled using SOLID45 elements. The solid finite element models generally maintain the same element size of 0.25". In the transition regions around the weld, finer element sizes are used. Six layers of element are modeled across the plate thickness, therefore, providing adequate discretization through the plate thickness to capture the stress variations across the thickness. The entire model consists of approximately 86,000 nodes and 76,000 solid elements. The following Figure 3-8 shows the finite element mesh for the solid finite element models.

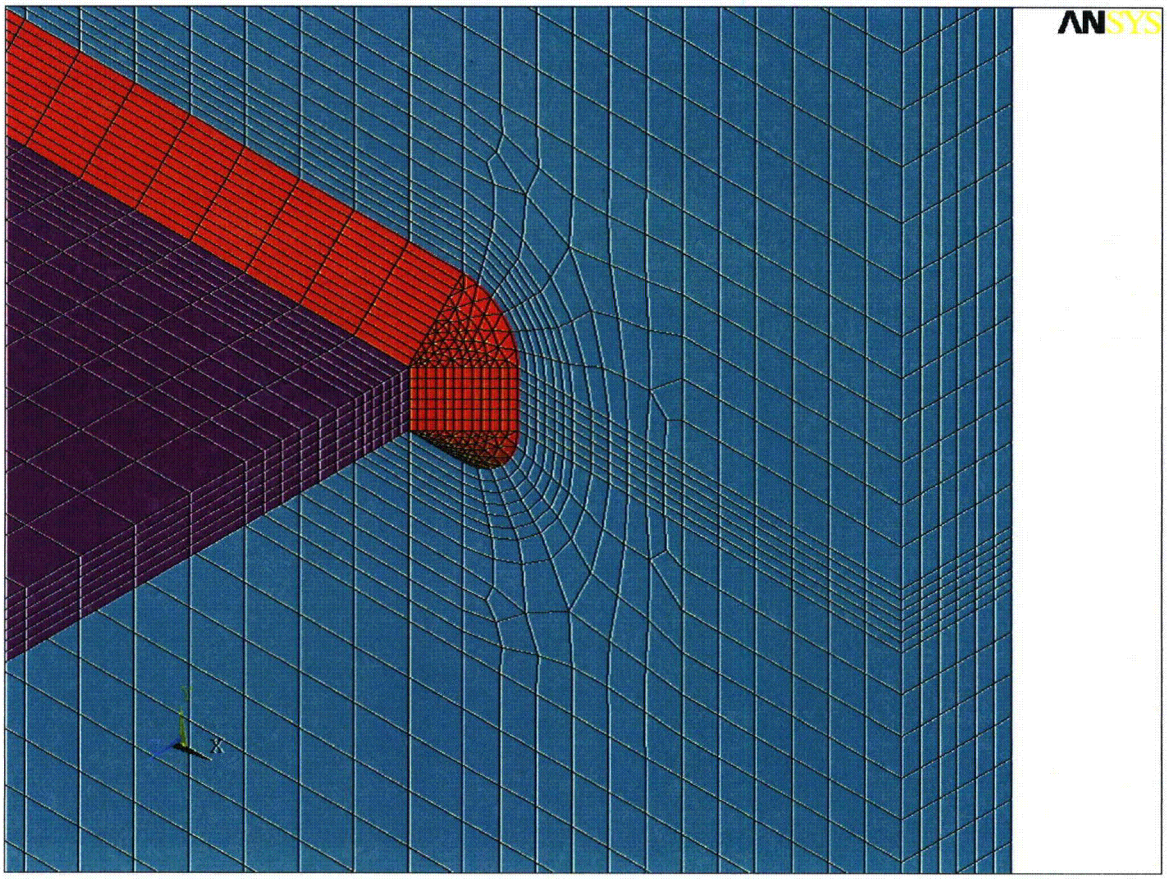

Figure 3-8
Solid Finite Element Model Mesh

3.3 Stress Paths

Linearization stress paths are taken from the weld root to the component surface in the vicinity of the high stress region. In addition, linearization stress paths are also taken from the weld toe to the opposite surface of the connected parts. The stress paths used for the stiffener solid model are shown in the following Figure 3-9 and Figure 3-10.

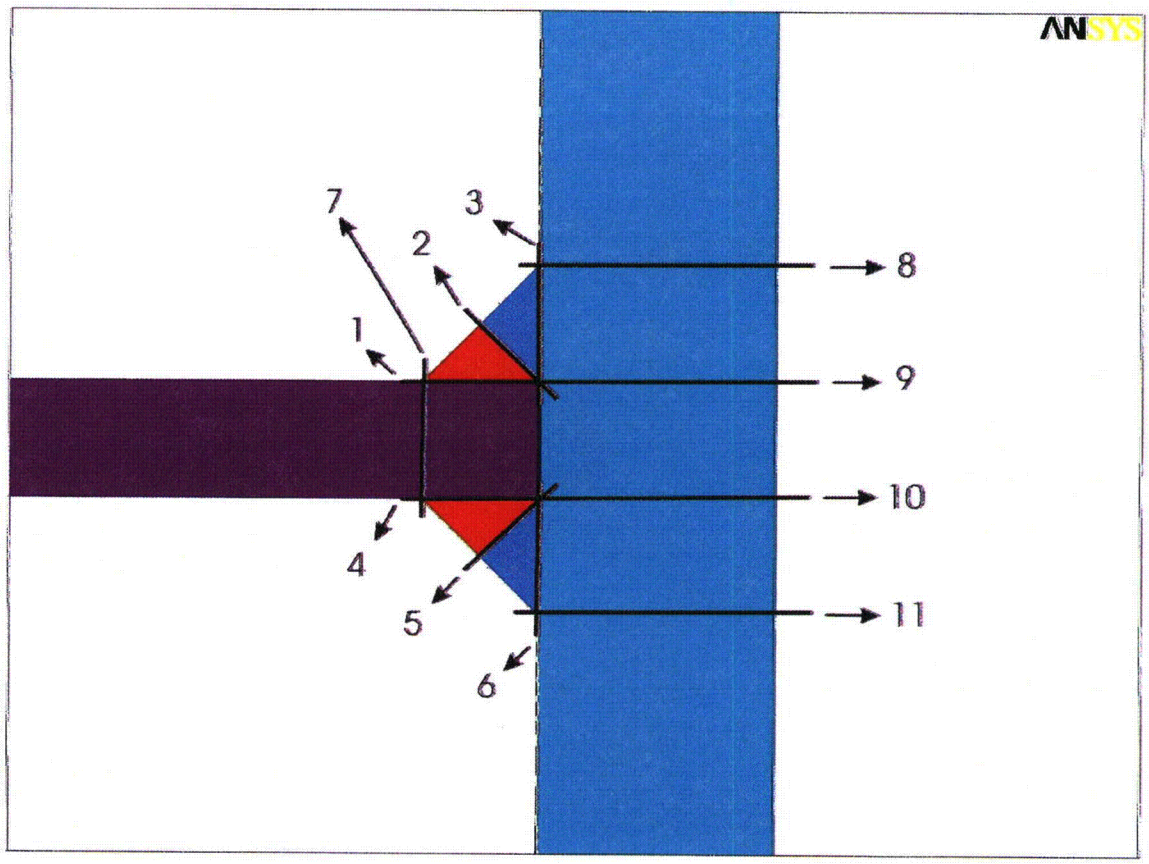

Figure 3-9
Solid Finite Element Model Stress Paths
(Side View)

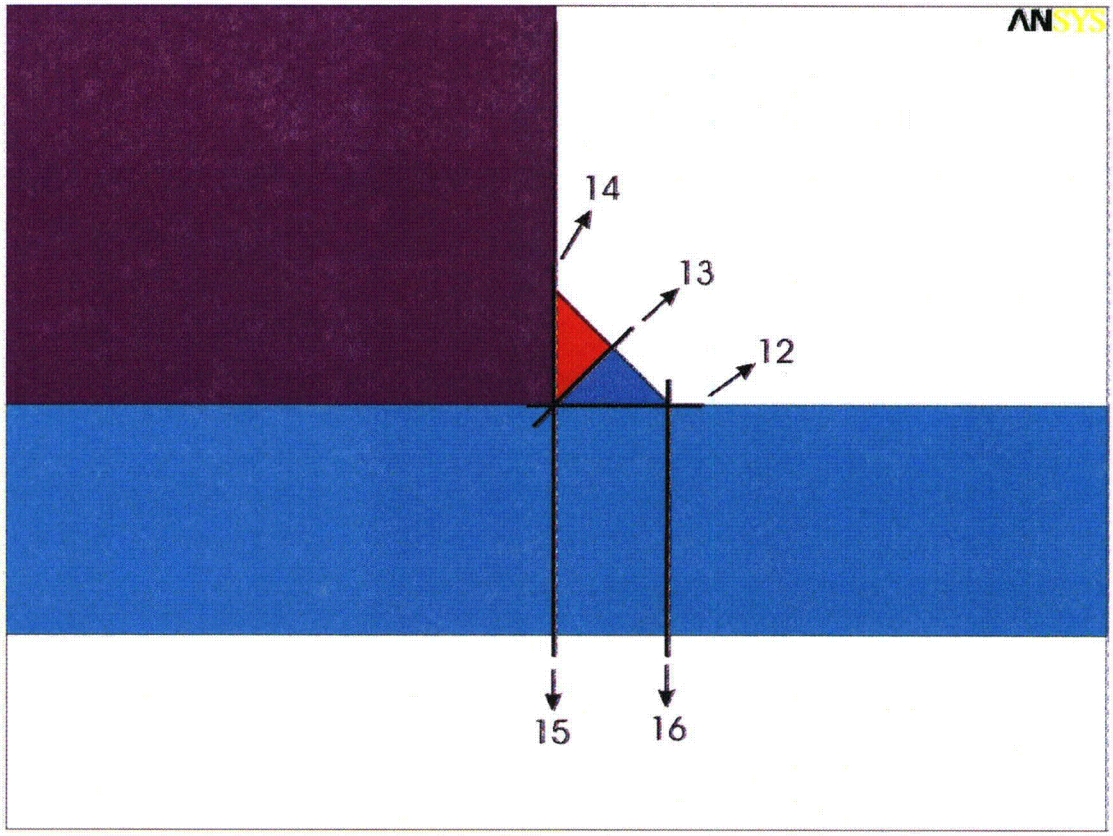

Figure 3-10
Solid Finite Element Model Stress Paths
(Top View)

4.0 LOAD CASES

4.1 Static Analysis Load Cases

Two static load cases are applied:

1. Vertical Load

   A uniform vertical load of 24 lb is applied along Edge C (see Figure 3-1). This load will generate primarily bending stress on the horizontal plate. In the submodel analysis, applied displacements will be used to match the stress intensity along the weld line.

2. Horizontal Load

   A uniform horizontal load of 480 lb is applied along Edge C in the Z direction (see Figure 3-1). This load will generate primarily membrane stress on the horizontal plate. In the submodel analysis, applied loads will be used to match the stress intensity along the weld line.

Static Analysis Objectives

The two static load cases accomplish the following objectives:

- Applying Displacement in Submodel Analysis

  This is accomplished in the Load Case #1.

- Applying Load in Submodel Analysis

  This is accomplished in the Load Case #2.

- Full Solid Finite Element Baseline Analysis

  This analysis provides a direct comparison with the full shell finite elemnt baseline analysis. This analysis removes any inherent approximation and assumption that is associated with the substructure and submodel analyses.

- Submodel #1 and Submodel #2

  Two submodels are used for substructure and submodel analyses. Submodel #1 is 1/2 the size of the full model, and submodel #2 is 3/4 the size of the full model. This different size will highlight the discrepancies, if any, in the substructure and submodel analyses.

4.2 Dynamic Analysis Load Cases

Two dynamic load cases are applied:

1. Vertical Load

   A harmonic uniform vertical load of 24 lb, applied along Edge C (see Figure 3-1). The freqeuncy of the load is set at 25 Hz. The maximum magnitude of this load is similar to the corresponding static analysis load case.

2. Horizontal Load

   A harmonic uniform horizontal load of 480 lb is applied along Edge C in the Z direction (see Figure 3-1). The frequency of the load is set at 25 Hz. The maximum magnitude of this load is similar to the corresponding static analysis load case.

Dynamic Analysis Objectives

The two dynamic load cases accomplish the following objectives:

- Applying Displacement in Submodel Analysis

  This is accomplished in the Load Case #1.

- Applying Load in Submodel Analysis

  This is accomplished in the Load Case #2.

- Comparing the effectiveness of substructure analysis and submodel analysis.

5.0 STATIC ANALYSIS RESULTS

5.1 Static Load Case #1

5.1.1 Full Shell Finite Element Analysis

Stress Plot

The maximum stress intensity is 5,189 psi, and the stress plot is provided in the following Figure 5-1. This analysis is the full shell model baseline analysis, and the maximum stress intensity of 5,189 psi is used to determine the SRF in the other analyses.

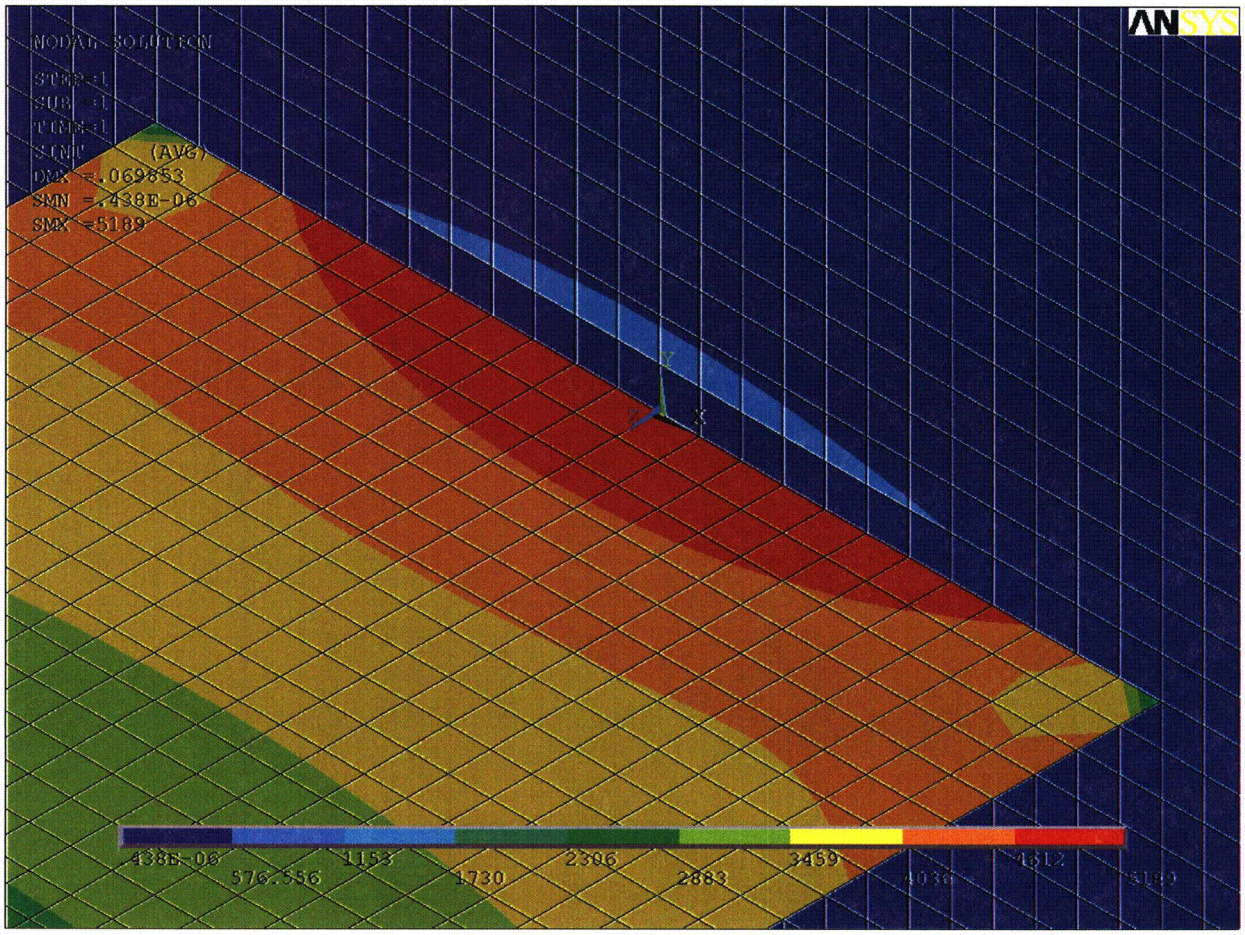

Figure 5-1
Full Shell Model
Stress Plot for Case #1
(Full Shell Model Baseline Analysis)

5.1.2 Full Solid Finite Element Analysis

Stress Plot

The maximum non-linearized stress intensity is 5,608 psi, and the stress plot is provided in the following Figure 5-2. This analysis is the full solid model baseline analysis.

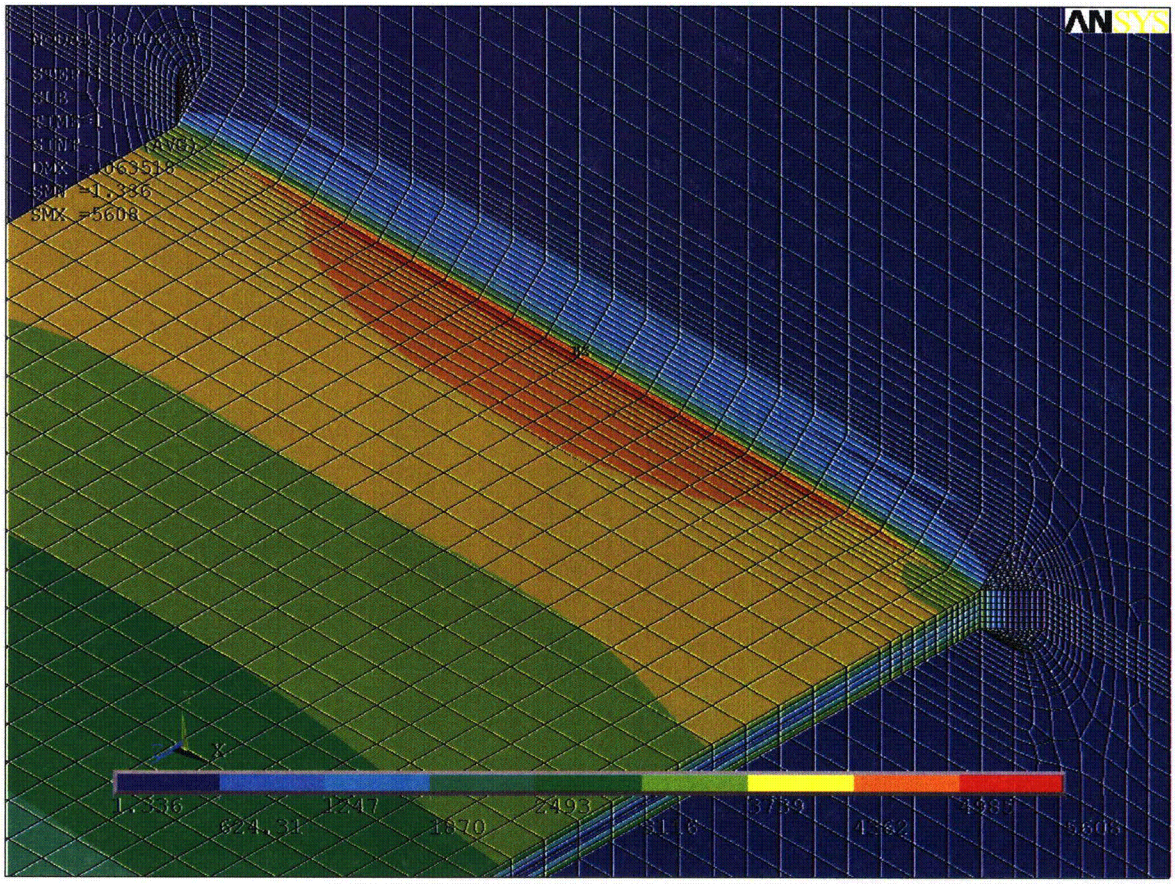

Figure 5-2
Full Solid Model Analysis
Stress Plot for Load Case #1
(Full Solid Model Baseline Analysis)

SRF Table

Table 5-1
Full Solid Model Baseline Analysis SRF
for Static Load Case #1

Path #	Solid (psi)	Shell (psi)	SRF
1	3,043	5,189	0.59
2	1,223		0.24
3	799		0.15
4	3,043		0.59
5	1,223		0.24
6	799		0.15
7	3,020		0.58
8	549		0.11
9	746		0.14
10	746		0.14
11	549		0.11
12	373		0.07
13	417		0.08
14	1,726		0.33
15	364		0.07
16	265		0.05
		Maximum =	**0.59**

5.1.3 Substructure Analysis Using Shell Submodel #1

With reference to Figure 3-3, the displacements along Edges A and C computed in the full shell finite element analysis (Section 5.1.1) are applied onto this shell submodel.

Stress Plot

The maximum stress intensity is 5,198 psi, and the stress plot is provided in the following Figure 5-3.

The maximum stress intensity is the same as the full shell baseline analysis maximum stress intensity, and the stress contours are very similar (see Figure 5-1). This confirms that the shell substructure analysis produces the same stress results as the full shell baseline analysis.

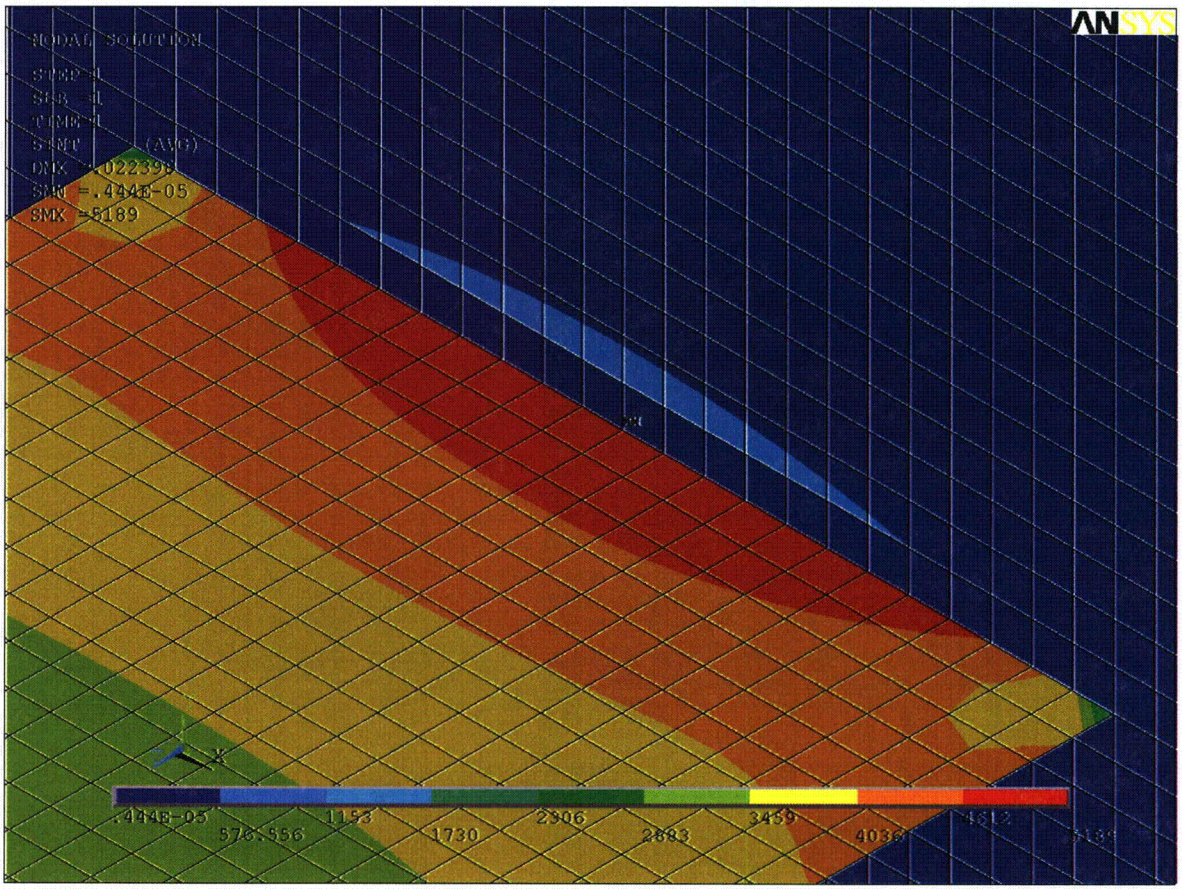

Figure 5-3
Substructure Analysis using Shell Submodel #1
Stress Plot for Load Case #1

5.1.4 Substructure Analysis Using Shell Submodel #2

With reference to Figure 3-5, the displacements along Edges A and C computed in the full shell finite element analysis (Section 5.1.1) are applied onto this shell submodel.

Stress Plot

The maximum stress intensity is 5,198 psi, and the stress plot is provided in the following Figure 5-4.

The maximum stress intensity is the same as the full shell baseline analysis maximum stress intensity, and the stress contours are very similar (see Figure 5-1). This confirms that the shell substructure analysis produces the same stress results as the full shell baseline analysis.

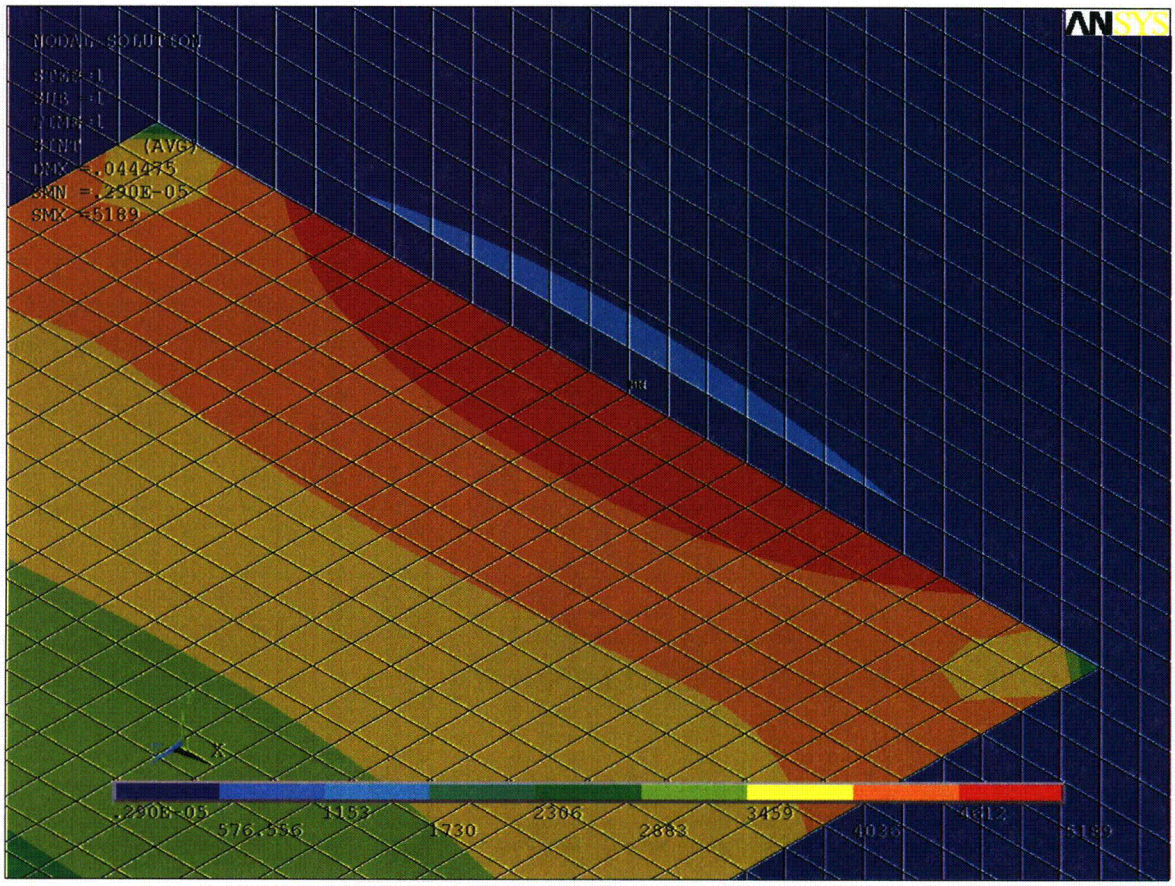

Figure 5-4
Substructure Analysis using Shell Submodel #2
Stress Plot for Load Case #1

5.1.5 Substructure Analysis Using Solid Submodel #1

With reference to Figure 3-4, the displacements along Edges A and C computed in the full shell finite element analysis (Section 5.1.1) are applied onto this solid submodel.

Stress Plot

The maximum non-linearized stress intensity is 7,033 psi, and the stress plot is provided in the following Figure 5-5.

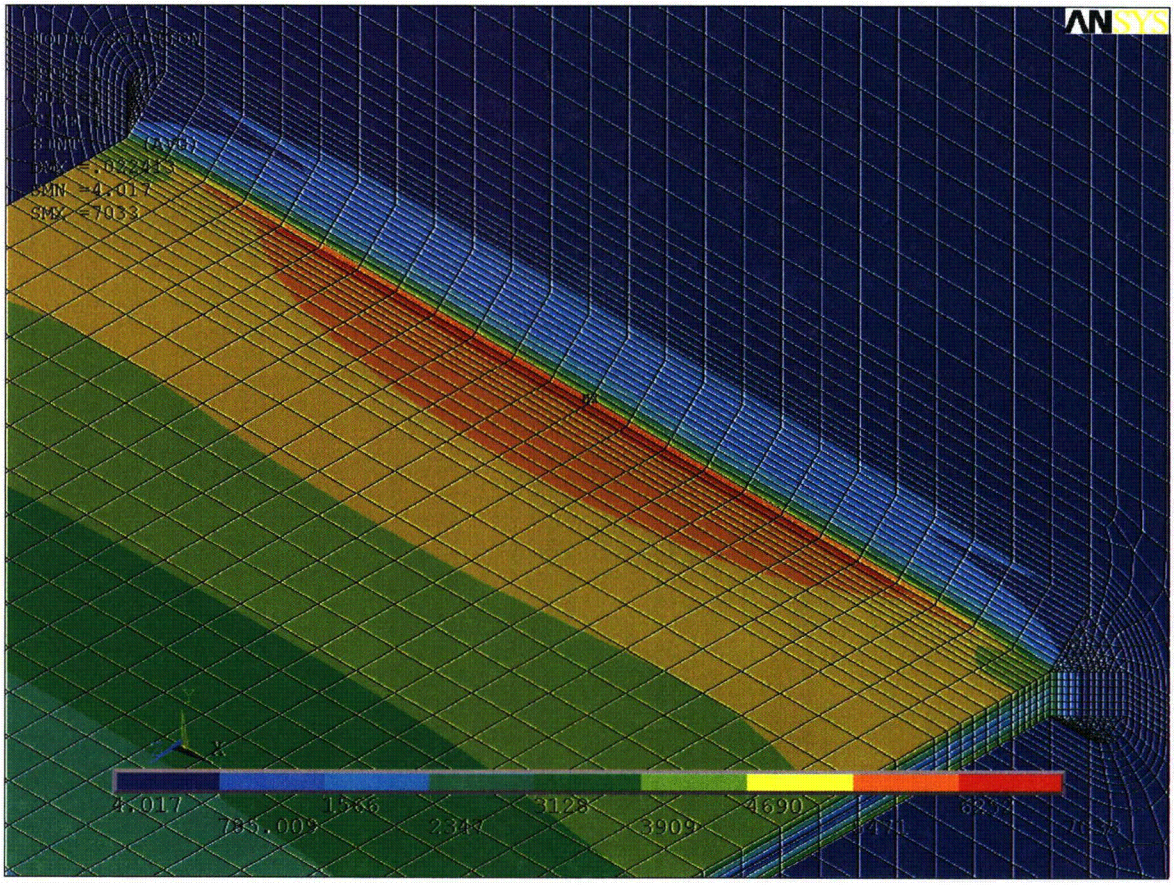

Figure 5-5
Substructure Analysis using Solid Submodel #1
Stress Plot for Load Case #1

SRF Table

Table 5-2
Substructure Analysis (Submodel #1) SRF
for Static Load Case #1

Path #	Solid (psi)	Shell (psi)	SRF
1	3,822	5,189	0.74
2	1,543		0.30
3	1,003		0.19
4	3,822		0.74
5	1,543		0.30
6	1,003		0.19
7	3,785		0.73
8	696		0.13
9	936		0.18
10	936		0.18
11	696		0.13
12	488		0.09
13	546		0.11
14	2,239		0.43
15	477		0.09
16	364		0.07
		Maximum =	**0.74**

5.1.6 Substructure Analysis Using Solid Submodel #2

With reference to Figure 3-6, the displacements along Edges A and C computed in the full shell finite element analysis (Section 5.1.1) are applied onto this solid submodel.

Stress Plot

The maximum non-linearized stress intensity is 6,568 psi, and the stress plot is provided in the following Figure 5-6.

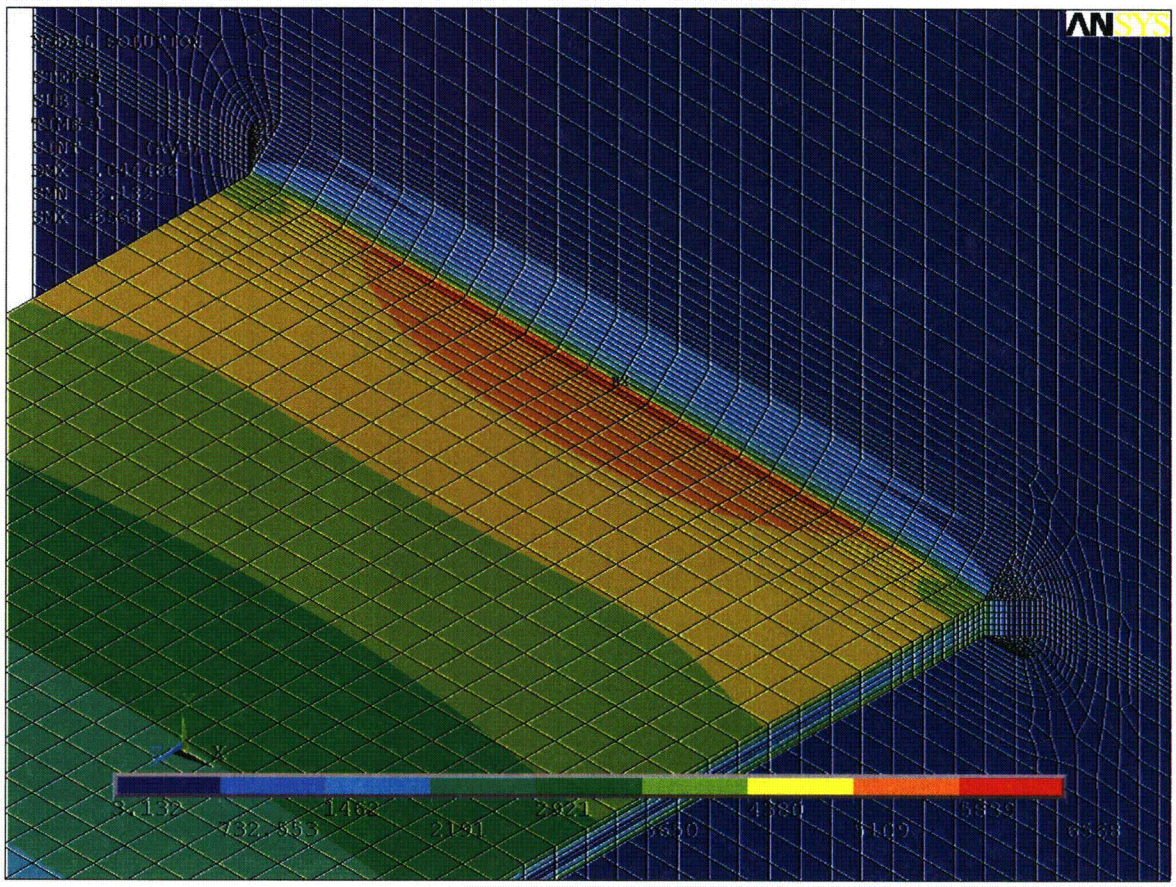

Figure 5-6
Substructure Analysis using Solid Submodel #2
Stress Plot for Load Case #1

SRF Table

Table 5-3
Substructure Analysis (Submodel #2) SRF
for Static Load Case #1

Path #	Solid (psi)	Shell (psi)	SRF
1	3,565	5,189	0.69
2	1,435		0.28
3	936		0.18
4	3,565		0.69
5	1,435		0.28
6	936		0.18
7	3,536		0.68
8	646		0.12
9	874		0.17
10	874		0.17
11	646		0.12
12	445		0.09
13	498		0.10
14	2,051		0.40
15	434		0.08
16	321		0.06
		Maximum =	**0.69**

5.1.7 Submodel Analysis Using Submodel #1

Matching Stress Profile

The stress profile matching is performed along the weld line connecting the vertical plate to the horizontal plate. The matching is accomplished by imposing vertical displacements along the Edge C (see Figure 3-3) of the submodel. Fixed boundary condition is applied to the top and bottom edges. The applied displacements and the comparison of the stress profiles are shown in the following Figure 5-7 and Figure 5-8, respectively.

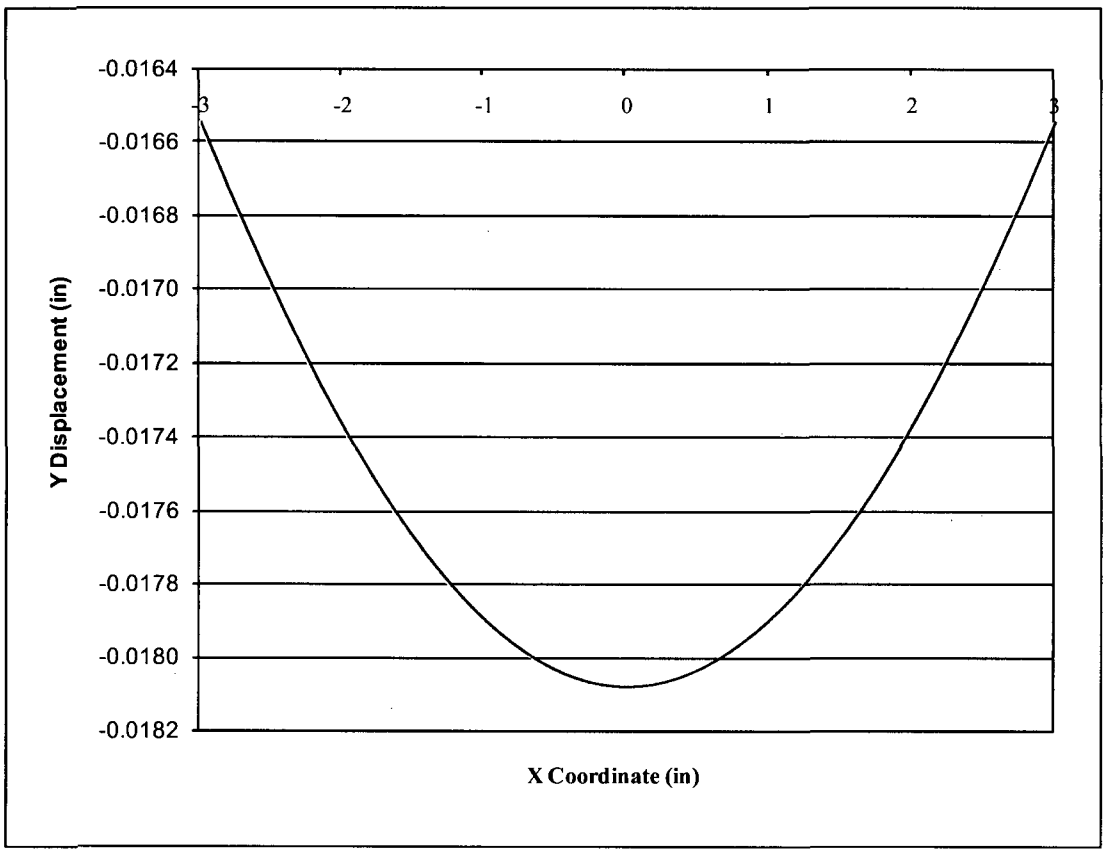

Figure 5-7
Submodel Analysis using Submodel #1
Applied Displacements for Load Case #1

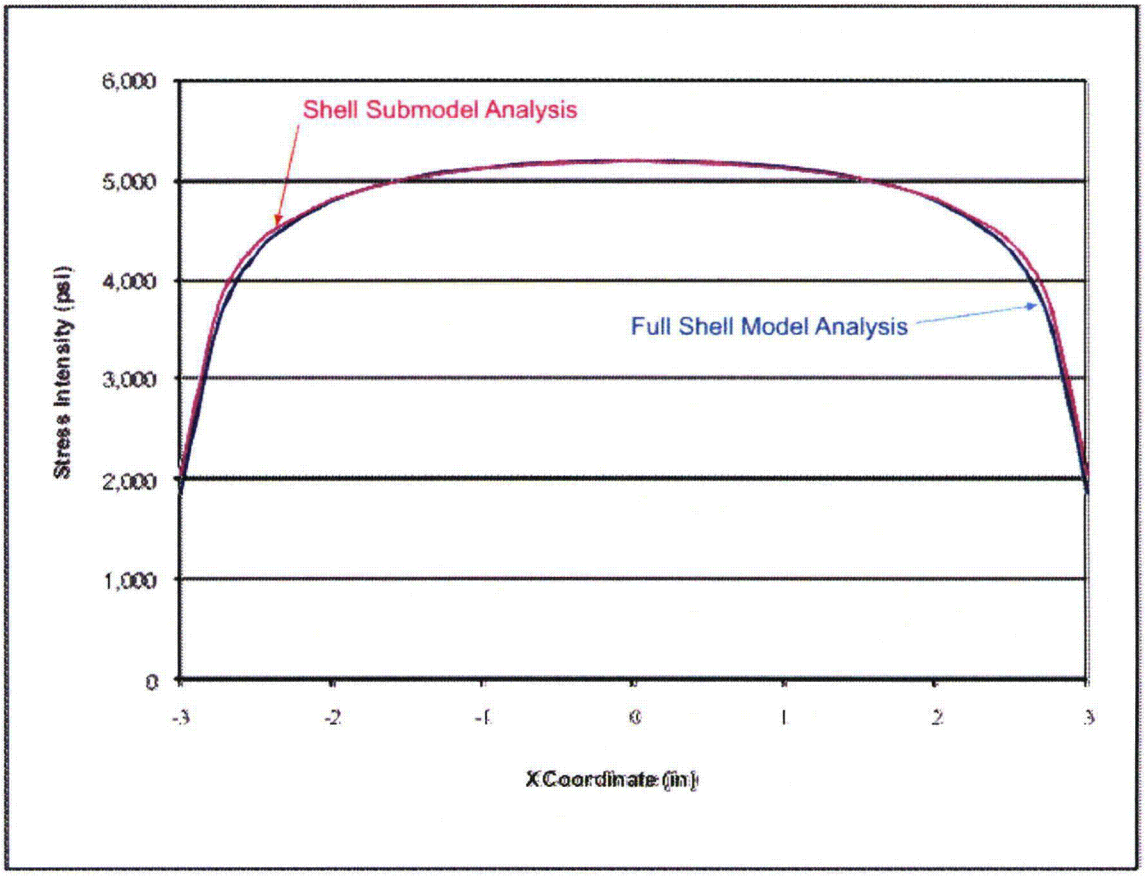

Figure 5-8
Submodel Analysis using Submodel #1
Stress Profile Comparison for Load Case #1

Stress Plot

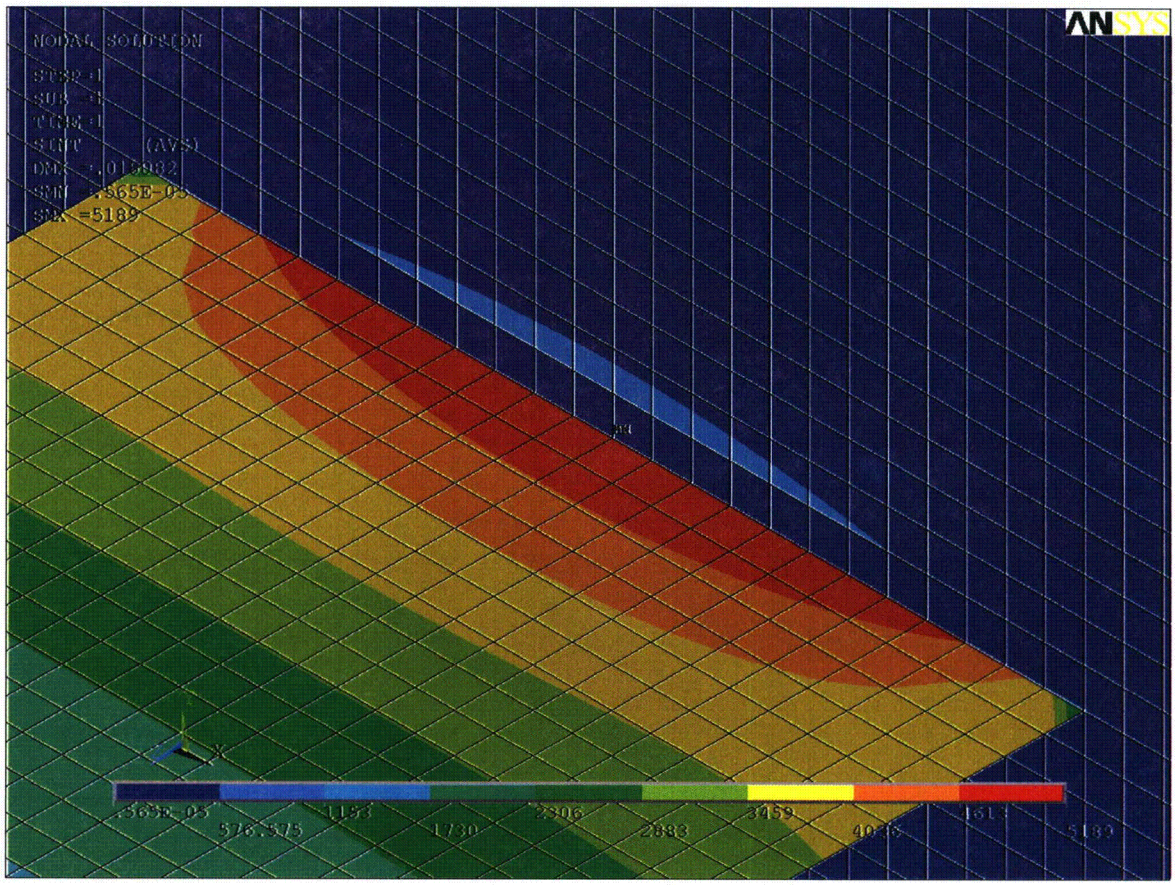

Figure 5-9
Submodel Analysis using Submodel #1
Shell Model Stress Plot for Load Case #1

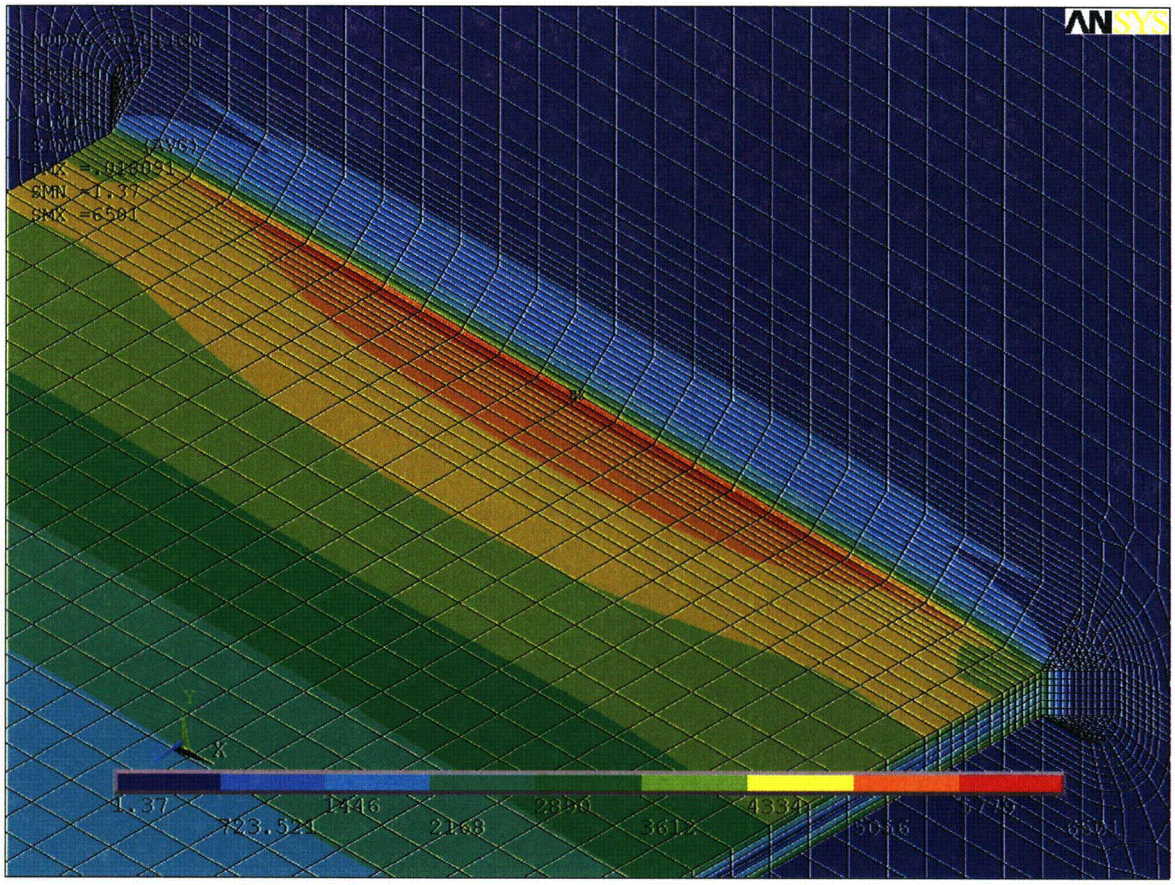

Figure 5-10
Submodel Analysis using Submodel #1
Solid Model Stress Plot for Load Case #1

SRF Table

Table 5-4
Submodel Analysis (Submodel #1) SRF
for Static Load Case #1

Path #	Solid (psi)	Shell (psi)	SRF
1	3,543	5,189	0.68
2	1,443		0.28
3	929		0.18
4	3,543		0.68
5	1,443		0.28
6	929		0.18
7	3,495		0.67
8	645		0.12
9	865		0.17
10	865		0.17
11	645		0.12
12	456		0.09
13	499		0.10
14	2,084		0.40
15	437		0.08
16	367		0.07
		Maximum =	**0.68**

5.1.8 Submodel Analysis Using Submodel #2

Matching Stress Profile

The stress profile matching is performed along the weld line connecting the vertical plate to the horizontal plate. The matching is accomplished by imposing vertical displacements along the Edge C (see Figure 3-5) of the submodel. Fixed boundary condition is applied to the top and bottom edges. The applied displacements and the comparison of the stress profiles are shown in the following Figure 5-11 and Figure 5-12, respectively.

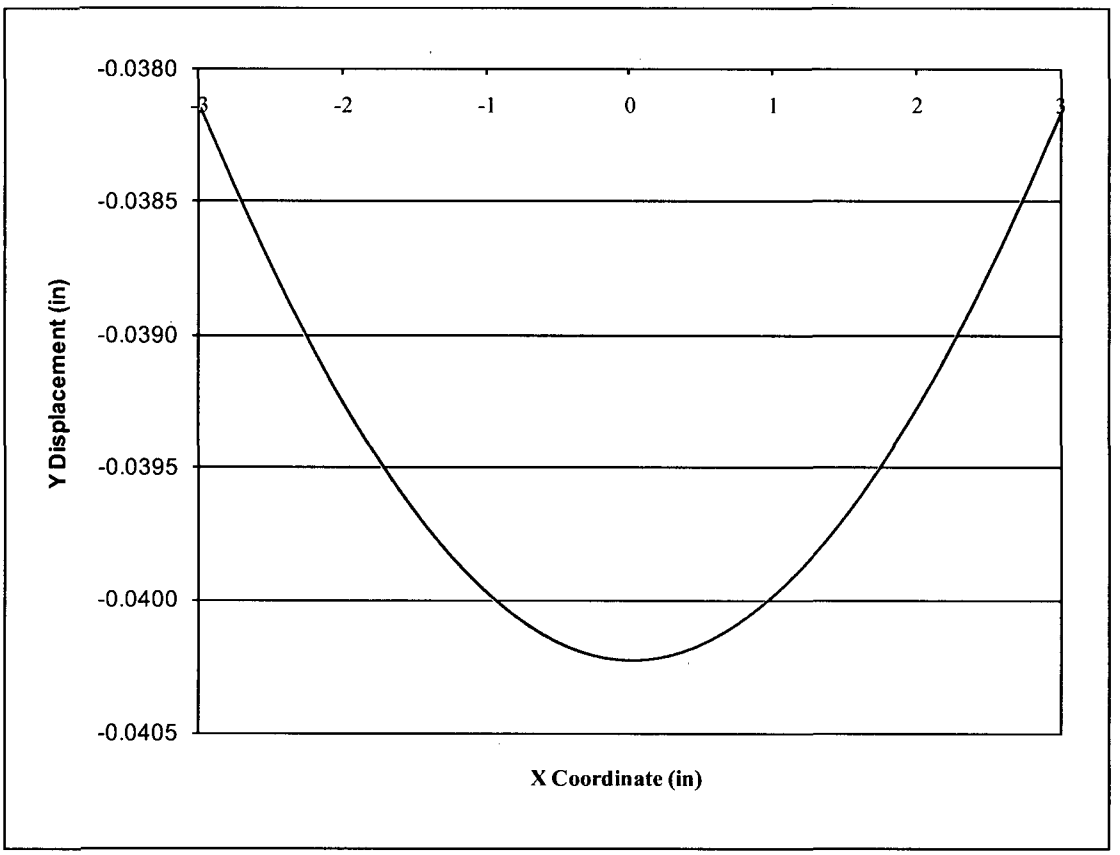

Figure 5-11
Submodel Analysis using Submodel #2
Applied Displacements for Load Case #1

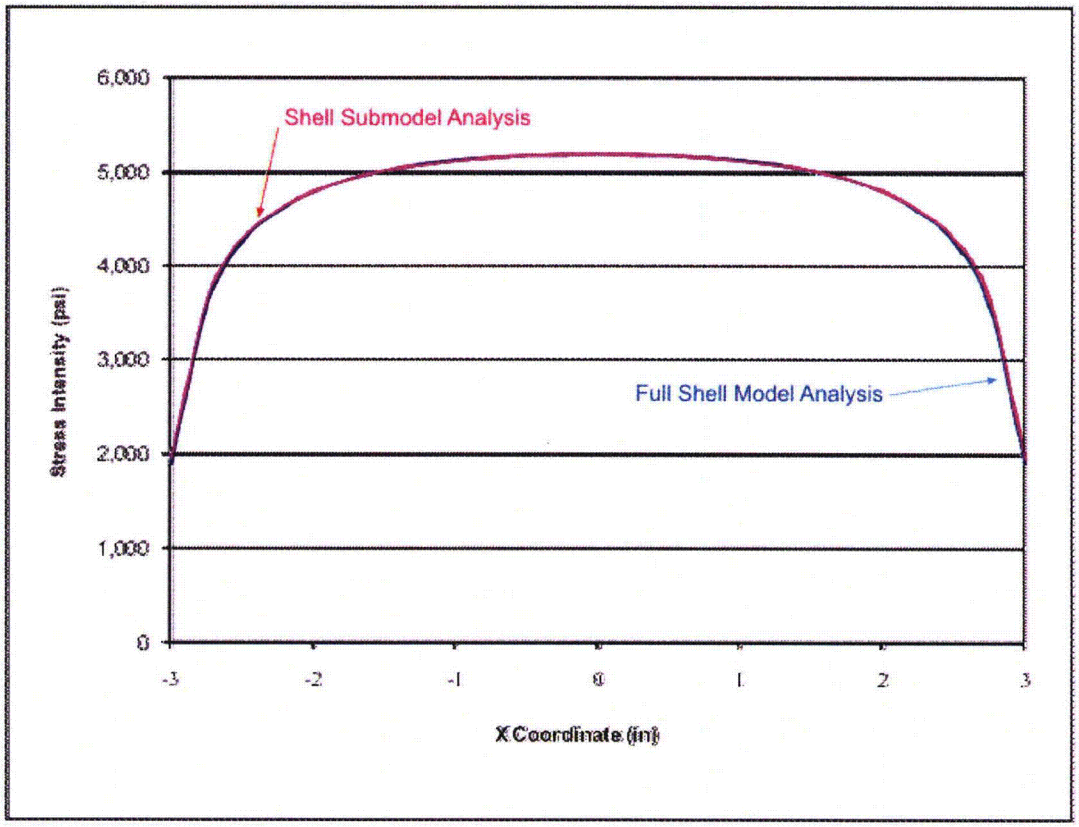

Figure 5-12
Submodel Analysis using Submodel #2
Stress Profile Comparison for Load Case #1

Stress Plot

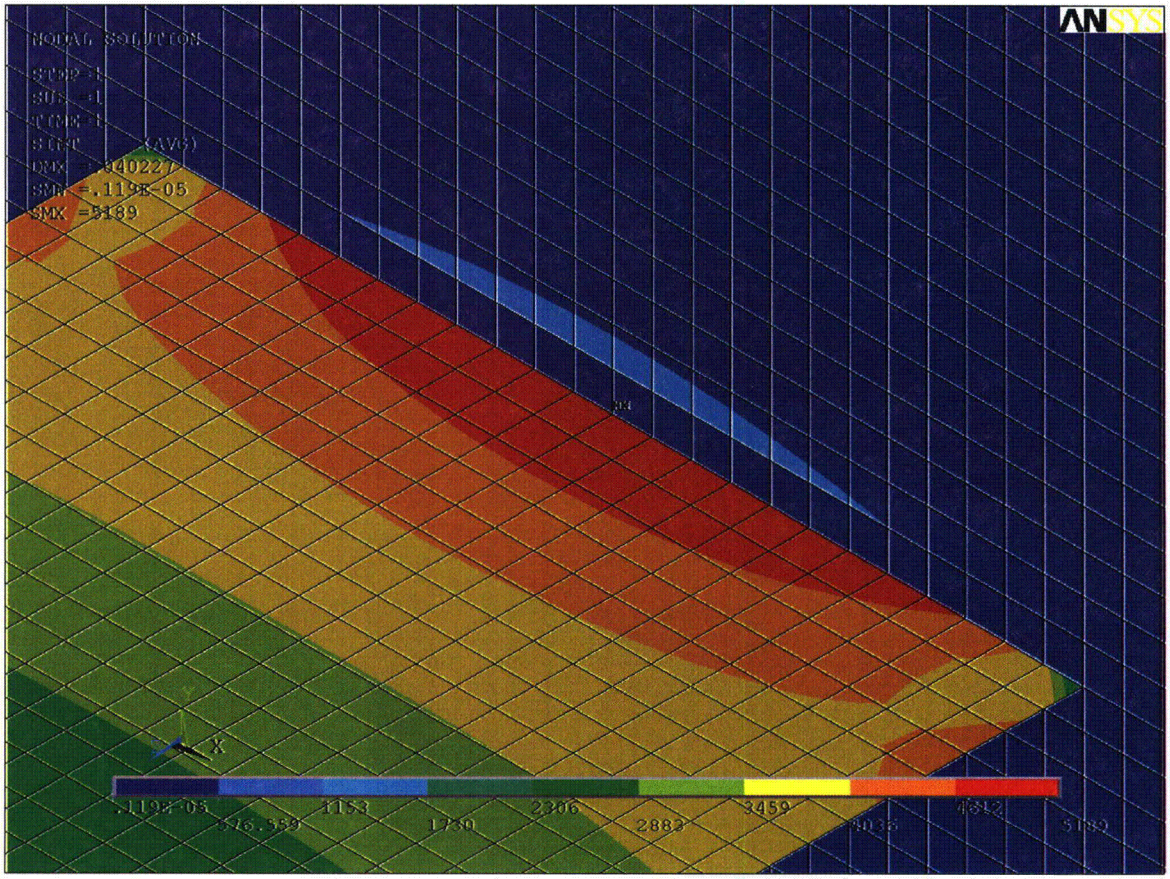

Figure 5-13
Submodel Analysis using Submodel #2
Shell Model Stress Plot for Load Case #1

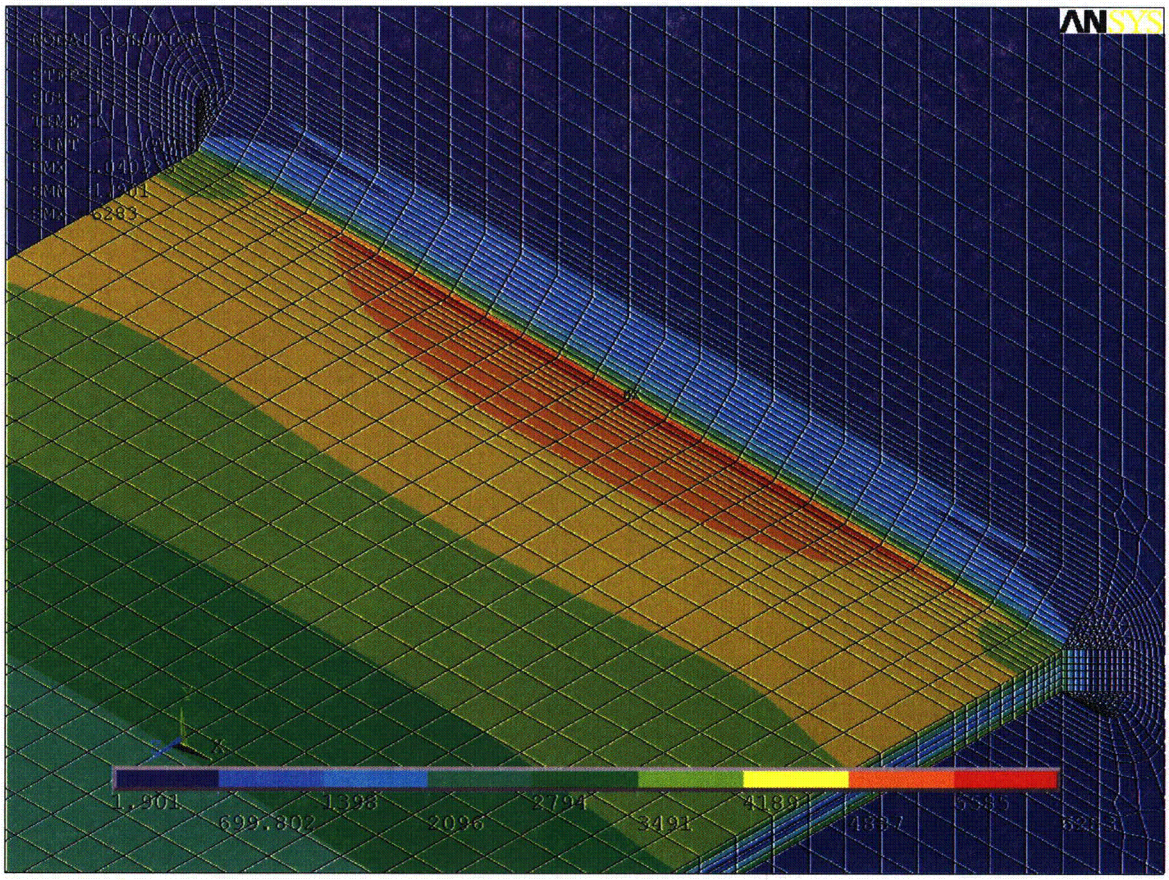

Figure 5-14
Submodel Analysis using Submodel #2
Solid Model Stress Plot for Load Case #1

SRF Table

Table 5-5
Submodel Analysis (Submodel #2) SRF
for Static Load Case #1

Path #	Solid (psi)	Shell (psi)	SRF
1	3,414	5,189	0.66
2	1,378		0.27
3	896		0.17
4	3,414		0.66
5	1,378		0.27
6	896		0.17
7	3,381		0.65
8	618		0.12
9	836		0.16
10	836		0.16
11	618		0.12
12	422		0.08
13	472		0.09
14	1,950		0.38
15	412		0.08
16	318		0.06
		Maximum =	0.66

5.2 Static Load Case #2

5.2.1 Full Shell Finite Element Analysis

Stress Plot

The maximum stress intensity is 6,579 psi, and the stress plot is provided in the following Figure 5-15. This analysis is the full shell model baseline analysis, and the maximum stress intensity of 6,579 psi is used to determine the SRF in the other analyses.

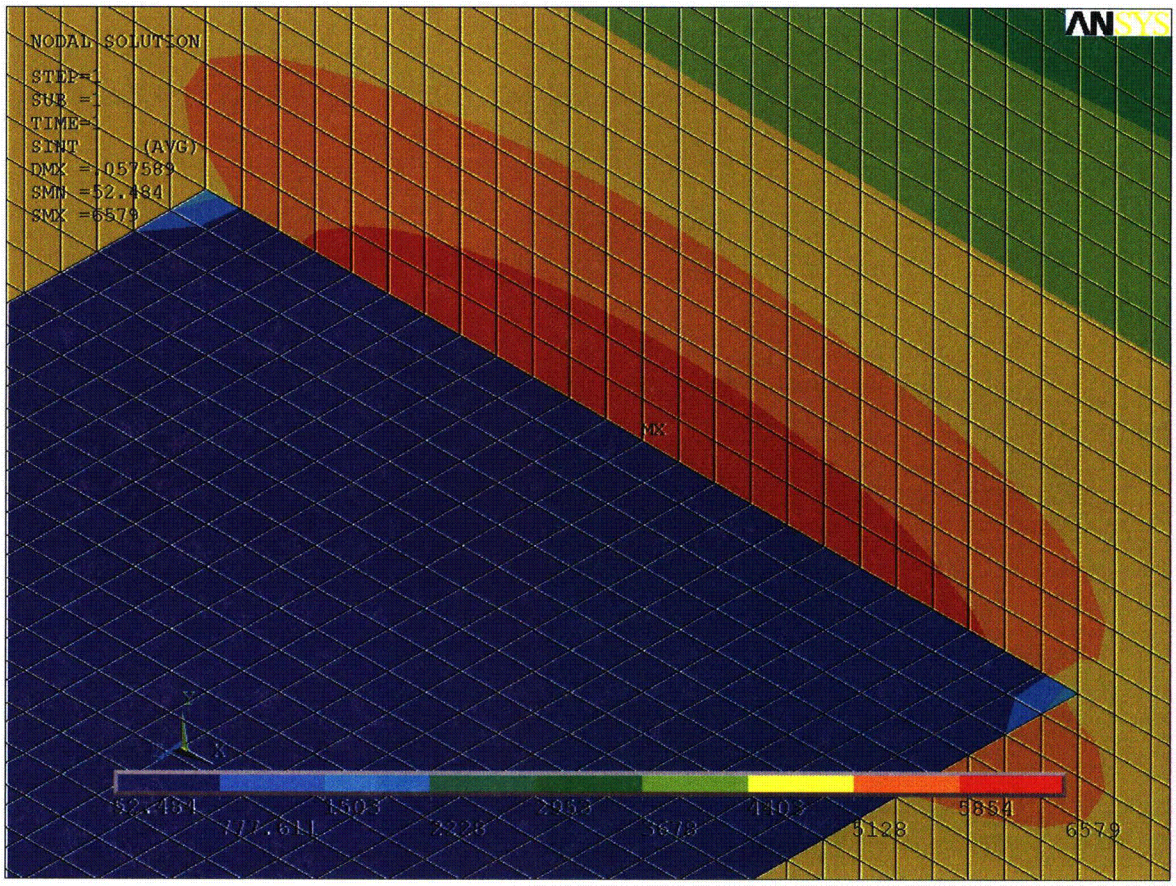

Figure 5-15
Full Shell Model
Stress Plot for Case #2
(Full Shell Model Baseline Analysis)

5.2.2 *Full Solid Finite Element Analysis*

Stress Plot

The maximum non-linearized stress intensity is 10,470 psi, and the stress plot is provided in the following Figure 5-16. This analysis is the full solid model baseline analysis.

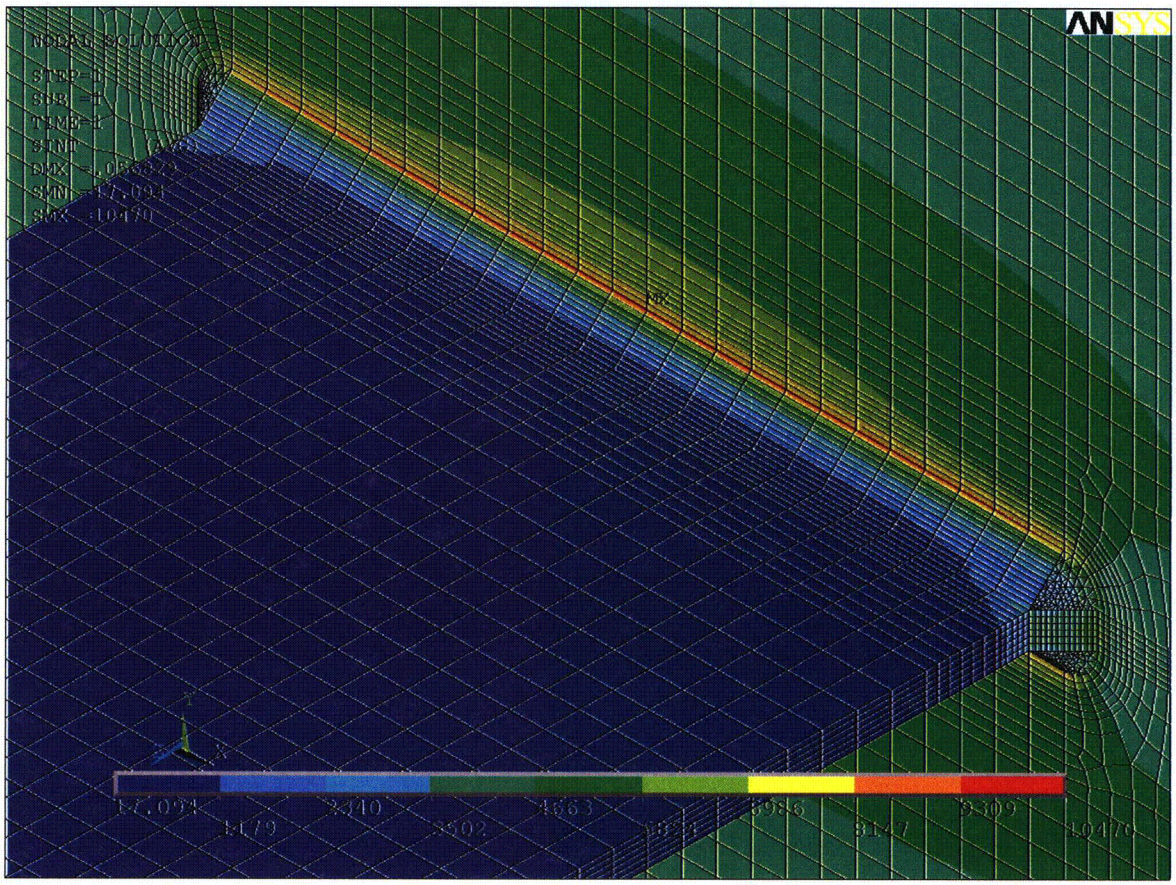

Figure 5-16
Full Solid Model Analysis
Stress Plot for Load Case #2
(Full Solid Model Baseline Analysis)

SRF Table

Table 5-6
Full Solid Model Baseline Analysis SRF
for Static Load Case #2

Path #	Solid (psi)	Shell (psi)	SRF
1	3,760	6,579	0.57
2	3,789		0.58
3	5,733		0.87
4	3,760		0.57
5	3,789		0.58
6	5,733		0.87
7	2,939		0.45
8	5,872		0.89
9	4,731		0.72
10	4,731		0.72
11	5,872		0.89
12	5,042		0.77
13	4,358		0.66
14	3,667		0.56
15	3,720		0.57
16	4,954		0.75
		Maximum =	**0.89**

5.2.3 Substructure Analysis Using Shell Submodel #1

With reference to Figure 3-3, the displacements along Edges A and C computed in the full shell finite element analysis (Section 5.2.1) are applied onto this solid submodel.

Stress Plot

The maximum stress intensity is 6,579 psi, and the stress plot is provided in the following Figure 5-17.

The maximum stress intensity is the same as the full shell baseline analysis maximum stress intensity, and the stress contours are very similar (see Figure 5-15). This confirms that the shell substructure analysis produces the same stress results as the full shell baseline analysis.

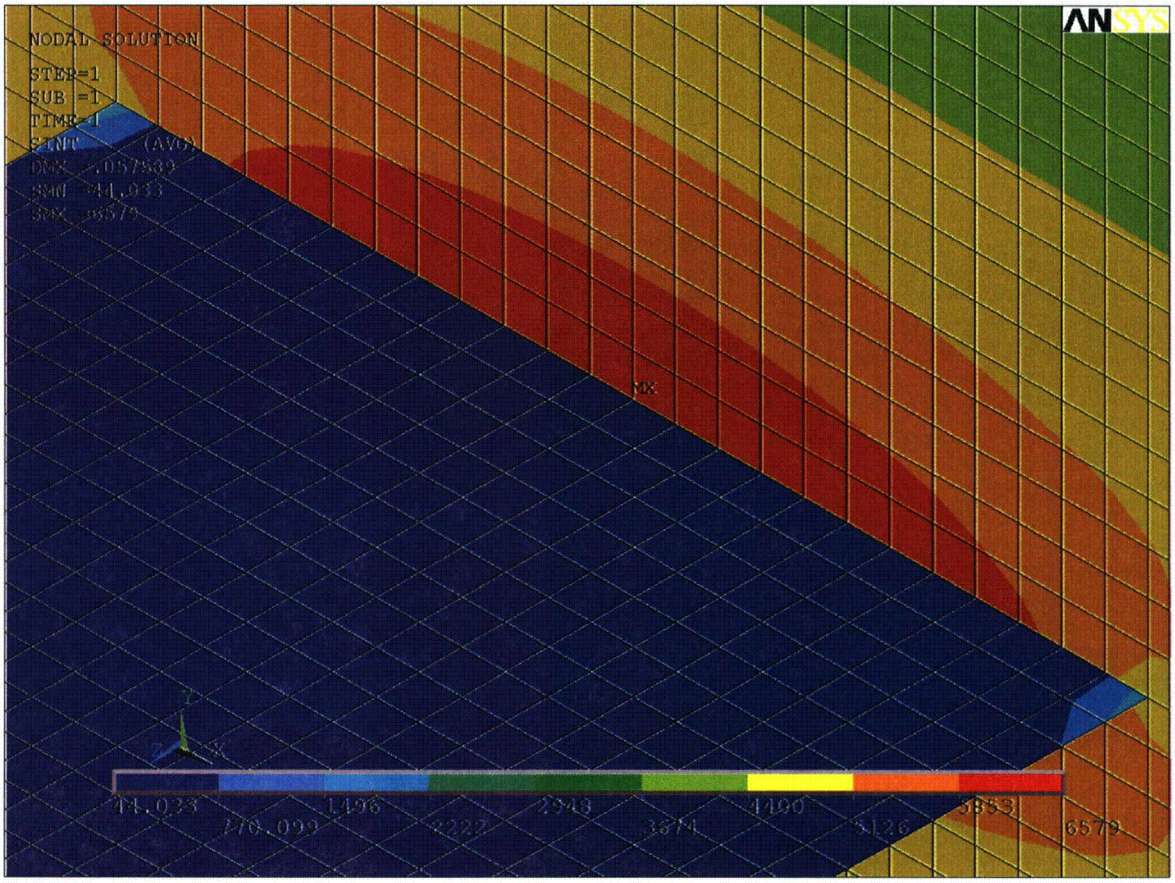

Figure 5-17
Substructure Analysis using Shell Submodel #1
Stress Plot for Load Case #2

5.2.4 *Substructure Analysis Using Shell Submodel #2*

With reference to Figure 3-5, the displacements along Edges A and C computed in the full shell finite element analysis (Section 5.2.1) are applied onto this solid submodel.

Stress Plot

The maximum stress intensity is 6,579 psi, and the stress plot is provided in the following Figure 5-18.

The maximum stress intensity is the same as the full shell baseline analysis maximum stress intensity, and the stress contours are very similar (see Figure 5-15). This confirms that the shell substructure analysis produces the same stress results as the full shell baseline analysis.

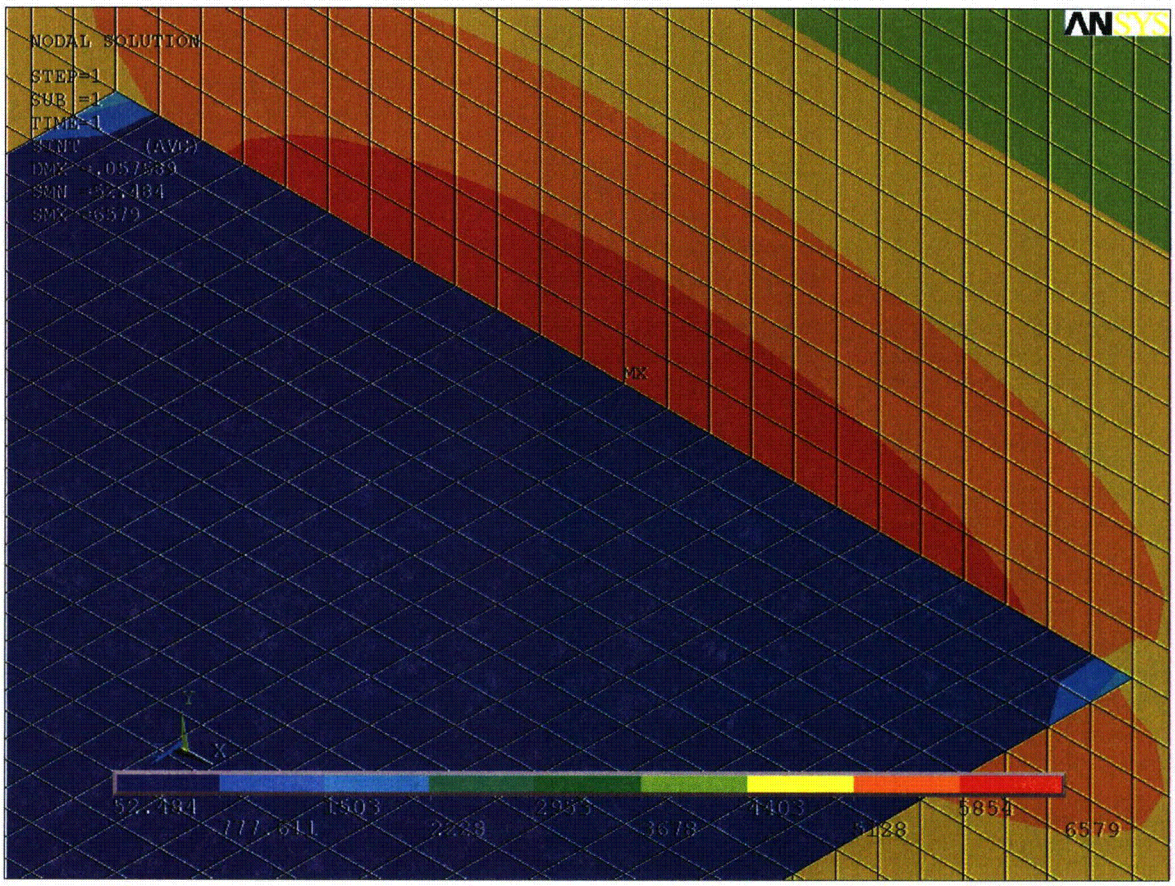

Figure 5-18
Substructure Analysis using Shell Submodel #2
Stress Plot for Load Case #2

5.2.5 *Substructure Analysis Using Solid Submodel #1*

With reference to Figure 3-3, the displacements along Edges A and C computed in the full shell finite element analysis (Section 5.2.1) are applied onto this solid submodel.

Stress Plot

The maximum non-linearized stress intensity is 10,789 psi, and the stress plot is provided in the following Figure 5-19.

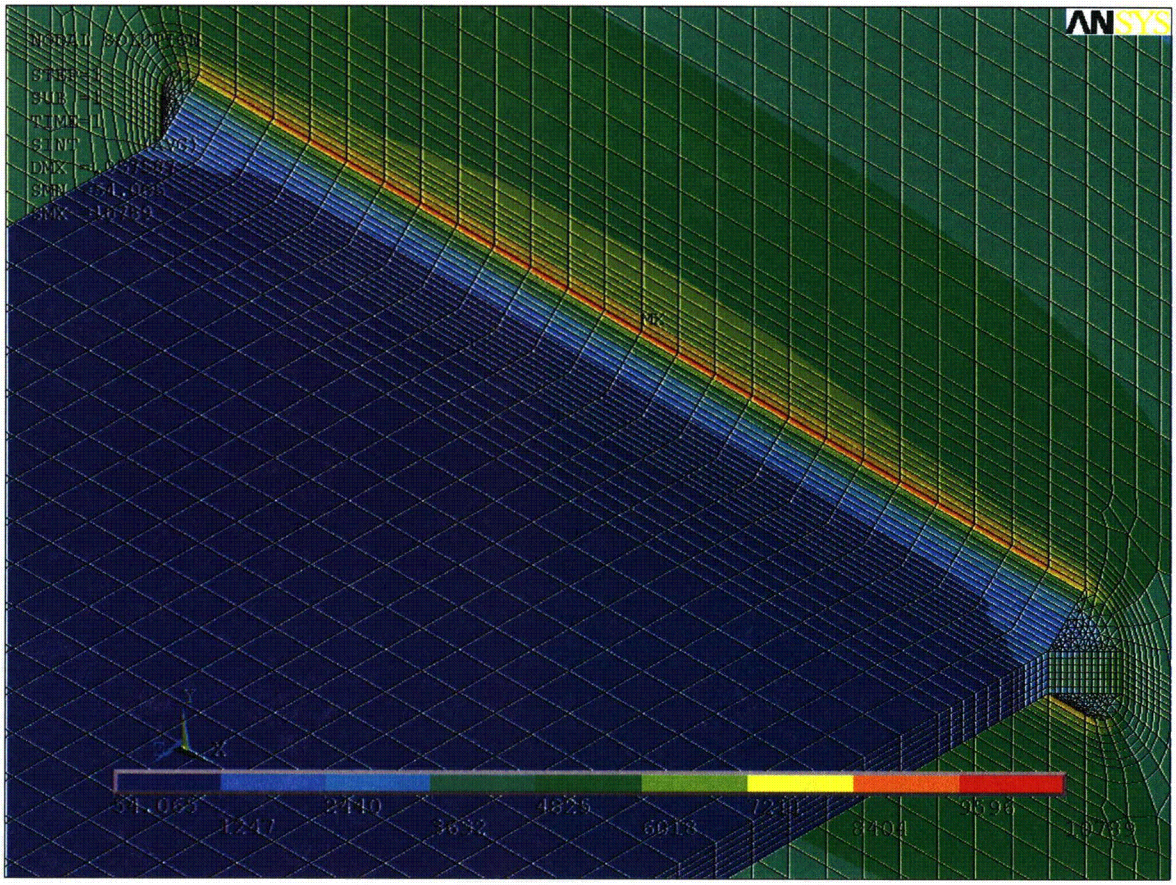

Figure 5-19
Substructure Analysis using Solid Submodel #1
Stress Plot for Load Case #2

SRF Table

Table 5-7
Substructure Analysis (Submodel #1) SRF
for Static Load Case #2

Path #	Solid (psi)	Shell (psi)	SRF
1	3,874	6,579	0.59
2	3,904		0.59
3	5,909		0.90
4	3,874		0.59
5	3,904		0.59
6	5,909		0.90
7	2,965		0.45
8	6,036		0.92
9	4,861		0.74
10	4,861		0.74
11	6,036		0.92
12	5,207		0.79
13	4,456		0.68
14	3,768		0.57
15	3,825		0.58
16	5,109		0.78
		Maximum =	**0.92**

5.2.6 *Substructure Analysis Using Solid Submodel #2*

With reference to Figure 3-3, the displacements along Edges A and C computed in the full shell finite element analysis (Section 5.2.1) are applied onto this solid submodel.

Stress Plot

The maximum non-linearized stress intensity is 10,673 psi, and the stress plot is provided in the following Figure 5-20.

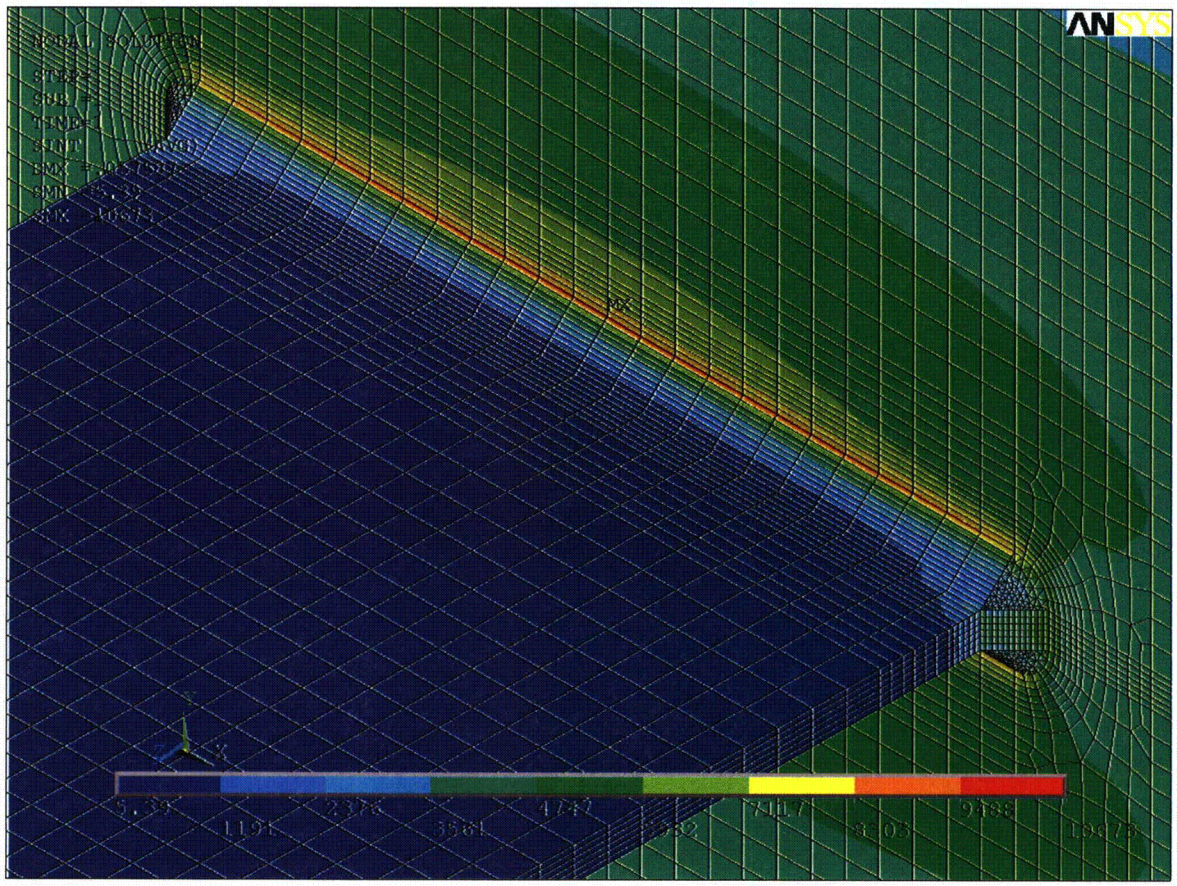

Figure 5-20
Substructure Analysis using Solid Submodel #2
Stress Plot for Load Case #2

SRF Table

Table 5-8
Substructure Analysis (Submodel #2) SRF
for Static Load Case #2

Path #	Solid (psi)	Shell (psi)	SRF
1	3,833	6,579	0.58
2	3,863		0.59
3	5,845		0.89
4	3,833		0.58
5	3,863		0.59
6	5,845		0.89
7	2,981		0.45
8	5,981		0.91
9	4,818		0.73
10	4,818		0.73
11	5,981		0.91
12	5,142		0.78
13	4,434		0.67
14	3,736		0.57
15	3,791		0.58
16	5,051		0.77
		Maximum =	**0.91**

5.2.7 *Submodel Analysis Using Submodel #1*

Matching Stress Profile

The stress profile matching is performed along the weld line connecting the vertical plate to the horizontal plate. The matching is accomplished by applying a horizontal (Z) load along the Edge C (see Figure 3-3) of the submodel. The nodes at the top and bottom edges are restrained in X and Z translations. The applied loads and the comparison of the stress profiles are shown in the following Figure 5-21 and Figure 5-22, respectively.

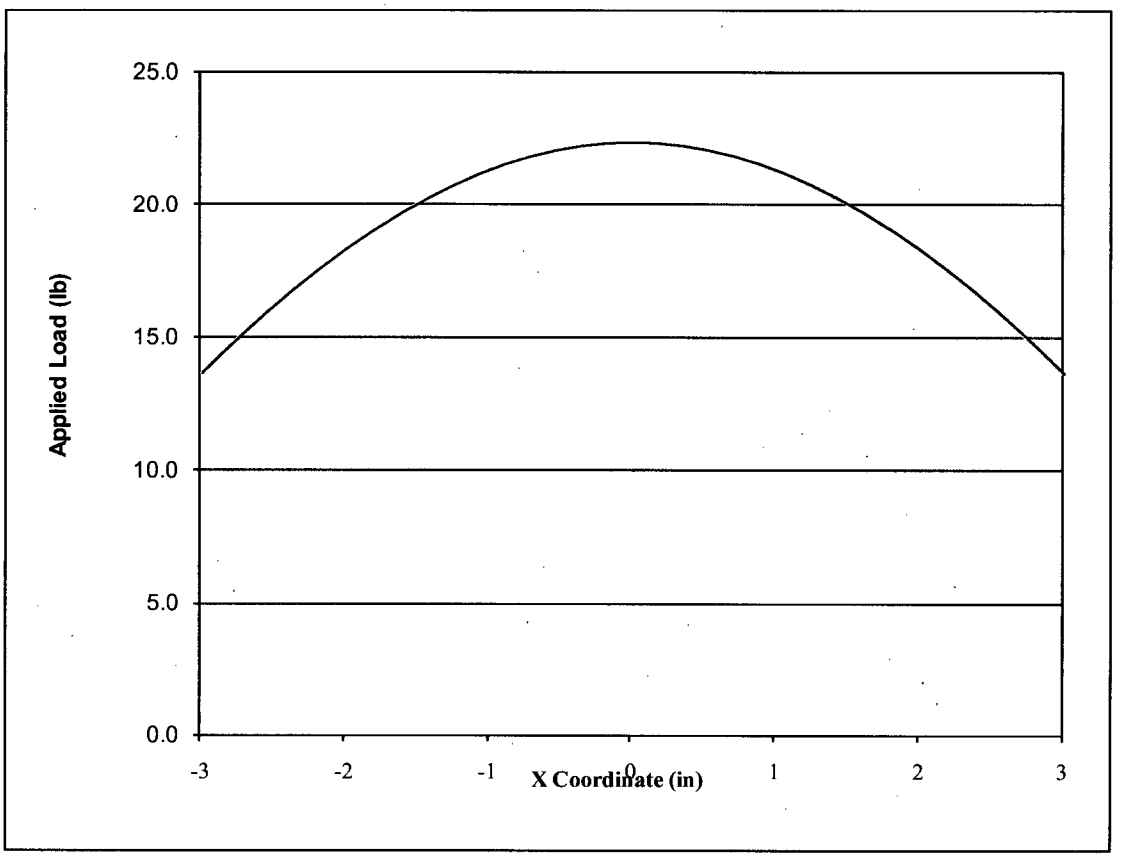

Figure 5-21
Submodel Analysis using Submodel #1
Applied Loads for Load Case #2

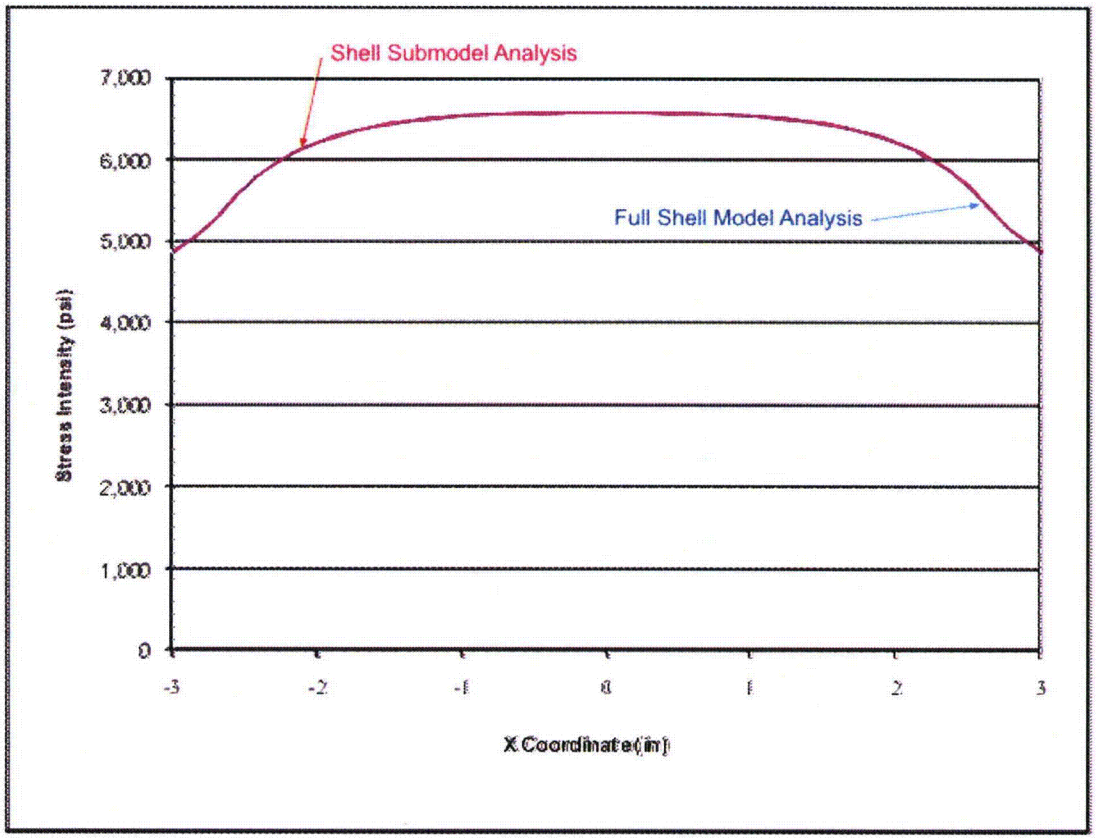

Figure 5-22
Submodel Analysis using Submodel #1
Stress Profile Comparison for Load Case #2

Stress Plot

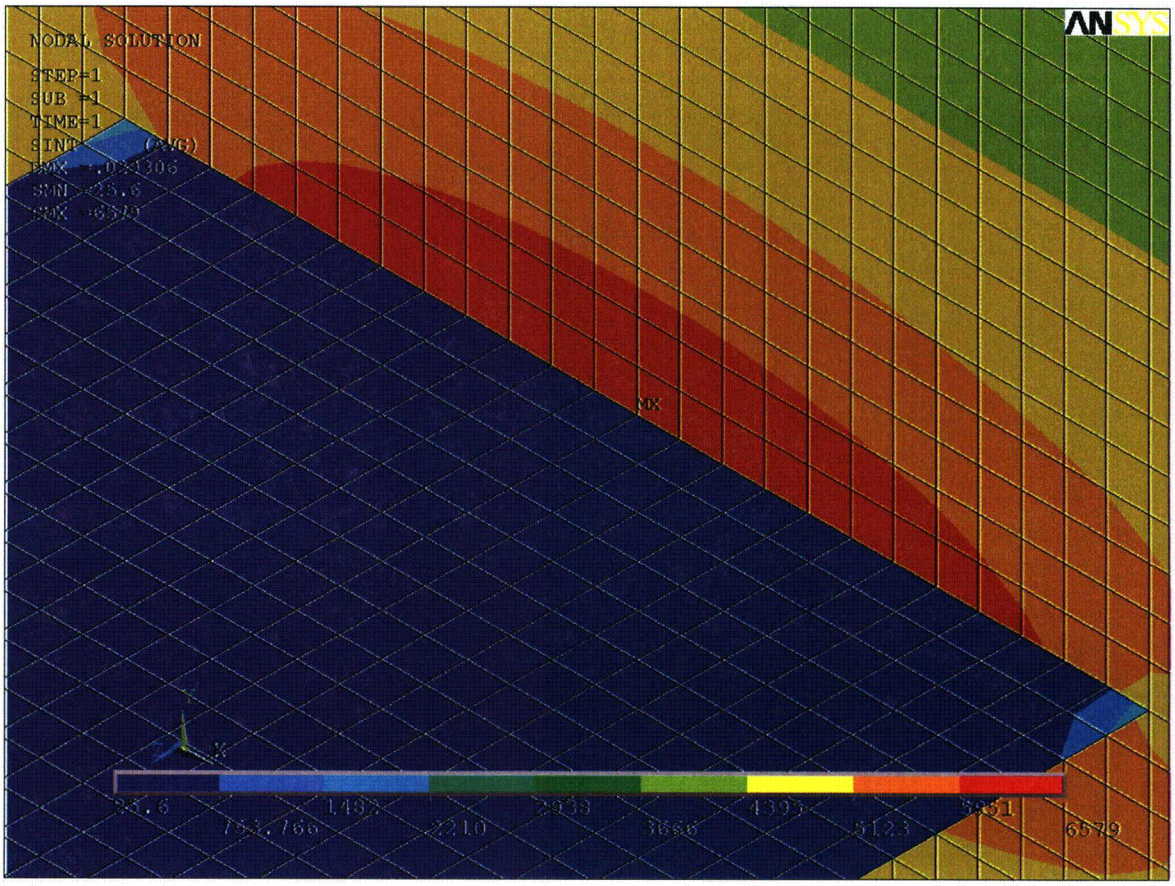

Figure 5-23
Submodel Analysis using Submodel #1
Shell Model Stress Plot for Load Case #2

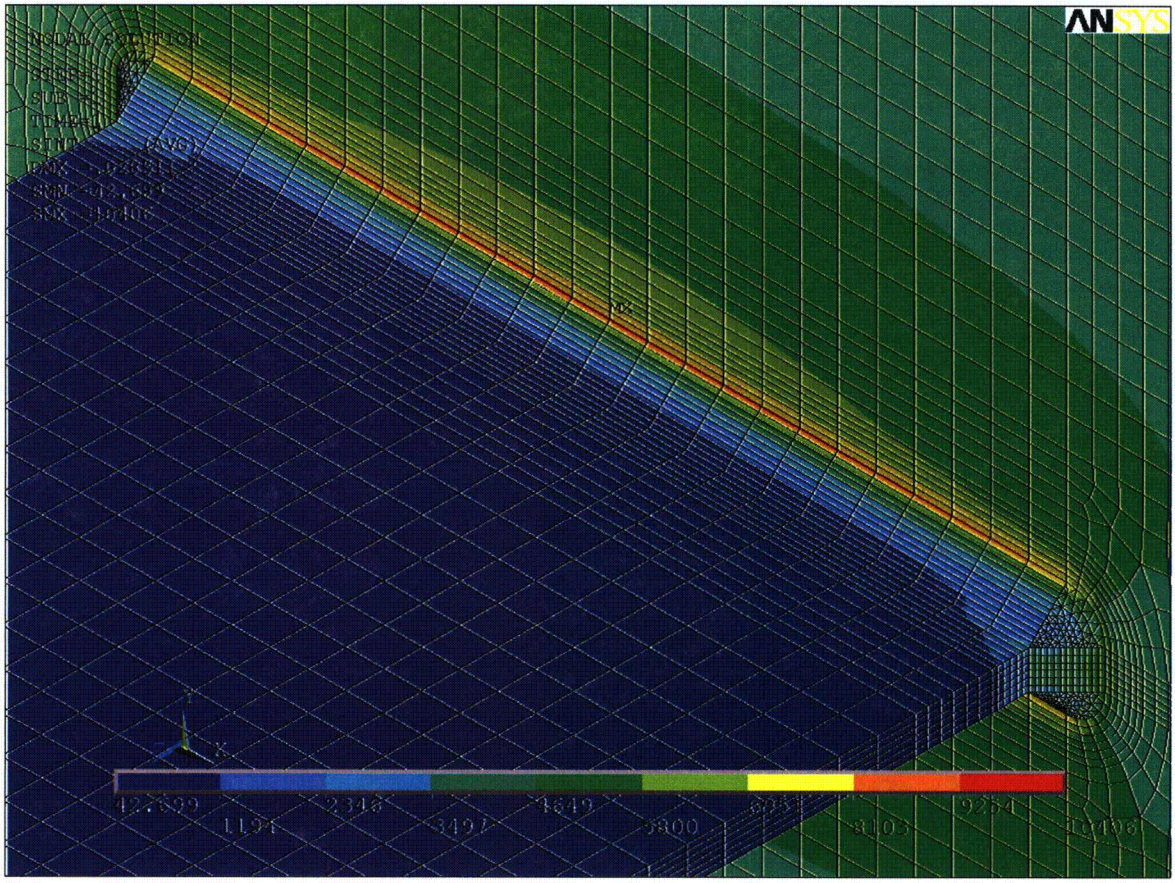

Figure 5-24
Submodel Analysis using Submodel #1
Solid Model Stress Plot for Load Case #2

SRF Table

Table 5-9
Submodel Analysis (Submodel #1) SRF
for Static Load Case #2

Path #	Solid (psi)	Shell (psi)	SRF
1	3,737	6,579	0.57
2	3,765		0.57
3	5,697		0.87
4	3,737		0.57
5	3,765		0.57
6	5,697		0.87
7	2,911		0.44
8	5,849		0.89
9	4,715		0.72
10	4,715		0.72
11	5,849		0.89
12	5,014		0.76
13	4,326		0.66
14	3,644		0.55
15	3,697		0.56
16	4,924		0.75
		Maximum =	**0.89**

5.2.8 Submodel Analysis Using Submodel #2

Matching Stress Profile

The stress profile matching is performed along the weld line connecting the vertical plate to the horizontal plate. The matching is accomplished by applying a horizontal (Z) load along the Edge C (see Figure 3-5) of the submodel. The nodes at the top and bottom edges (i.e., Edge A) are fixed. The applied loads and the comparison of the stress profiles are shown in the following Figure 5-25 and Figure 5-26, respectively.

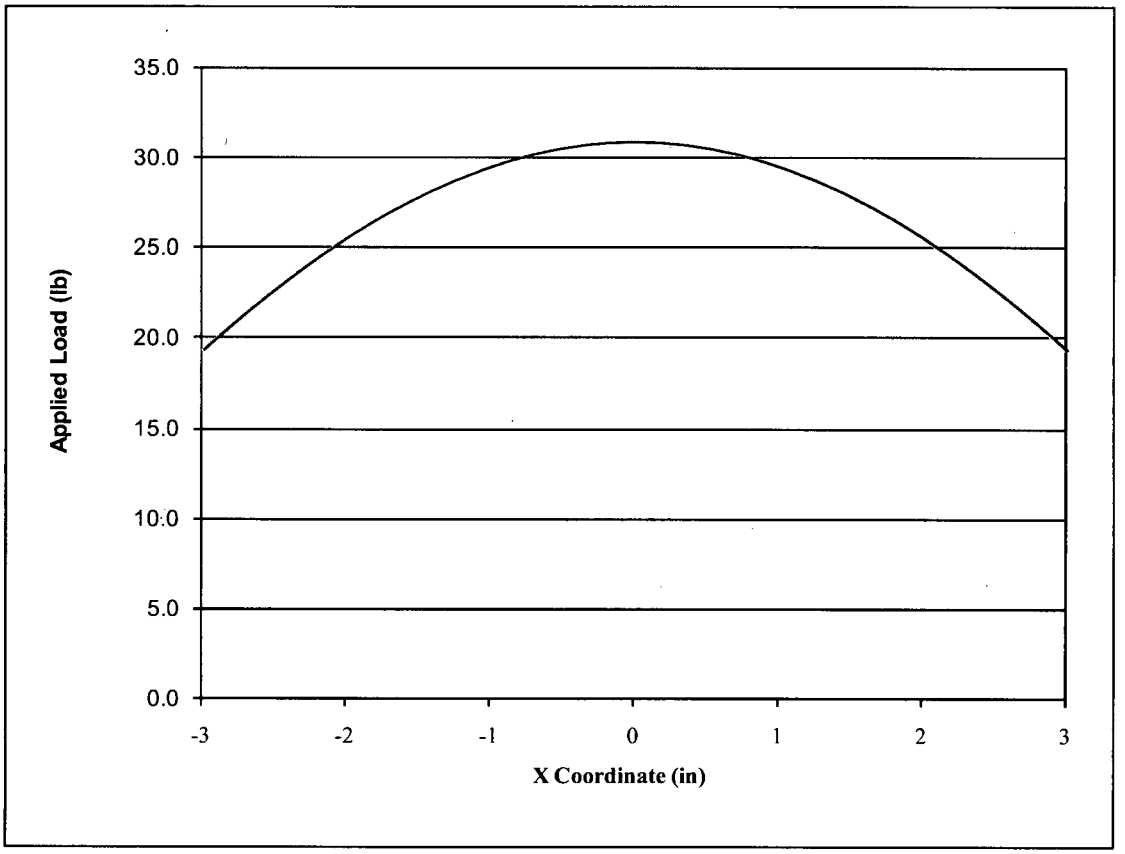

Figure 5-25
Submodel Analysis using Submodel #2
Applied Loads for Load Case #2

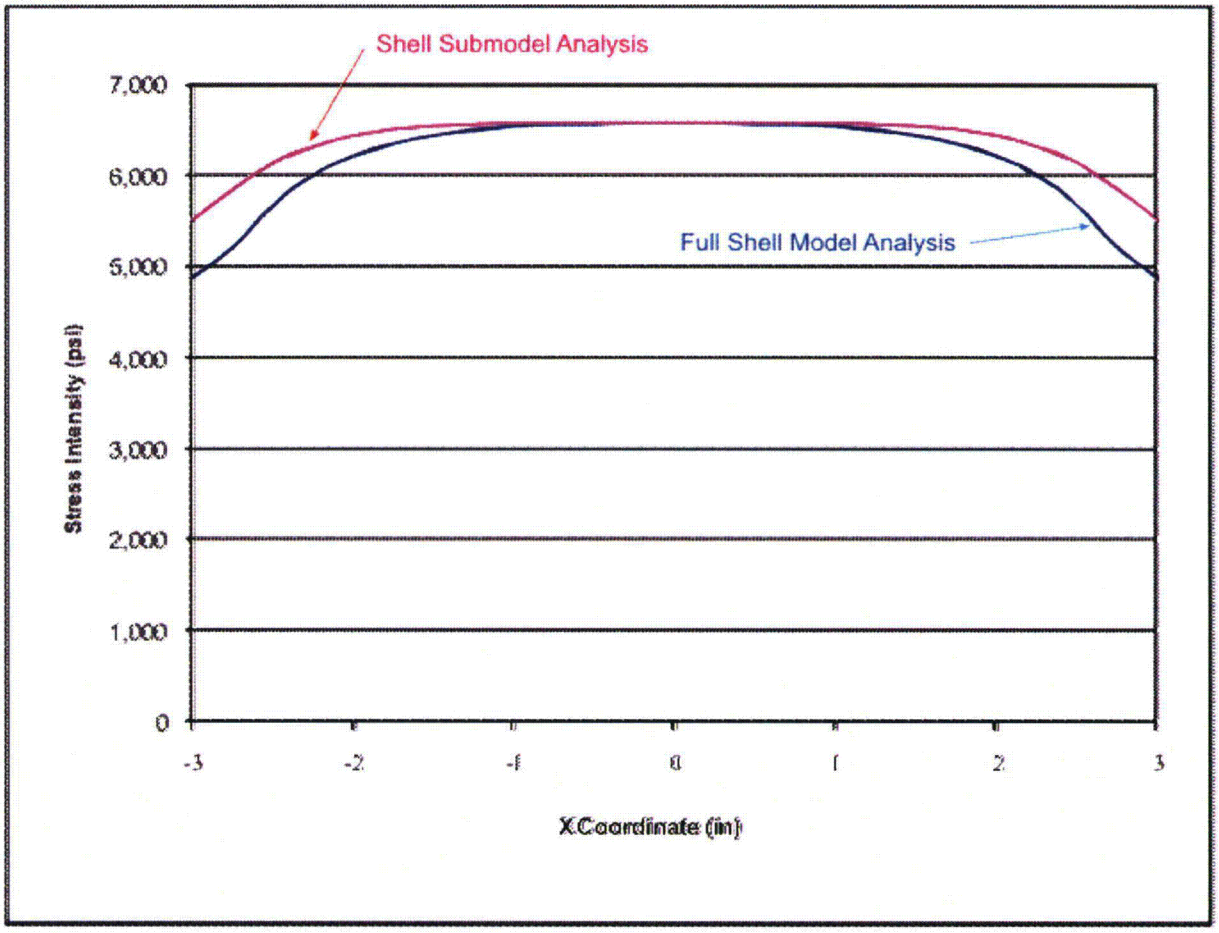

Figure 5-26
Submodel Analysis using Submodel #2
Stress Profile Comparison for Load Case #2

Stress Plot

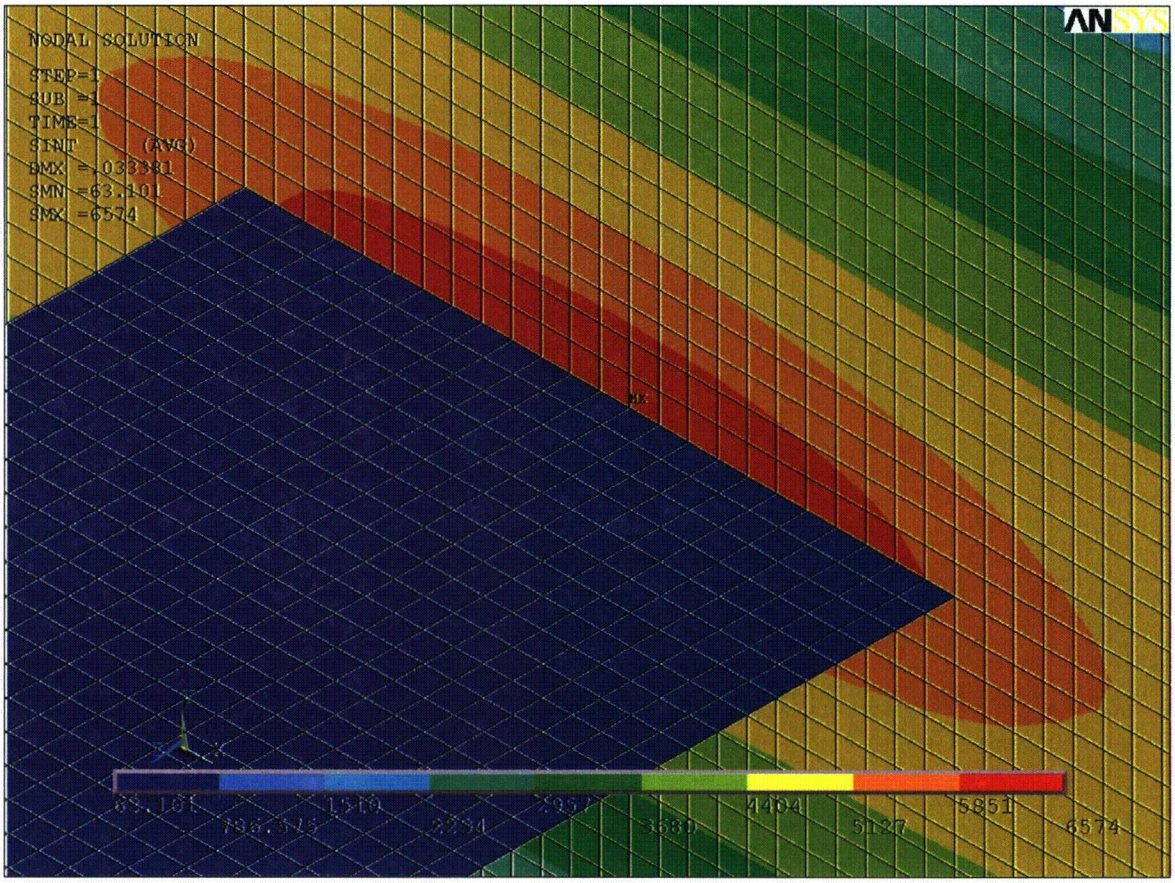

Figure 5-27
Submodel Analysis using Submodel #2
Shell Model Stress Plot for Load Case #2

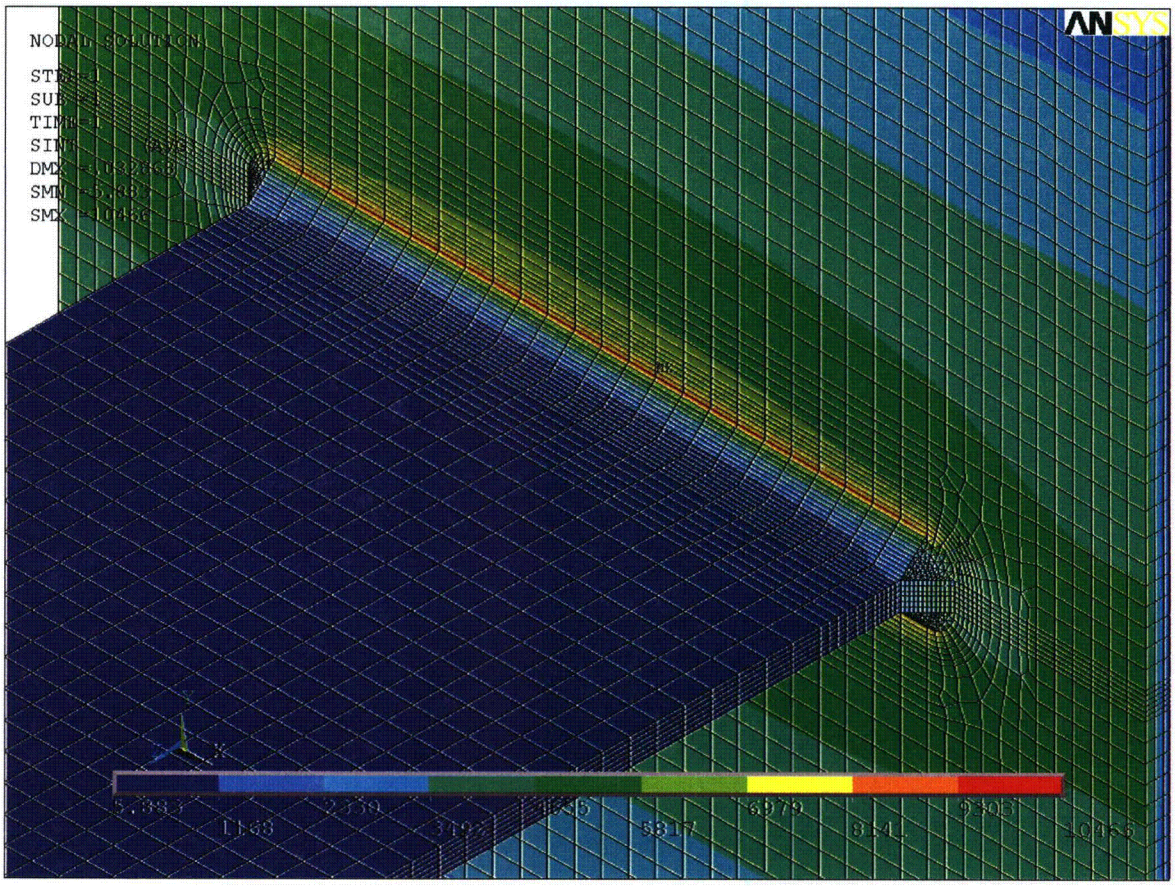

Figure 5-28
Submodel Analysis using Submodel #2
Solid Model Stress Plot for Load Case #2

SRF Table

Table 5-10
Submodel Analysis (Submodel #2) SRF
for Static Load Case #2

Path #	Solid (psi)	Shell (psi)	SRF
1	3,755	6,579	0.57
2	3,784		0.58
3	5,736		0.87
4	3,755		0.57
5	3,784		0.58
6	5,736		0.87
7	1,763		0.27
8	5,851		0.89
9	4,719		0.72
10	4,719		0.72
11	5,851		0.89
12	5,482		0.83
13	3,706		0.56
14	3,504		0.53
15	3,608		0.55
16	5,143		0.78
		Maximum =	**0.89**

6.0 DYNAMIC ANALYSIS RESULTS

6.1 Structural Modal Frequencies

Modal analysis of the structure is performed to determine the fundamental frequencies of the system. The following Table 6-1 and Table 6-2 summarize the major frequencies in the vertical (Y direction) and the horizontal (Z direction) directions, which correspond to the directions of the Load Cases #1 and #2, respectively.

Table 6-1
Structural Vertical (Y direction) Modal Frequencies

Mode # (1)	Frequency (Hz)	Period	Participation Factor	Effective Mass	Cumulative Mass Fraction
1	2.64	0.379	1.779	3.164	0.759
4	8.69	0.115	0.050	0.002	0.760
7	16.77	0.060	-1.000	1.000	1.000
10	28.24	0.035	-0.027	0.001	1.000

Note: (1) Insignificant modes have been excluded from the table.

Table 6-2
Structural Horizontal (Z direction) Modal Frequencies

Mode # (1)	Frequency (Hz)	Period	Participation Factor	Effective Mass	Cumulative Mass Fraction
2	2.82	0.354	6.604	43.614	0.848
6	15.80	0.063	2.798	7.827	1.000

Note: (1) Insignificant modes have been excluded from the table.

6.2 Structural Damping Values

For the purpose of this study, assume that the structural critical damping value is 4%.

The damping used in the dynamic transient analysis is the Alpha and Beta damping, also known as the Rayleigh damping and is defined by Rayleigh damping constants α and β. The damping matrix, C, is calculated by using these constants to multiply the mass matrix, M, and the stiffness matrix, K:

$$C = \alpha M + \beta K$$

The values of α and β are calculated from modal damping ratio, ξ_i, which is the ratio of actual damping to critical damping for a particular mode of vibration, i. If ω_i is the natural frequency of the mode i, α and β satisfy the relation:

$$\xi_i = \alpha/2\omega_i + \beta\omega_i/2$$ (Reference 4, Structural Analysis Guide, Section 5.9.3)

Therefore, given ξ and a frequency range between ω_i and ω_j, two simultaneous equations can be solved for α and β.

In this analysis, the frequency range is 2.0 Hz and 28.2 Hz, which cover the frequency range from mode #1 to mode #10(see Table 6-1 and Table 6-2). The calculated values are:

α = 0.939

β = 4.216E-4

The calculations of α and β are documented in the spreadsheet *Damping.xls* (described in Appendix A).

6.3 Time History Analysis Integration Time Step

The accuracy of the transient dynamic solution depends on the integration time step. For the Newmark time integration used herein, it is recommended that using approximately twenty points per cycle of the highest frequency of interest results in a reasonably accurate solution. That is, if f is the frequency (in Hz), the integration time step (ITS) is given by:

$$ITS = 1/(20f)$$ (Reference 4, Structural Analysis Guide, Section 5.9.1)

The modal analysis shows that the highest major mode is 28.2 Hz, in the vertical direction (see Table 6-1). The applied harmonic load frequency is set at 25 Hz (see Section 4.2). Therefore, conservatively use 50 Hz as the highest frequency of interest.

$$ITS = 1/(20*50)$$

$$= 0.001 \text{ seconds}$$

6.4 Dynamic Load Case #1

6.4.1 Full Shell Finite Element Analysis

Transient Displacement Plot

The maximum vertical displacement occurs at the edge node of the load application line. The following Figure 6-1 shows a plot of the nodal transient displacements.

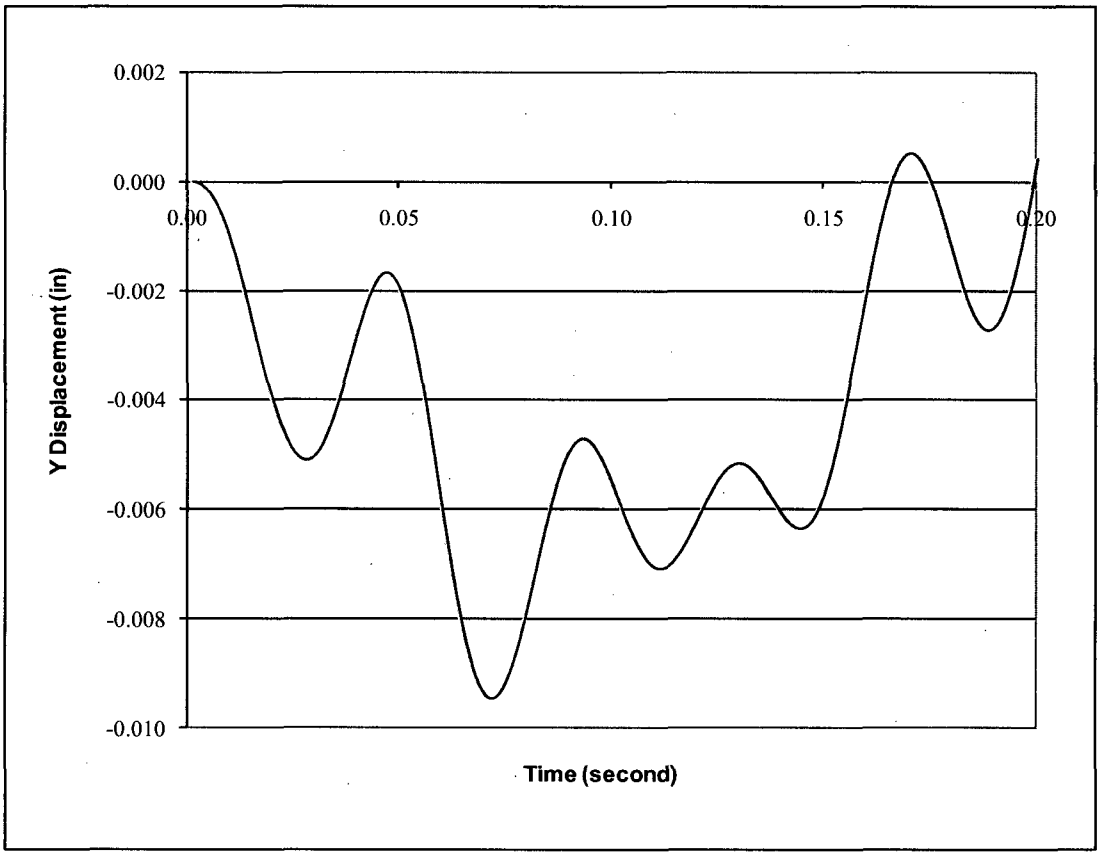

Figure 6-1
Full Shell Model Dynamic Analysis
Vertical Transient Displacement for Load Case #1

Transient Stress Intensity Plot

The maximum stress intensity occurs at one of the weld line nodes. The following Figure 6-2 shows a plot of the nodal transient stress intensities. The maximum stress intensity is 2,100 psi, which occurs at 0.048 seconds time step.

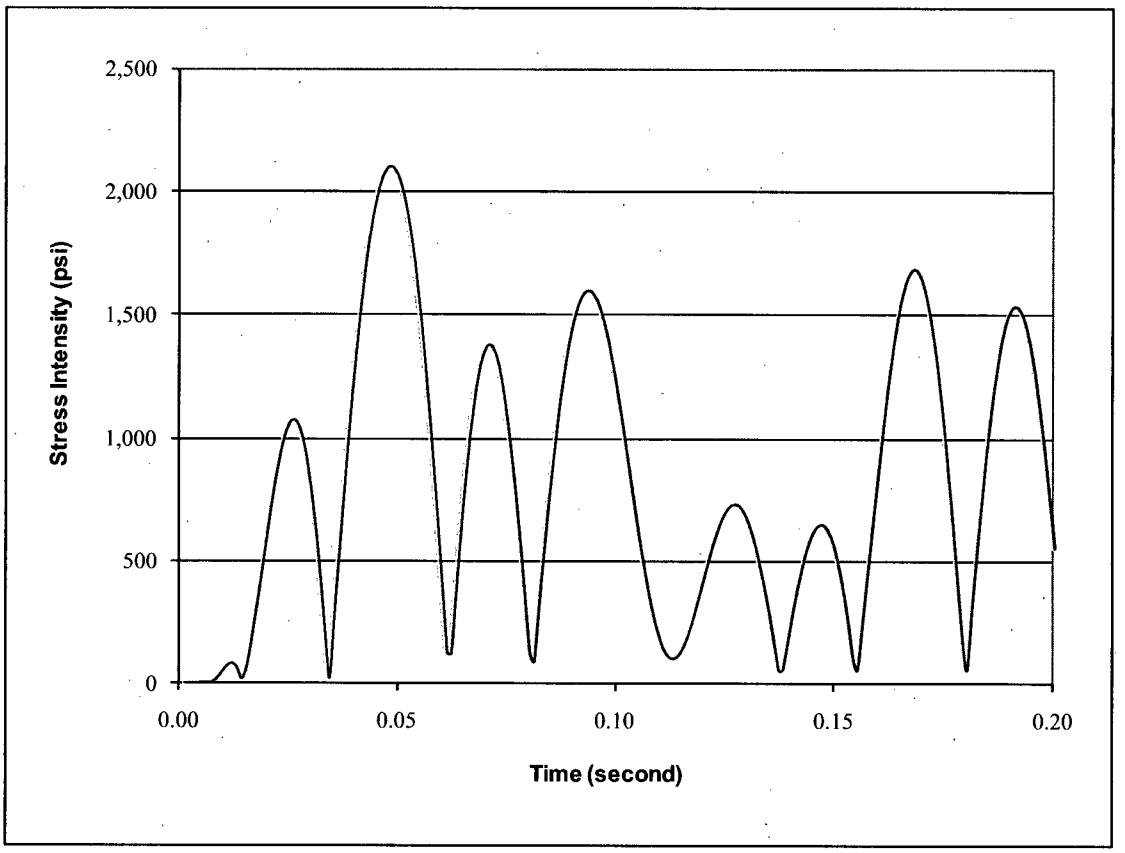

Figure 6-2
Full Shell Model Dynamic Analysis
Nodal Stress Intensity for Load Case #1

Vertical Displacement Plot

The following Figure 6-3 shows the vertical displacements at 0.048 seconds time step, when the maximum stress intensity occurs. The nodal displacements (for 6 degrees of freedom) at the submodel boundaries at this time step are used for subsequent substructure analyses.

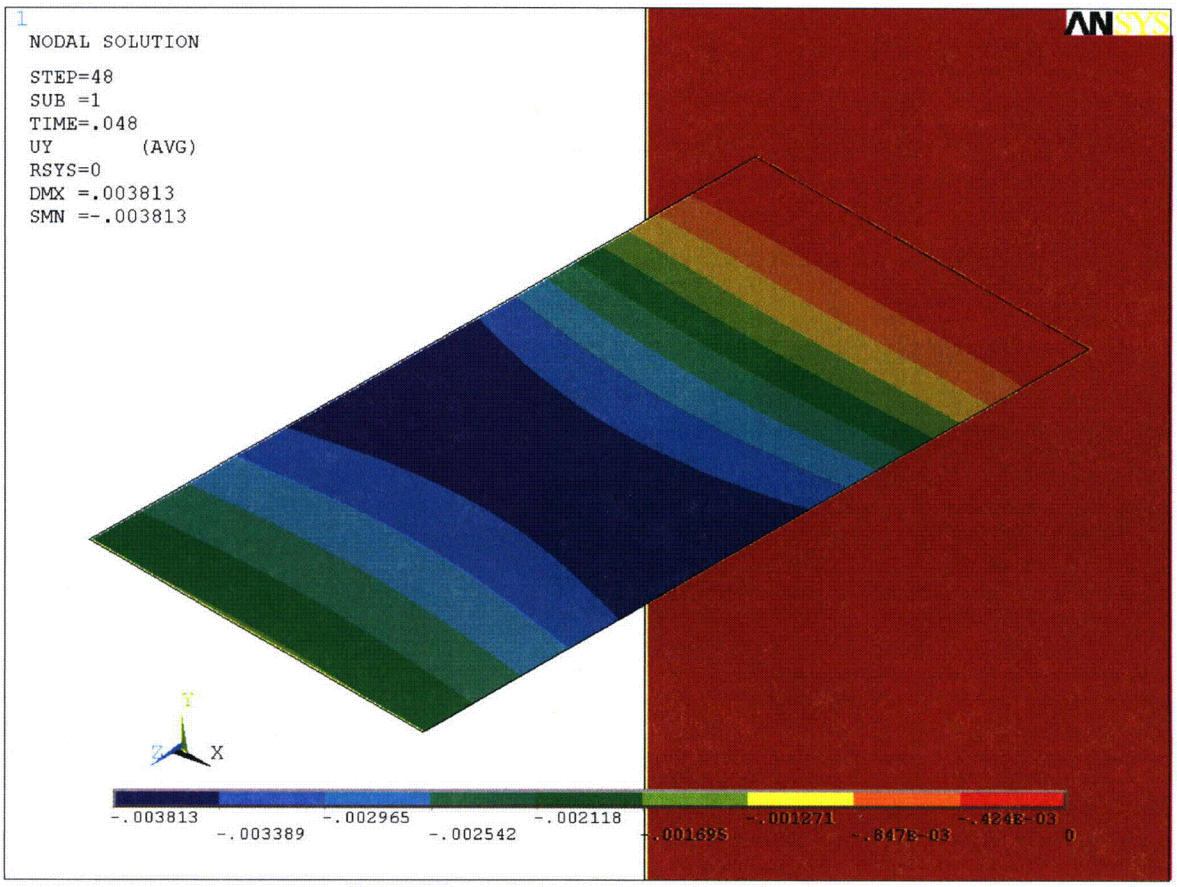

Figure 6-3
Full Shell Model Dynamic Analysis
Vertical Displacement Plot for Load Case #1
(Full Shell Model Baseline Analysis)

Maximum Stress Plot

The maximum stress intensity is 2,100 psi, which occurs at 0.048 seconds time step. The stress plot at that time step is provided in the following Figure 6-4. This analysis is the full shell model baseline analysis, and the maximum stress intensity of 2,100 psi is used to determine the SRF in the other analysis.

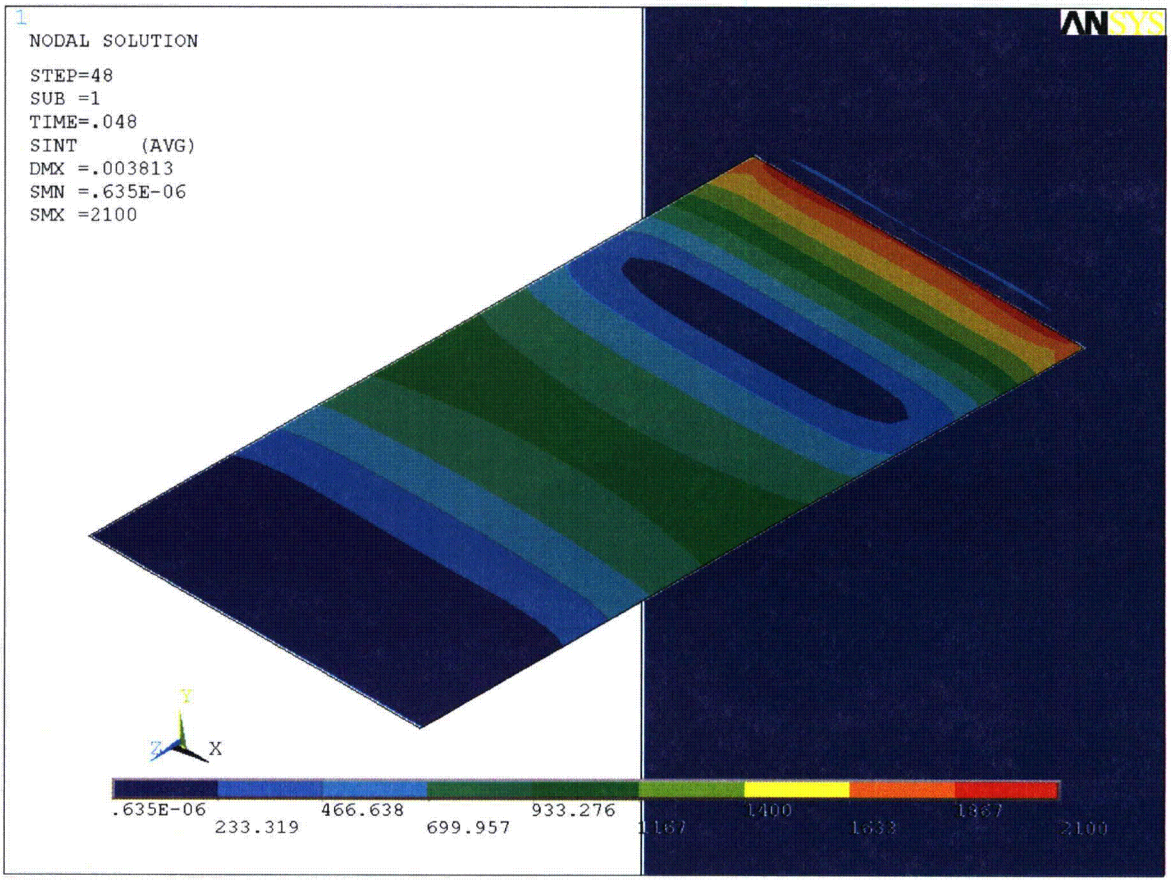

Figure 6-4
Full Shell Model Dynamic Analysis
Maximum Stress Plot for Load Case #1
(Full Shell Model Baseline Analysis)

6.4.2 *Substructure Analysis Using Shell Submodel #2*

With reference to Figure 3-5, the displacements along Edges A and C computed in the full shell finite element analysis (Section 6.4.1) are applied onto this shell submodel.

Vertical Displacement Plot

The maximum vertical displacement plot is provided in the following Figure 6-5.

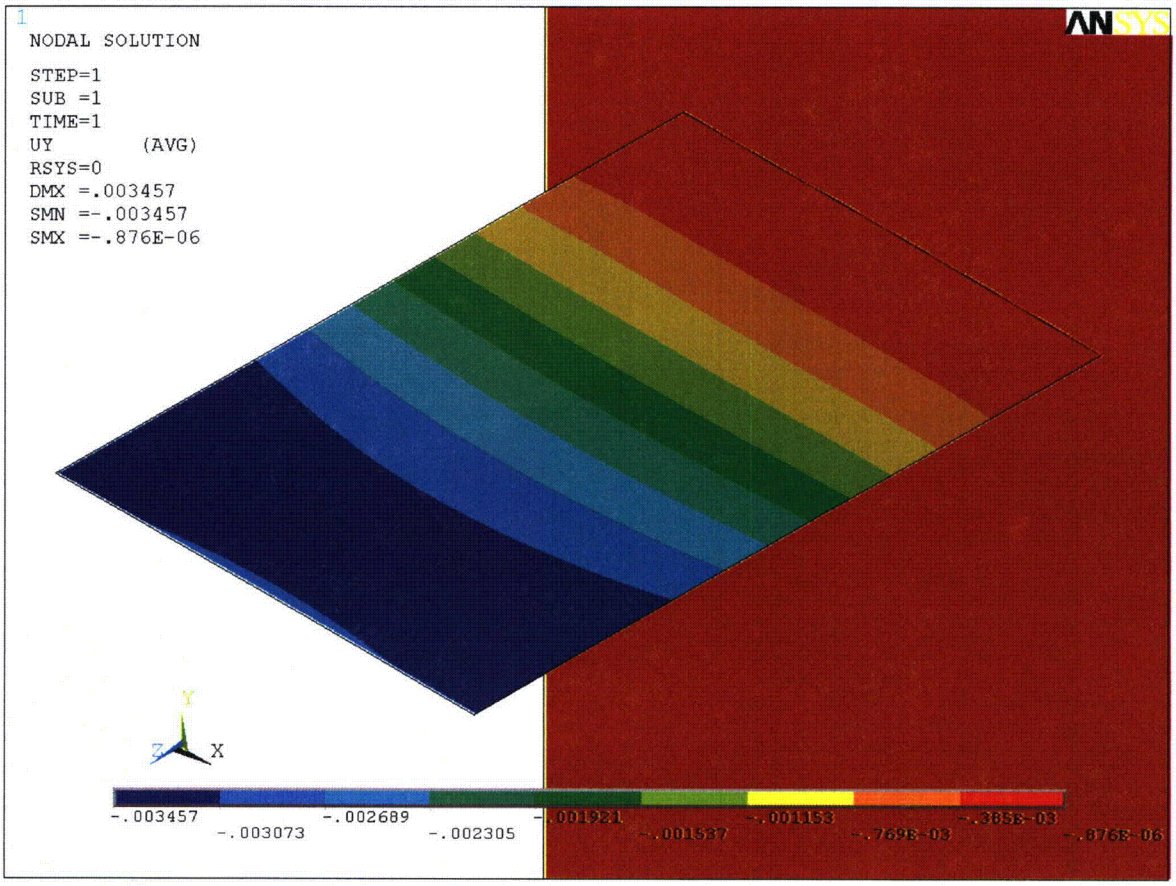

Figure 6-5
Substructure Analysis using Shell Submodel #2
Vertical Displacement Plot for Load Case #1

Stress Plot

The maximum stress intensity is 1,564 psi, and the stress plot is provided in the following Figure 6-6.

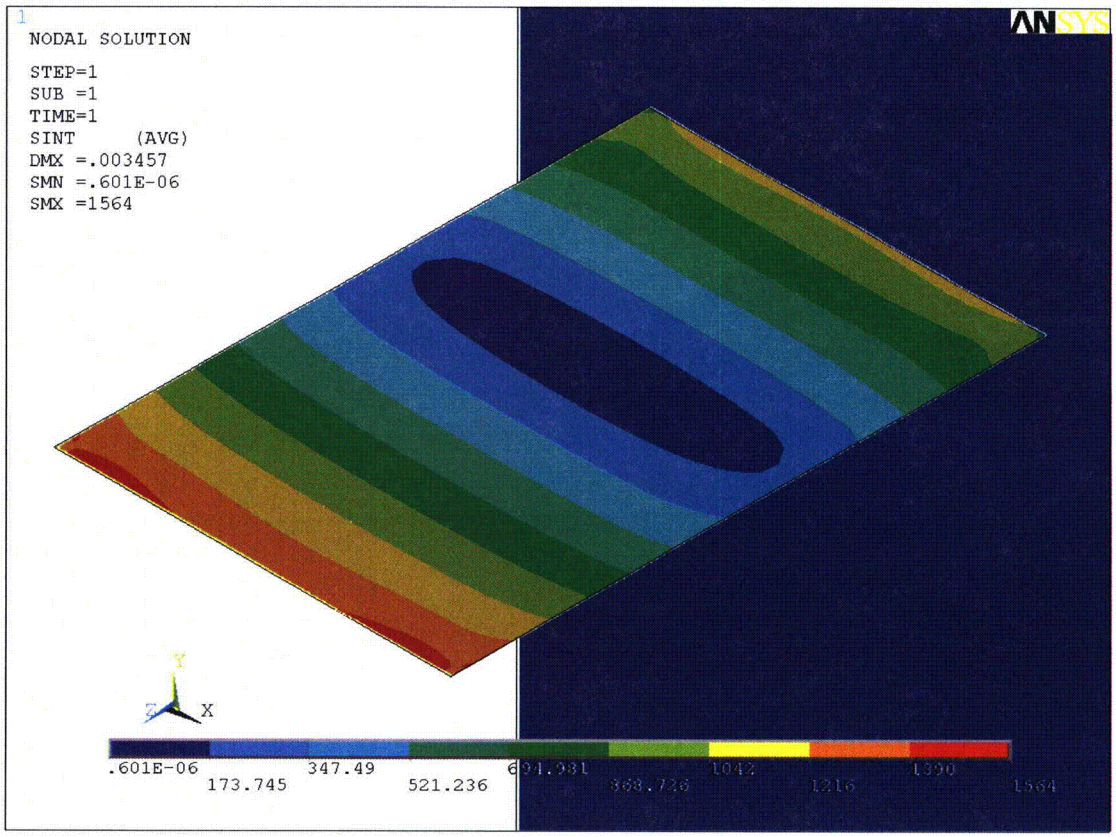

Figure 6-6
Substructure Analysis using Shell Submodel #2
Stress Plot for Load Case #1

Observation

The maximum stress intensity of 1,564 psi is significantly lower than the full shell baseline analysis maximum stress intensity of 2,100 psi. The stress pattern is also different. The maximum stress intensity for the substructure analysis is located along the edge, not at the weld line.

In this analysis, only the displacements at the boundaries are mapped from the full shell model to the submodel. The shell internal displacements, influenced by the dynamic inertia effects, are not captured in the substructure analysis. Without imposing the dynamic characteristic displacements within the submodel boundaries, the substructure analysis is not able to duplicate the stress pattern of the full shell model.

6.4.3 *Substructure Analysis Using Solid Submodel #2*

With reference to Figure 3-6, the displacements along Edges A and C computed in the full shell finite element analysis (Section 6.4.1) are applied onto this solid submodel.

Stress Plot

The maximum non-linearized stress intensity is 1,596 psi, and the stress plot is provided in the following Figure 6-7.

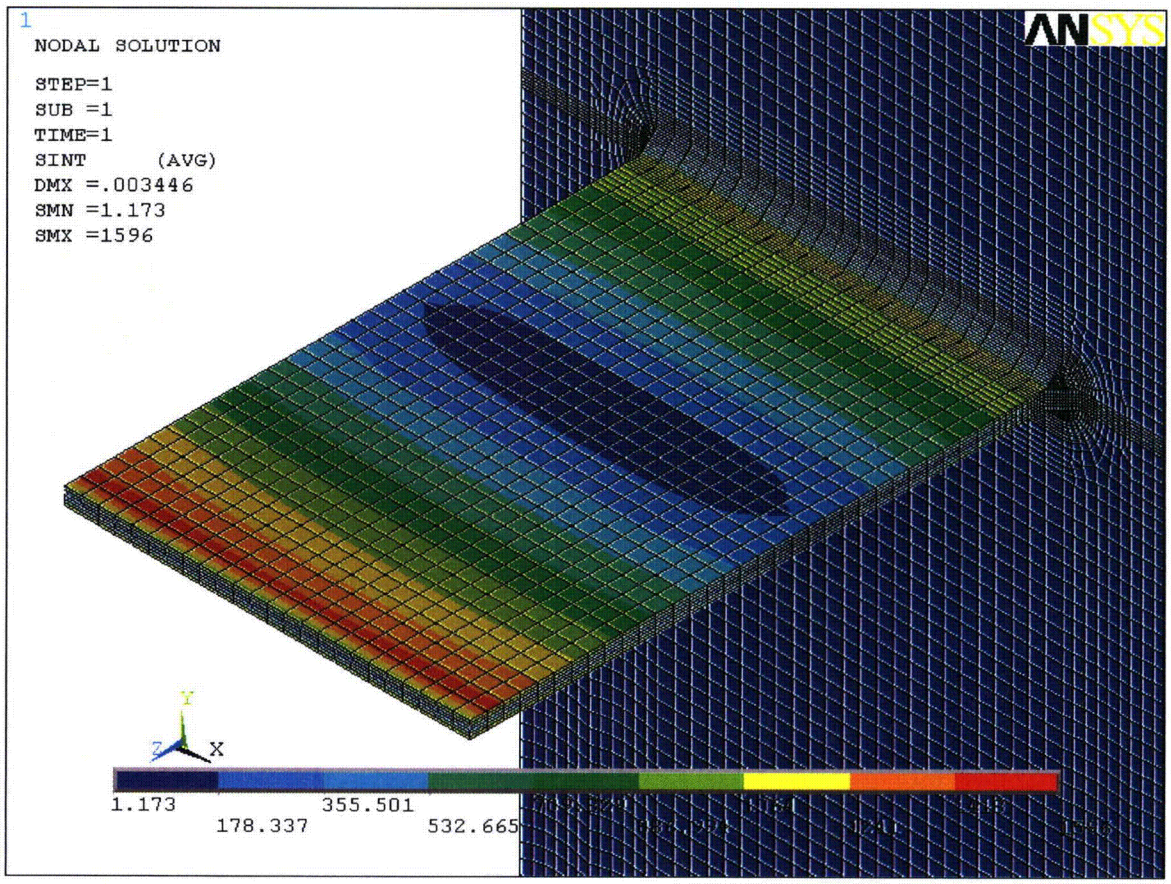

Figure 6-7
Substructure Analysis using Solid Submodel #2
Stress Plot for Load Case #1

SRF Table

Table 6-3
Substructure Dynamic Analysis (Submodel #2) SRF for Dynamic Load Case #1

Path #	Solid (psi)	Shell (psi)	SRF
1	711	2,100	0.34
2	297		0.14
3	186		0.09
4	711		0.34
5	297		0.14
6	186		0.09
7	780		0.37
8	133		0.06
9	173		0.08
10	173		0.08
11	133		0.06
12	124		0.06
13	144		0.07
14	567		0.27
15	107		0.05
16	93		0.04
		Maximum =	**0.37**

6.4.4 Submodel Analysis Using Submodel #2

Matching Stress Profile

The stress profile matching is perform along the weld line connecting the vertical plate to the horizontal plate. The matching is accomplished by imposing vertical displacements along the Edge C (see Figure 3-3) of the submodel. Fixed boundary condition is applied to the top and bottom edges. The applied displacements and the comparison of the stress profiles are shown in the following Figure 6-8 and Figure 6-9, respectively.

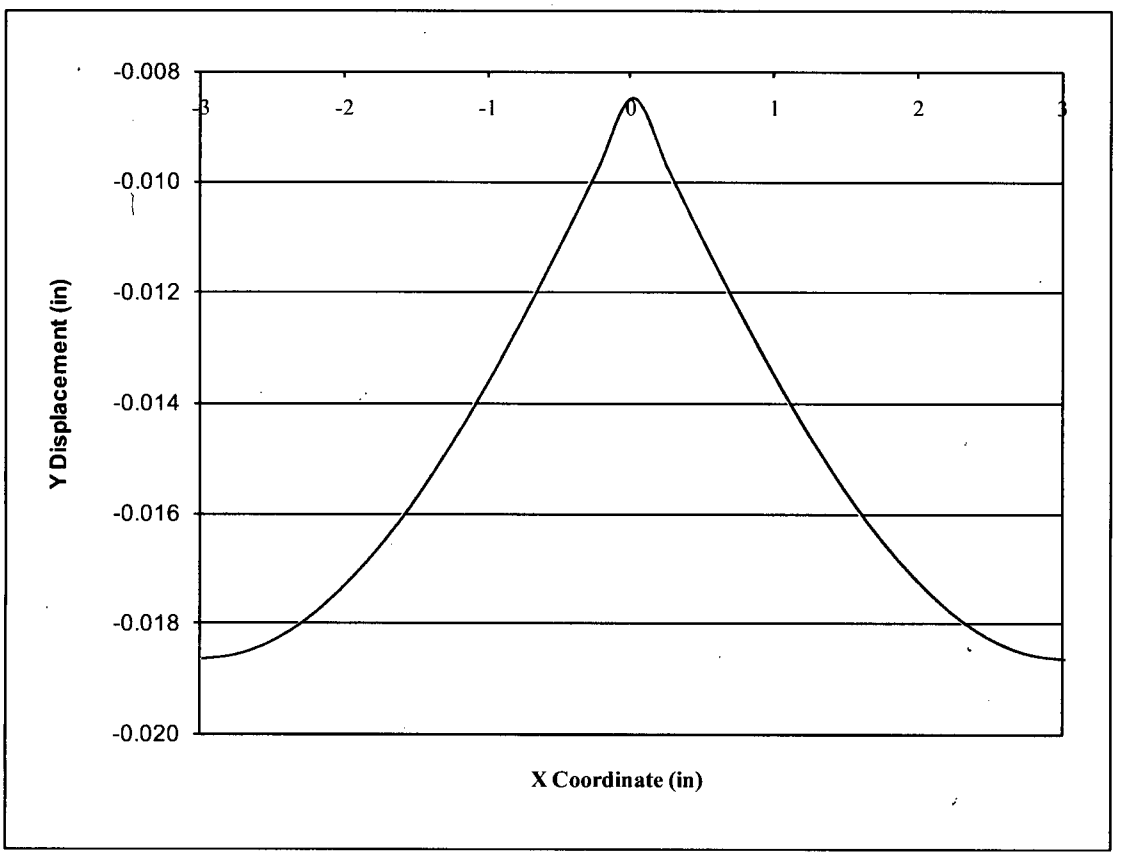

Figure 6-8
Submodel Analysis using Submodel #2
Applied Displacements for Load Case #1

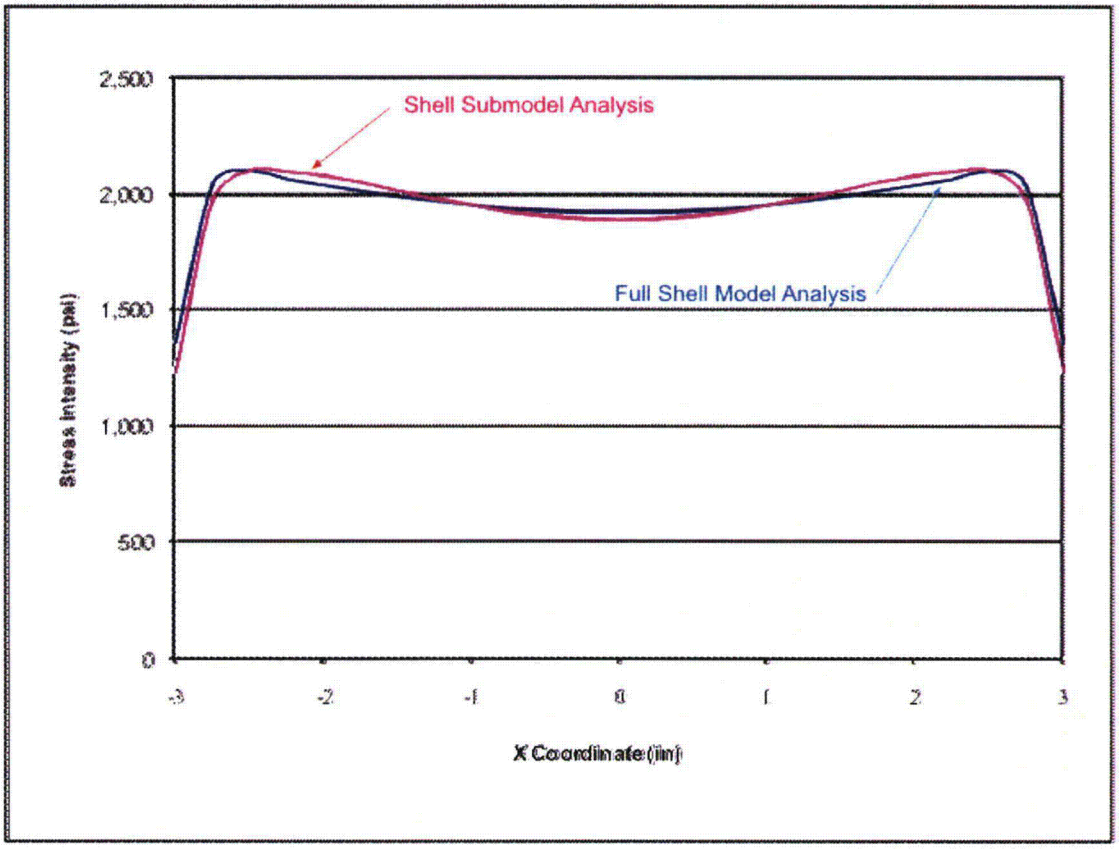

Figure 6-9
Submodel Analysis using Submodel #2
Stress Profile Comparison for Load Case #1

Stress Plot

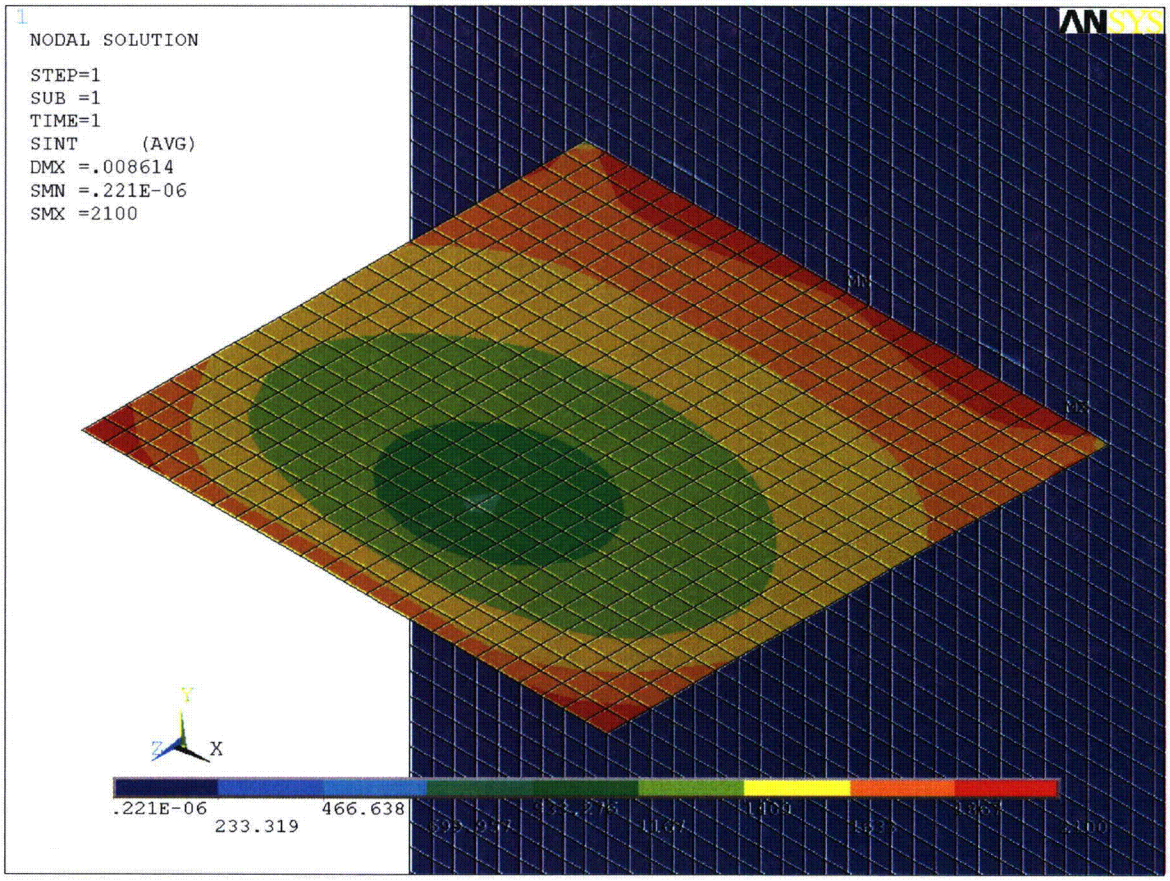

Figure 6-10
Submodel Analysis using Submodel #2
Shell Model Stress Plot for Load Case #1

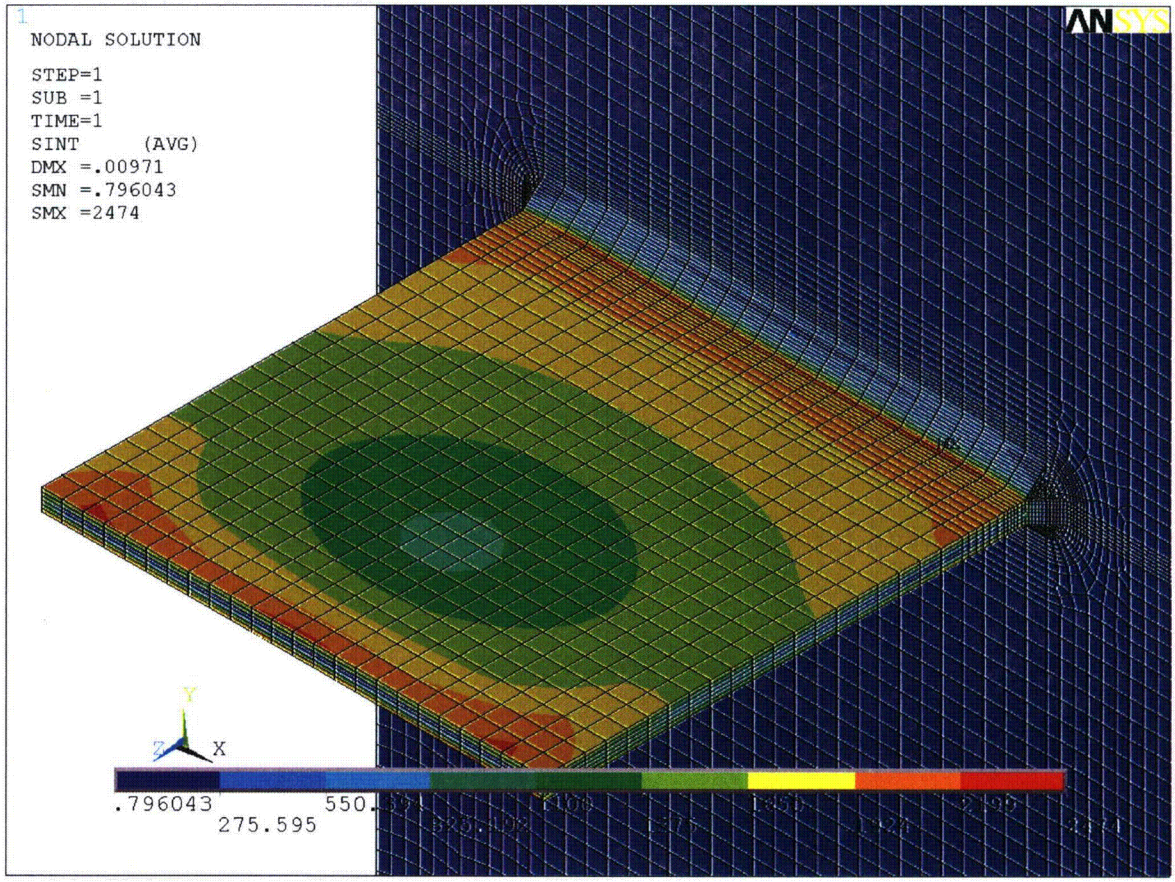

Figure 6-11
Submodel Analysis using Submodel #2
Solid Model Stress Plot for Load Case #1

SRF Table

Table 6-4
Submodel Analysis (Submodel #2) SRF
for Dynamic Load Case #1

Path #	Solid (psi)	Shell (psi)	SRF
1	1,351	2,100	0.64
2	550		0.26
3	351		0.17
4	1,351		0.64
5	550		0.26
6	351		0.17
7	1,512		0.72
8	233		0.11
9	325		0.15
10	325		0.15
11	233		0.11
12	213		0.10
13	256		0.12
14	1,073		0.51
15	207		0.10
16	158		0.08
		Maximum =	**0.72**

6.5 Dynamic Load Case #2

6.5.1 Full Shell Finite Element Analysis

Transient Displacement Plot

The maximum horizontal displacement in the applied load Z direction occurs at the edge node of the load application line. The following Figure 6-12 shows a plot of the nodal transient displacements.

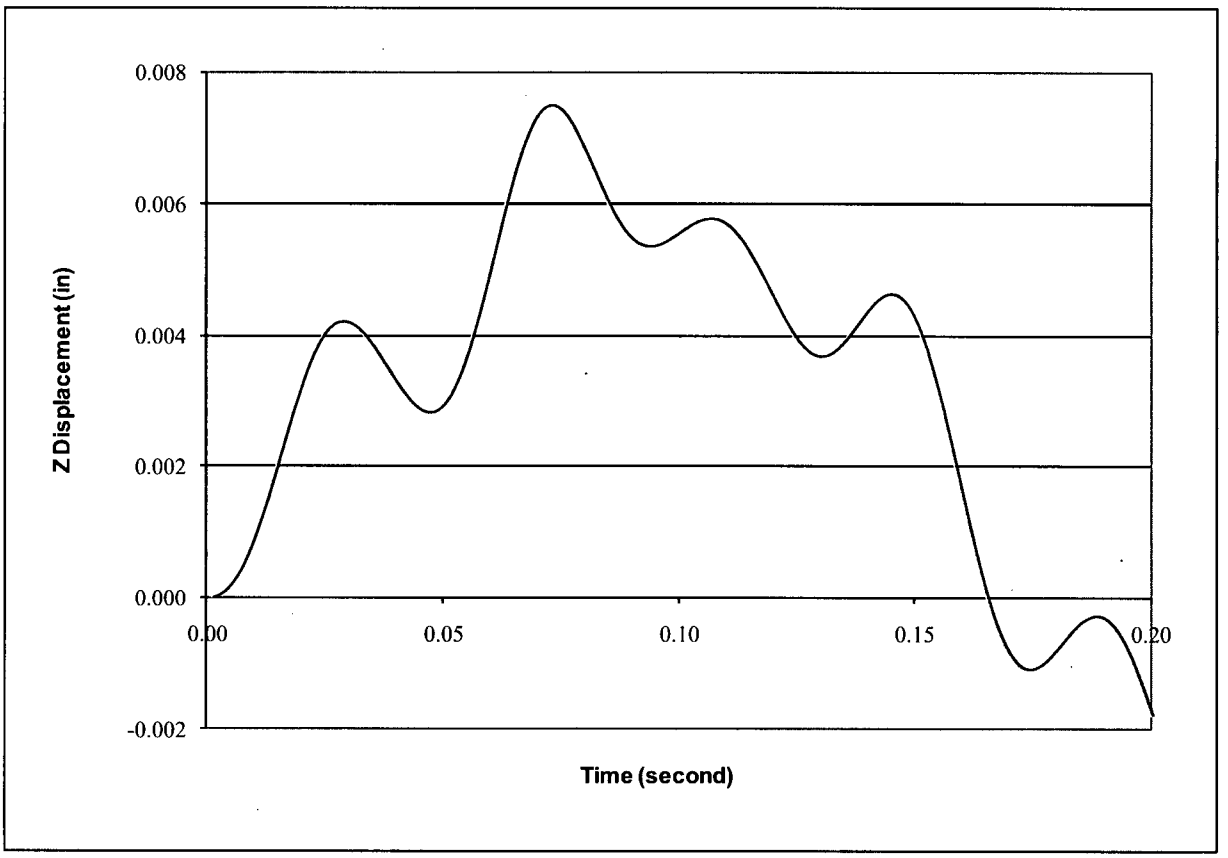

Figure 6-12
Full Shell Model Dynamic Analysis
Horizontal Transient Displacement for Load Case #2

Transient Stress Intensity Plot

The maximum stress intensity occurs at the one of the weld line nodes. The following Figure 6-13 shows a plot of the nodal transient stress intensities. The maximum stress intensity is 2,262 psi, which occurs at 0.031 seconds time step.

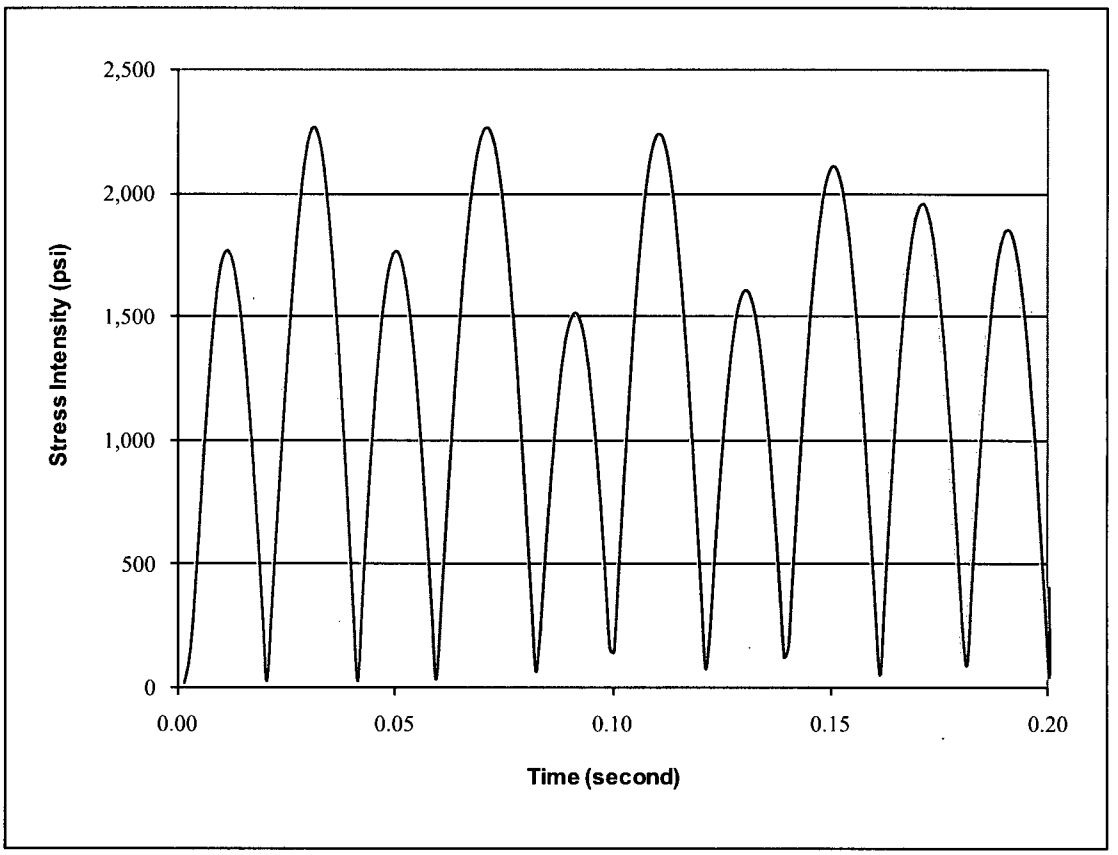

Figure 6-13
Full Shell Model Dynamic Analysis
Nodal Stress Intensity for Load Case #2

Horizontal Displacement Plot

The following Figure 6-14 shows the horizontal Z displacements at 0.031 seconds time step, when the maximum stress intensity occurs. The nodal displacements (for 6 degrees of freedom) at the submodel boundaries at this time step are used for subsequent substructure analyses.

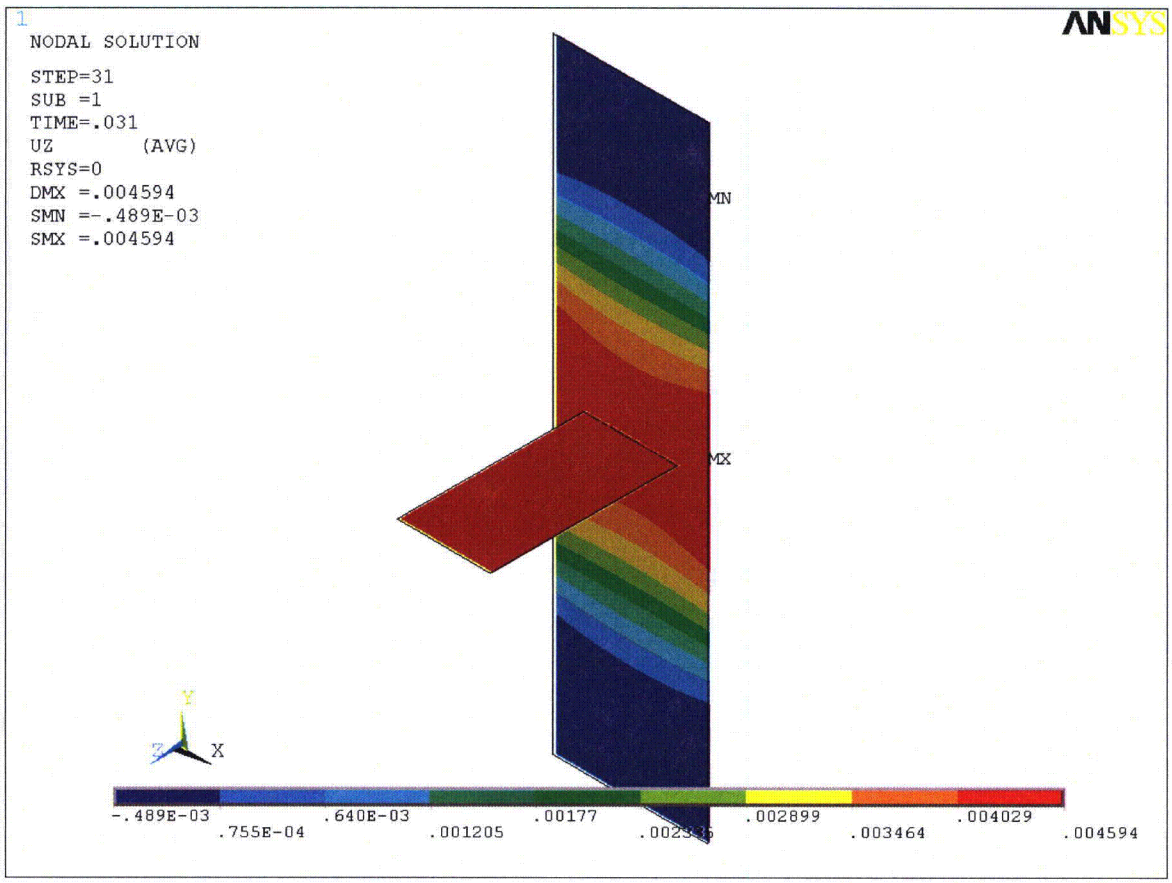

Figure 6-14
Full Shell Model Dynamic Analysis
Horizontal Displacement Plot for Load Case #2
(Full Shell Model Baseline Analysis)

Maximum Stress Plot

The maximum stress intensity is 2,262 psi, which occurs at 0.031 seconds time step. The stress plot at that time step is provided in the following Figure 6-15. This analysis is the full shell model baseline analysis, and the maximum stress intensity of 2,262 psi is used to determine the SRF in the other analysis.

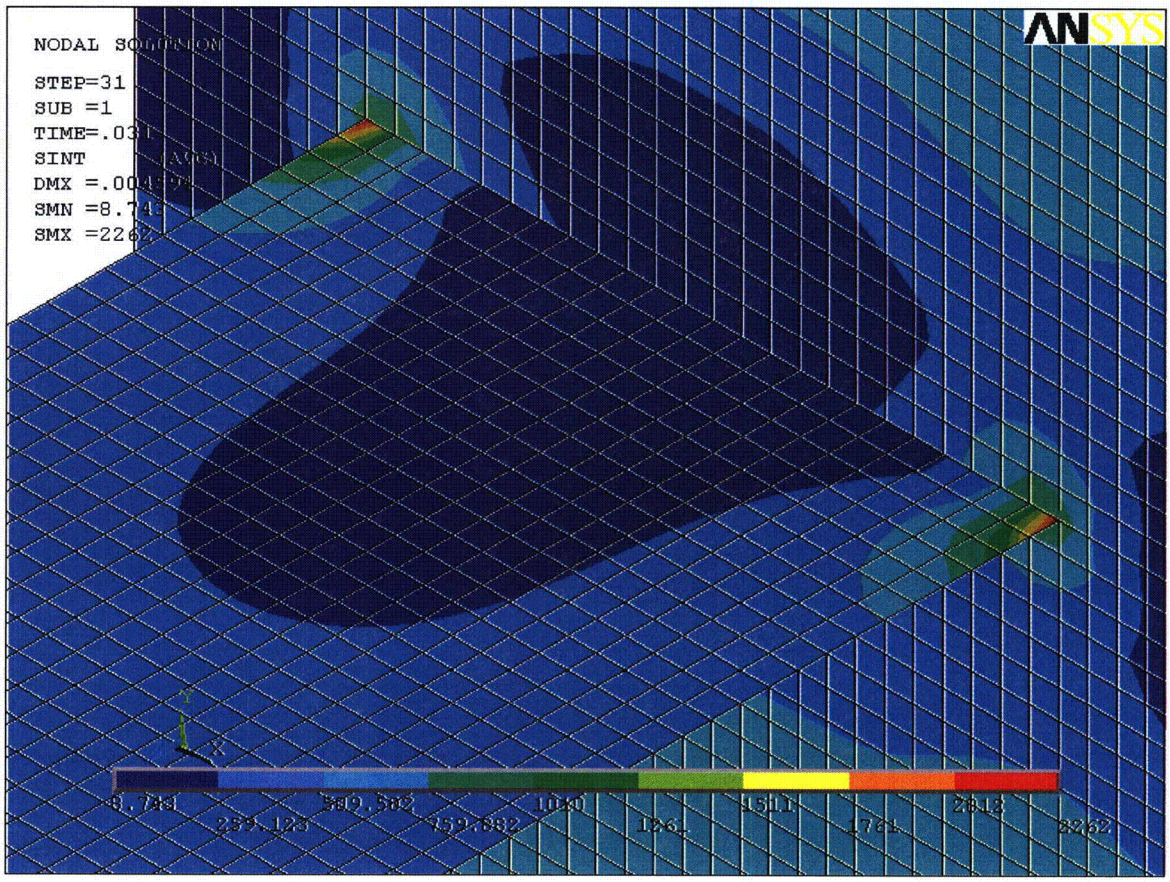

Figure 6-15
Full Shell Model Dynamic Analysis
Maximum Stress Plot for Load Case #2
(Full Shell Model Baseline Analysis)

6.5.2 Substructure Analysis Using Shell Submodel #2

With reference to Figure 3-5, the displacements along Edges A and C computed in the full shell finite element analysis (Section 6.5.1) are applied onto this shell submodel.

Horizontal Displacement Plot

The maximum horizontal displacement plot is provided in the following Figure 6-16.

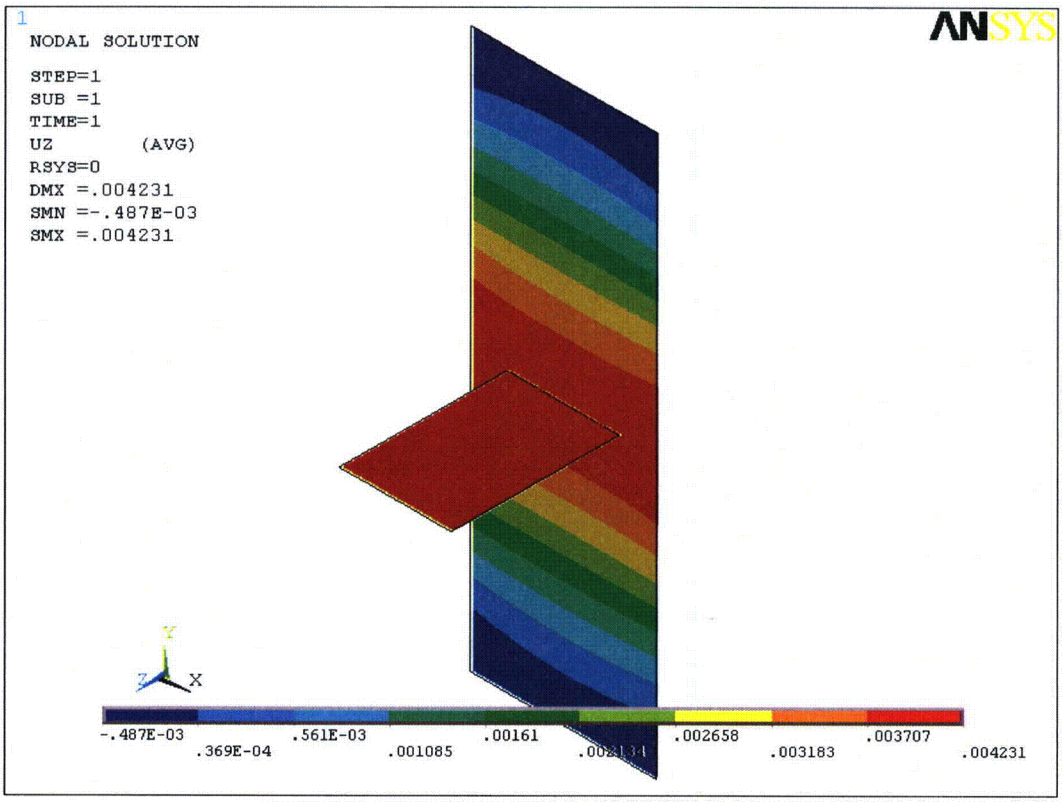

Figure 6-16
Substructure Analysis using Shell Submodel #2
Horizontal Displacement Plot for Load Case #2

Stress Plot

The maximum stress intensity is 948 psi, and the stress plot is provided in the following figure.

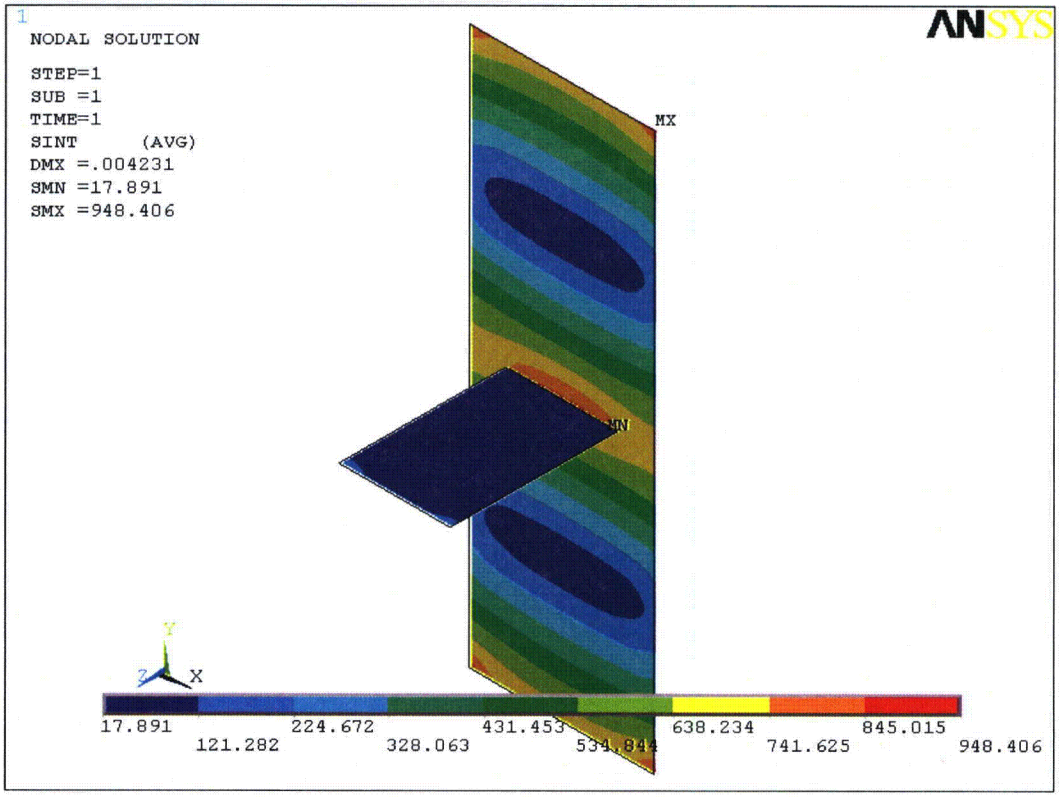

Figure 6-17
Substructure Analysis using Shell Submodel #2
Stress Plot for Load Case #2

Observation

The maximum stress intensity of 948 psi is significantly lower than the full shell baseline analysis maximum stress intensity of 2,262 psi. The stress pattern is also different. The maximum stress intensity for the substructure analysis is located along the top edge, not at the weld line.

In this analysis, only the displacements at the boundaries are mapped from the full shell model to the submodel. The shell internal displacements, influenced by the dynamic inertia effects, are not captured in the substructure analysis. Without imposing the dynamic characteristic displacements within the submodel boundaries, the substructure analysis is not able to duplicate the stress pattern of the full shell model.

6.5.3 *Substructure Analysis Using Solid Submodel #2*

With reference to Figure 3-6, the displacements along Edges A and C computed in the full shell finite element analysis (Section 6.5.1) are applied onto this solid submodel.

Stress Plot

The maximum non-linearized stress intensity is 1,389 psi, and the stress plot is provided in the following Figure 6-18.

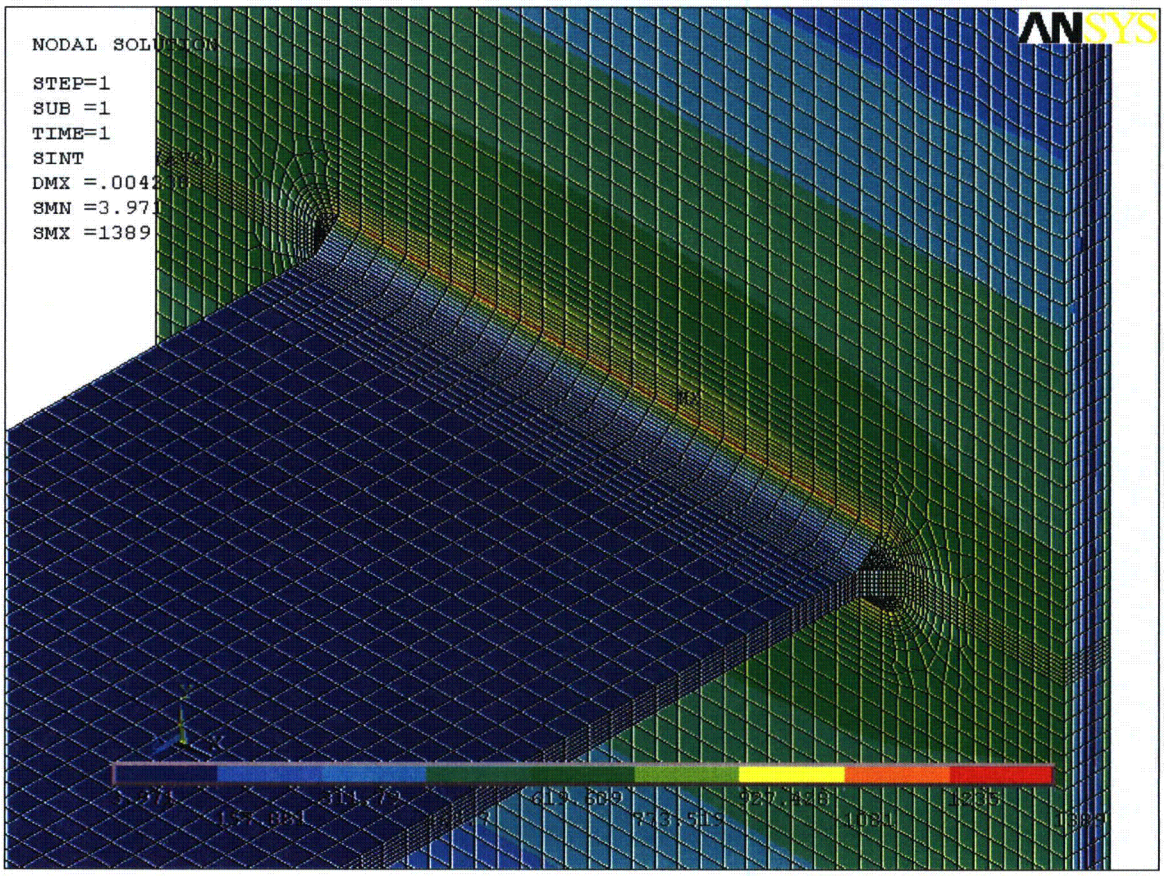

Figure 6-18
Substructure Analysis using Solid Submodel #2
Stress Plot for Load Case #2

SRF Table

Table 6-5
Substructure Dynamic Analysis (Submodel #2) SRF for Dynamic Load Case #2

Path #	Solid (psi)	Shell (psi)	SRF
1	500	2,262	0.22
2	503		0.22
3	762		0.34
4	500		0.22
5	503		0.22
6	762		0.34
7	239		0.11
8	777		0.34
9	627		0.28
10	627		0.28
11	777		0.34
12	730		0.32
13	496		0.22
14	469		0.21
15	482		0.21
16	686		0.30
		Maximum =	**0.34**

6.5.4 *Submodel Analysis Using Submodel #2*

Matching Stress Profile

The stress profile matching is perform along the weld line connecting the vertical plate to the horizontal plate. The matching is accomplished by imposing horizontal forces along the two vertical edges (i.e., Edge B, see Figure 3-3) of the submodel. The nodes at the top and bottom edges (i.e. Edge A) are restrained in UX and UZ translations. Fix boundary condition is applied to Edge C. The applied loads and the comparison of the stress profiles are shown in the following Figure 6-19 and Figure 6-20, respectively.

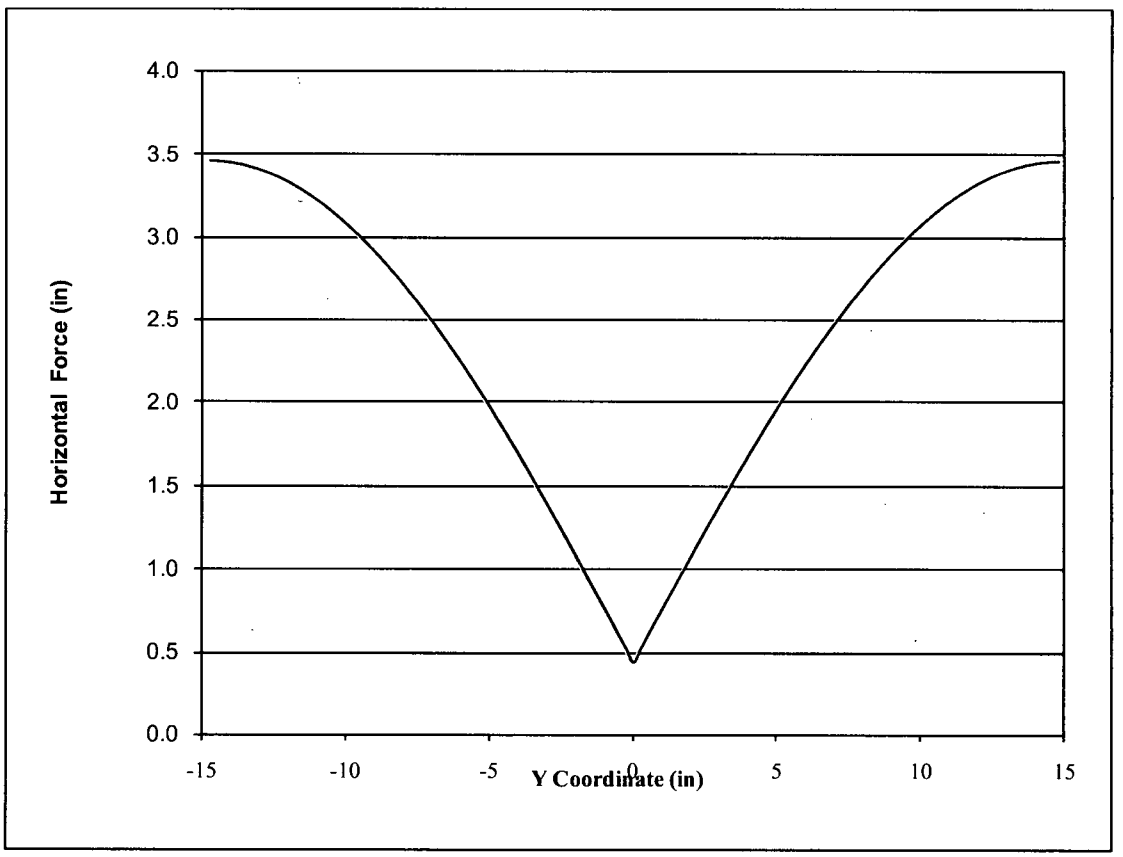

Figure 6-19
Submodel Analysis using Submodel #2
Applied Horizontal Loads for Load Case #2

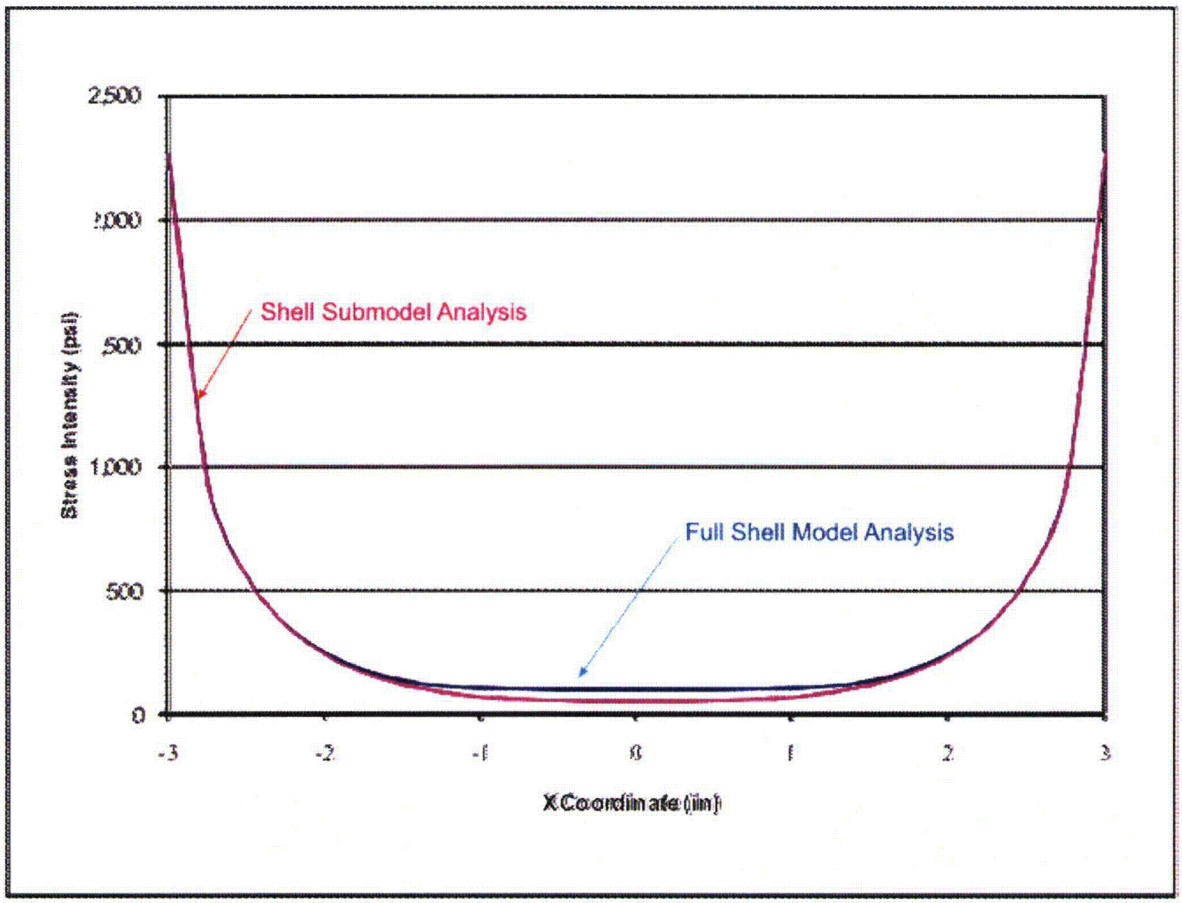

Figure 6-20
Submodel Analysis using Submodel #2
Stress Profile Comparison for Load Case #2

Stress Plot

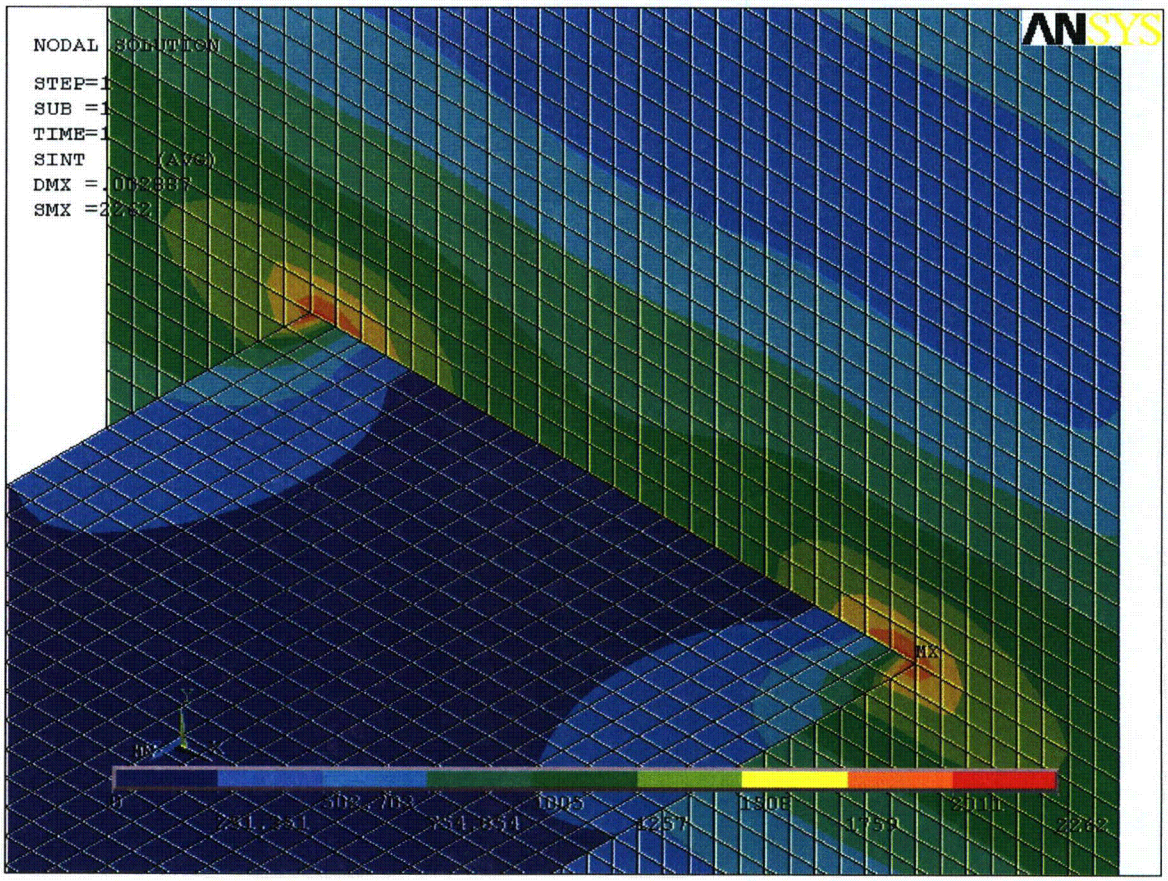

Figure 6-21
Submodel Analysis using Submodel #2
Shell Model Stress Plot for Load Case #2

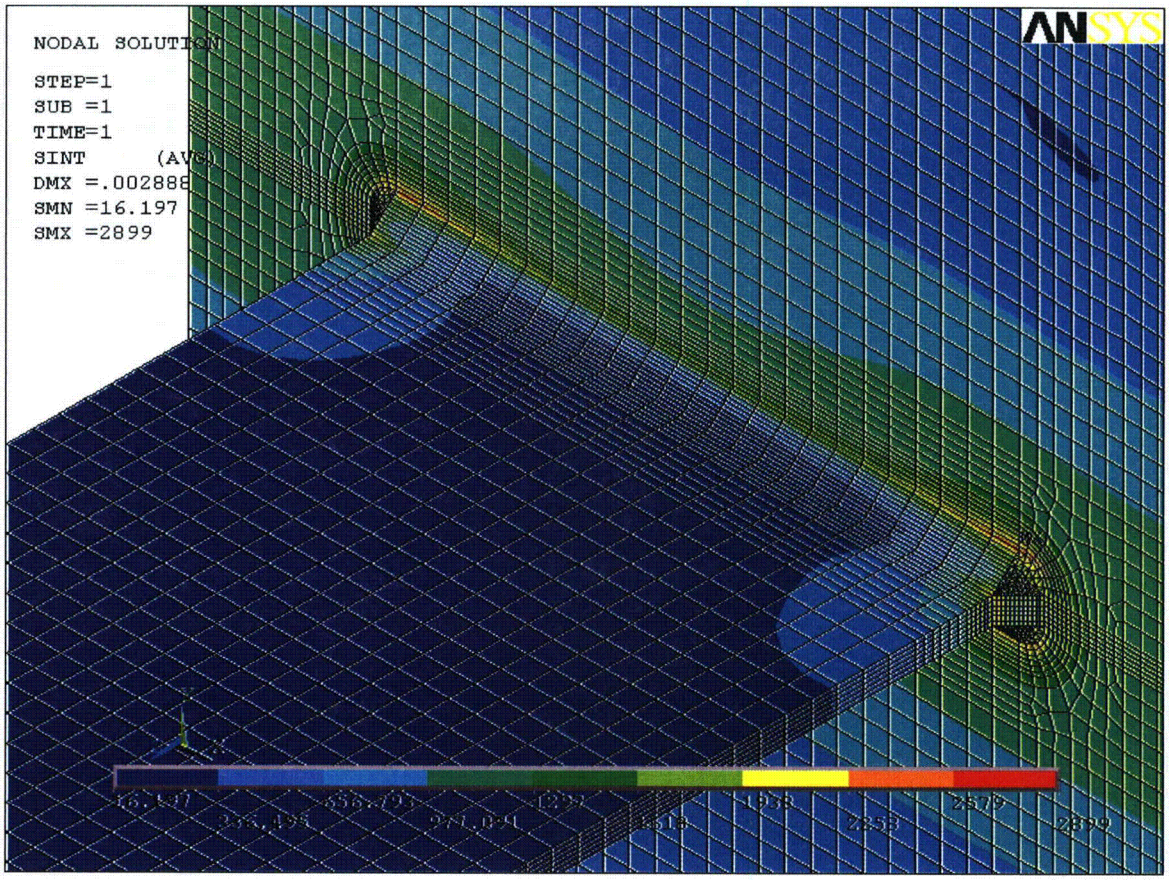

Figure 6-22
Submodel Analysis using Submodel #2
Solid Model Stress Plot for Load Case #2

SRF Table

Table 6-6
Submodel Analysis (Submodel #2) SRF
for Dynamic Load Case #2

Path #	Solid (psi)	Shell (psi)	SRF
1	1,871	2,262	0.83
2	1,233		0.55
3	1,820		0.80
4	1,871		0.83
5	1,233		0.55
6	1,820		0.80
7	1,888		0.83
8	1,467		0.65
9	1,228		0.54
10	1,228		0.54
11	1,467		0.65
12	1,905		0.84
13	1,259		0.56
14	1,871		0.83
15	832		0.37
16	1,619		0.72
		Maximum =	**0.84**

7.0 SUMMARY STRESS REDUCTION FACTORS

7.1 Static Analysis SRF

Static Load Case #1

Table 7-1
Summary SRF for Static Load Case #1

Analysis Approach	SRF
Full Solid Model Baseline Analysis	0.59
Substructure Analysis (Submodel #1)	0.74
Substructure Analysis (Submodel #2)	0.69
Submodel Analysis (Submodel #1)	0.68
Submodel Analysis (Submodel #2)	0.66

Static Load Case #2

Table 7-2
Summary SRF for Static Load Case #2

Analysis Approach	SRF
Full Solid Model Baseline Analysis	0.89
Substructure Analysis (Submodel #1)	0.92
Substructure Analysis (Submodel #2)	0.91
Submodel Analysis (Submodel #1)	0.89
Submodel Analysis (Submodel #2)	0.89

7.2 Dynamic Analysis SRF

Dynamic Load Case #1

Table 7-3
Summary SRF for Dynamic Load Case #1

Analysis Approach	SRF
Substructure Analysis (Submodel #2)	0.37
Submodel Analysis (Submodel #2)	0.72

Dynamic Load Case #2

Table 7-4
Summary SRF for Dynamic Load Case #2

Analysis Approach	SRF
Substructure Analysis (Submodel #2)	0.34
Submodel Analysis (Submodel #2)	0.84

8.0 DISCUSSIONS

The comparisons of the SRF and the different analyses lead to the following observation and deduction.

8.1 Static Analysis

Substructure Analysis Using Shell Submodels

The substructure analyses using the shell submodels show that the results are the same as the full shell model. The maximum stress intensities from both the shell submodel and the full shell model analyses are the same. The stress plots of both the submodel and full model analyses also show that the stress patterns are the same.

Substructure Analysis Using Solid Submodels

The substructure analysis using the solid submodel predicts higher SRF than the SRF computed in the full solid model baseline analysis (see Table 7-1 and Table 7-2). The reason that they are different is because the shell model is more flexible than the solid model, which models in the detailed weld configuration.

The local region of the solid model that models in the weld configuration becomes stiffer than the corresponding region in the shell model. When the displacements from the more flexible shell model analysis are applied onto the more rigid solid submodel, higher stresses are computed for the solid submodel.

To better predict the local stresses using the substructure analysis, the boundaries of the submodel need to be extended to a reasonable distance. This is evident when the submodel #1 and submodel #2 substructure analysis results are compared. When the boundaries are extended from submodel #1 to submodel #2, the SRF is lowered (see Table 7-1 and Table 7-2).

Submodel Analysis

The study shows that when the matching of the stress intensity profile along the high stress weld line is achieved, the submodel analysis is a reasonable approach for calculating the SRF. For Load Cases #1 and #2, the submodel analyses have computed SRFs that show good agreement with the full solid model baseline analysis.

The SRFs computed using submodels #1 and #2 are very similar. This similarity in SRFs demonstrate that after satisfactory stress intensity profile matching, the computation of SRFs is not sensitive to the size of the submodel.

8.2 Dynamic Analysis

Substructure Analysis Using Shell Submodels

The maximum stress intensity calculated using a substructure shell analysis is significantly lower than the maximum stress intensity computed using full shell baseline analysis. The stress patterns of the two analyses are also different.

In the substructure analysis, only the displacements at the boundaries are mapped from the full shell model to the submodel boundaries. The shell internal displacements, caused by the dynamic inertia effects, are not captured in the substructure analysis. Without imposing the dynamic characteristic displacements at regions within the submodel boundaries, the substructure analysis is not able to duplicate the stress pattern of the full shell model. This results in predicting lower shell submodel stresses at the weld line.

Substructure Analysis Using Solid Submodels

Similar to the substructure analysis using shell submodel, the substructure analysis using solid submodel also does not capture the internal displacements at regions within the submodel boundaries, and therefore the full dynamic inertia effects of the structure have not been accurately represented. This also results in predicting lower solid submodel stresses at the weld line. Consequently, the SRF computed using the substructure analysis shows an unreasonably low value (see Table 7-3 and Table 7-4).

Submodel Analysis

Similar to the static analysis, the study shows that when the matching of the stress intensity profile along the high stress weld line is achieved, the submodel analysis is a reasonable approach for the calculation of the SRF.

For both Load Cases #1 and #2, the SRFs computed using the submodel analysis are significantly higher than the SRFs computed using the substructure analysis. However, they demonstrate reasonable agreement with the SRFs computed in the static analysis.

9.0 CONCLUSIONS

The comparison study documented in this calculation fully addresses the issues identified in the RAI 199/156 from NRC (Reference 3).

Two Load Cases have been considered in this calculation:

Load Case #1

This load case examines the scenario where the weld is subjected to mainly bending action. To match the stress profile, imposed displacements are used. This is similar to the submodel analysis approach used to determine the stresses at the bottom of the skirt/drain channel junction.

Load Case #2

This load case examines the scenario where the weld is subjected to mainly membrane action. To match the stress profile, imposed loads are used. This is similar to the submodel analysis approach used to determine the stresses at the intersection between the bottom of the inner hood, stiffener and base plate.

Two analysis options have been evaluated: the static analysis and the dynamic time history analysis. Together these analyses show that the SRFs computed using the TVA submodel analysis technique are accurate and acceptable.

In conclusion, this comparison study validates the submodel analysis approach adopted for the steam dryer stress analysis.

10.0 REFERENCES

1. Email with attachments from George Nelson (TVA) to Marcos Herrera (SI) on 04/22/08 at 9:02 am, "Steam Dryer - Drain Channel," SI File No. BFN-15-224.
2. Email with attachment from Rick Cutsinger (TVA) to Soo Bee Kok (SI) on May 20, 2008 @9:02 am, "RE: Weld Structure Evaluation," SI File No. BFN-15-227P.
3. Email with attachments from Denzel Housley (TVA) to Soo Bee Kok (SI) on 10/29/08 at 7:31 am, "RE: Editorial Changes to EMCB.199.156 R2", SI File No. BFN-15-229.
4. ANSYS Mechanical, Release 11.0 (w/ Service Pack 1), ANSYS, Inc., August 2007.
5. SI Calculation No. 0006982.302, Revision 0, "Project Specific Software Verification and Validation of ANSYS Release 11.0 (w/ Service Pack 1)"

Appendix A - Computer Files

General Application

Filename	Description
ShellFull.inp	Full shell finite element model development input file.
ShellSub1.inp	Shell submodel #1 finite element model development input file.
ShellSub2.inp	Shell submodel #2 finite element model development input file.
SolidFull.inp	Full solid finite element model development input file.
SolidSub1.inp	Solid submodel #1 finite element model development input file.
SolidSub2.inp	Solid submodel #2 finite element model development input file.
PPpath.mac	Stress path generation macro.

Static Load Case #1 Application

Filename	Description
T1E.inp	Full shell model baseline analysis for Load Case #1 input file.
C1E.inp	Substructure analysis using shell submodel #1 for Load Case #1 input file.
C2E.inp	Substructure analysis using shell submodel #2 for Load Case #1 input file.
T2E.inp	Substructure analysis using solid submodel #1 for Load Case #1 input file.
T2EPP.inp	Substructure analysis using solid submodel #1 for Load Case #1 post processing input file.
T2EPP.xls	Substructure analysis using solid submodel #1 for Load Case #1 SRF calculation spreadsheet.
T3E.inp	Substructure analysis using solid submodel #2 for Load Case #1 input file.
T3EPP.inp	Substructure analysis using solid submodel #2 for Load Case #1 post processing input file.
T3EPP.xls	Substructure analysis using solid submodel #2 for Load Case #1 SRF calculation spreadsheet.
T4E.inp	Full solid model baseline analysis for Load Case #1 input file.
T4EPP.inp	Full solid model baseline analysis for Load Case #1 post processing input file.
T4EPP.xls	Full solid model baseline analysis for Load Case #1 SRF calculation spreadsheet.
T5E.inp	Submodel stress intensity matching analysis using shell submodel #1 for Load Case #1 input file.
T6E.inp	Submodel analysis using solid submodel #1 for Load Case #1 input file.
T6EPP.inp	Submodel analysis using solid submodel #1 for Load Case #1 post processing input file.
T6EPP.xls	Submodel analysis using solid submodel #1 for Load Case #1 SRF calculation spreadsheet.
T7E.inp	Submodel stress intensity matching analysis using shell submodel #2 for Load Case #1 input file.
T8E.inp	Submodel analysis using solid submodel #2 for Load Case #1 input file.
T8EPP.inp	Submodel analysis using solid submodel #2 for Load Case #1 post processing input file.
T8EPP.xls	Submodel analysis using solid submodel #2 for Load Case #1 SRF calculation spreadsheet.

Static Load Case #2 Application

Filename	Description
T1D.inp	Full shell model baseline analysis for Load Case #2 input file.
C1D.inp	Substructure analysis using shell submodel #1 for Load Case #2 input file.
C2D.inp	Substructure analysis using shell submodel #2 for Load Case #2 input file.
T2D.inp	Substructure analysis using solid submodel #1 for Load Case #2 input file.
T2DPP.inp	Substructure analysis using solid submodel #1 for Load Case #2 post processing input file.
T2DPP.xls	Substructure analysis using solid submodel #1 for Load Case #2 SRF calculation spreadsheet.
T3D.inp	Substructure analysis using solid submodel #2 for Load Case #2 input file.
T3DPP.inp	Substructure analysis using solid submodel #2 for Load Case #2 post processing input file.
T3DPP.xls	Substructure analysis using solid submodel #2 for Load Case #2 SRF calculation spreadsheet.
T4D.inp	Full solid model baseline analysis for Load Case #2 input file.
T4DPP.inp	Full solid model baseline analysis for Load Case #2 post processing input file.
T4DPP.xls	Full solid model baseline analysis for Load Case #2 SRF calculation spreadsheet.
T5D.inp	Submodel stress intensity matching analysis using shell submodel #1 for Load Case #2 input file.
T6D.inp	Submodel analysis using solid submodel #1 for Load Case #2 input file.
T6DPP.inp	Submodel analysis using solid submodel #1 for Load Case #2 post processing input file.
T6DPP.xls	Submodel analysis using solid submodel #1 for Load Case #2 SRF calculation spreadsheet.
T7D.inp	Submodel stress intensity matching analysis using shell submodel #2 for Load Case #2 input file.
T8D.inp	Submodel analysis using solid submodel #2 for Load Case #2 input file.
T8DPP.inp	Submodel analysis using solid submodel #2 for Load Case #2 post processing input file.
T8DPP.xls	Submodel analysis using solid submodel #2 for Load Case #2 SRF calculation spreadsheet.

General Dynamic Analysis Application

Filename	Description
TH1E.inp	Full shell model modal analysis input file.
Damping.xls	Alpha and beta damping coefficient calculation spreadsheet.

Dynamic Load Case #1 Application

Filename	Description
TH2F.inp	Full shell model baseline time history analysis for Load Case #1 input file.
TH2FP1.inp	Full shell model baseline analysis for Load Case #1, 1st post processing input file.
TH2FP2.inp	Full shell model baseline analysis for Load Case #1, 2nd post processing input file.
TH3F.inp	Substructure analysis using shell submodel #2 for Load Case #1 input file.
TH6F.inp	Substructure analysis using solid submodel #2 for Load Case #1 input file.
TH6FPP.inp	Substructure analysis using solid submodel #2 for Load Case #1 post processing input file.
TH6FPP.xls	Substructure analysis using solid submodel #2 for Load Case #1 SRF calculation spreadsheet.
TH4F.inp	Submodel stress intensity matching analysis using shell submodel #2 for Load Case #1 input file.
TH5F.inp	Submodel analysis using solid submodel #2 for Load Case #1 input file.
TH5FPP.inp	Submodel analysis using solid submodel #2 for Load Case #1 post processing input file.
TH5FPP.xls	Submodel analysis using solid submodel #2 for Load Case #1 SRF calculation spreadsheet.

Dynamic Load Case #2 Application

Filename	Description
TH2G.inp	Full shell model baseline time history analysis for Load Case #2 input file.
TH2GP1.inp	Full shell model baseline analysis for Load Case #2, 1st post processing input file.
TH2GP2.inp	Full shell model baseline analysis for Load Case #2, 2nd post processing input file.
TH3G.inp	Substructure analysis using shell submodel #2 for Load Case #2 input file.
TH6G.inp	Substructure analysis using solid submodel #2 for Load Case #2 input file.
TH6GPP.inp	Substructure analysis using solid submodel #2 for Load Case #2 post processing input file.
TH6GPP.xls	Substructure analysis using solid submodel #2 for Load Case #2 SRF calculation spreadsheet.
TH4G.inp	Submodel stress intensity matching analysis using shell submodel #2 for Load Case #2 input file.
TH5G.inp	Submodel analysis using solid submodel #2 for Load Case #2 input file.
TH5GPP.inp	Submodel analysis using solid submodel #2 for Load Case #2 post processing input file.
TH5GPP.xls	Submodel analysis using solid submodel #2 for Load Case #2 SRF calculation spreadsheet.

ENCLOSURE 7

TENNESSEE VALLEY AUTHORITY
BROWNS FERRY NUCLEAR PLANT (BFN)
UNITS 1, 2, AND 3

TECHNICAL SPECIFICATIONS (TS) CHANGES TS-431 AND TS-418
EXTENDED POWER UPRATE (EPU)

CDI AFFIDAVIT

Attached is the CDI affidavit for the proprietary information contained in Enclosures 2, 3, 4, and 5.

Continuum Dynamics, Inc.

(609) 538-0444 (609) 538-0464 fax 34 Lexington Avenue Ewing, NJ 08618-2302

AFFIDAVIT

Re: C.D.I. Report 08-15P "Stress Assessment of Browns Ferry Nuclear Unit 1 Steam Dryer with Tie-Bar Modifications," Revision 2;
C.D.I. Report 08-14P "Flow-Induced Vibration in the Main Steam Lines at Browns Ferry Nuclear Units 1 and 2, With and Without Acoustic Side Branches, and Resulting Steam Dryer Loads," Revision 0;
C.D.I. Report 08-04P "Acoustic and Low Frequency Hydrodynamic Loads at CLTP Power Level on Browns Ferry Nuclear Unit 1 Steam Dryer to 250 Hz," Revision 2; and
C.D.I. Report 08-05P "Acoustic and Low Frequency Hydrodynamic Loads at CLTP Power Level on Browns Ferry Nuclear Unit 2 Steam Dryer to 250 Hz," Revision 3

I, Alan J. Bilanin, being duly sworn, depose and state as follows:

1. I hold the position of President and Senior Associate of Continuum Dynamics, Inc. (hereinafter referred to as C.D.I.), and I am authorized to make the request for withholding from Public Record the Information contained in the documents described in Paragraph 2. This Affidavit is submitted to the Nuclear Regulatory Commission (NRC) pursuant to 10 CFR 2.390(a)(4) based on the fact that the attached information consists of trade secret(s) of C.D.I. and that the NRC will receive the information from C.D.I. under privilege and in confidence.

2. The Information sought to be withheld, as transmitted to TVA Browns Ferry as attachment to C.D.I. Letter No. 08196 dated 31 October 2008 C.D.I. Report No. 08-15P "Stress Assessment of Browns Ferry Nuclear Unit 1 Steam Dryer with Tie-Bar Modifications," Revision 2; C.D.I. Report 08-14P "Flow-Induced Vibration in the Main Steam Lines at Browns Ferry Nuclear Units 1 and 2, With and Without Acoustic Side Branches, and Resulting Steam Dryer Loads," Revision 0; C.D.I. Report 08-04P "Acoustic and Low Frequency Hydrodynamic Loads at CLTP Power Level on Browns Ferry Nuclear Unit 1 Steam Dryer to 250 Hz," Revision 2; and C.D.I. Report 08-05P "Acoustic and Low Frequency Hydrodynamic Loads at CLTP Power Level on Browns Ferry Nuclear Unit 2 Steam Dryer to 250 Hz," Revision 3

3. The Information summarizes:

   (a) a process or method, including supporting data and analysis, where prevention of its use by C.D.I.'s competitors without license from C.D.I. constitutes a competitive advantage over other companies;

(b) Information which, if used by a competitor, would reduce his expenditure of resources or improve his competitive position in the design, manufacture, shipment, installation, assurance of quality, or licensing of a similar product;
(c) Information which discloses patentable subject matter for which it may be desirable to obtain patent protection.

The information sought to be withheld is considered to be proprietary for the reasons set forth in paragraphs 3(a), 3(b) and 3(c) above.

4. The Information has been held in confidence by C.D.I., its owner. The Information has consistently been held in confidence by C.D.I. and no public disclosure has been made and it is not available to the public. All disclosures to third parties, which have been limited, have been made pursuant to the terms and conditions contained in C.D.I.'s Nondisclosure Secrecy Agreement which must be fully executed prior to disclosure.

5. The Information is a type customarily held in confidence by C.D.I. and there is a rational basis therefore. The Information is a type, which C.D.I. considers trade secret and is held in confidence by C.D.I. because it constitutes a source of competitive advantage in the competition and performance of such work in the industry. Public disclosure of the Information is likely to cause substantial harm to C.D.I.'s competitive position and foreclose or reduce the availability of profit-making opportunities.

I declare under penalty of perjury that the foregoing affidavit and the matters stated therein are true and correct to be the best of my knowledge, information and belief.

Executed on this 31st day of October 2008.

Alan J. Bilanin
Continuum Dynamics, Inc.

Subscribed and sworn before me this day: October 31, 2008

Eileen P. Burmeister, Notary Public

EILEEN P. BURMEISTER
NOTARY PUBLIC OF NEW JERSEY
MY COMM. EXPIRES MAY 5 2012